

2003-08-18

Graphically Driven Interactive Stress Reanalysis for Machine Elements in the Early Design Stage

Sachin Sharad Terdalkar
Worcester Polytechnic Institute

Follow this and additional works at: <https://digitalcommons.wpi.edu/etd-theses>

Repository Citation

Terdalkar, Sachin Sharad, "Graphically Driven Interactive Stress Reanalysis for Machine Elements in the Early Design Stage" (2003). *Masters Theses (All Theses, All Years)*. 939.
<https://digitalcommons.wpi.edu/etd-theses/939>

This thesis is brought to you for free and open access by Digital WPI. It has been accepted for inclusion in Masters Theses (All Theses, All Years) by an authorized administrator of Digital WPI. For more information, please contact wpi-etd@wpi.edu.

Graphically Driven Interactive Stress Reanalysis for Machine Elements in the Early Design Stage

by

Sachin Sharad Terdalkar

A Thesis

Submitted to the Faculty

of the

WORCESTER POLYTECHNIC INSTITUTE

in partial fulfillment of the requirements for the

Degree of Master of Science

in

Mechanical Engineering

by

Sachin Sharad Terdalkar

August 2003

APPROVED:

Prof. Joseph J. Rencis
Advisor

Prof. Raymond R. Hagglund
Thesis Committee

Prof. Zikun Hou
Thesis Committee

Prof. John M. Sullivan, Jr.
Graduate Committee Representative

Abstract

In this work a new graphically driven interactive stress reanalysis finite element technique has been developed so that an engineer can easily carry out manual geometric changes in a machine element during the early design stage. The interface allow an engineer to model a machine element in the commercial finite element code ANSYS® and then modify part geometry graphically to see instantaneous graphical changes in the stress and displacement contour plots. A reanalysis technique is used to enhance the computational performance for solving the modified problem; with the aim of obtaining results of acceptable accuracy in as short a period of time in order to emphasize the interactive nature of the design process.

Three case studies are considered to demonstrate the effectiveness of the prototype graphically driven reanalysis finite element technique. The finite element type considered is a plane stress four-node quadrilateral based on a homogenous, isotropic, linear elastic material. The first two problems consider a plate with hole and plate with fillets. These two examples demonstrate that by changing the hole and fillet size/shape, an engineer can manually obtain an optimum design based on the stress concentration factor, i.e. engineer-driven optimization process. Each case study considered multiple redesigns. A combined approximation reanalysis method is used to solve each redesigned problem. The third case study considers a support bracket. The goal is to design the cantilever portion of the bracket to have uniform strength and to minimize the stress concentration at the fillet.

The major beneficiaries of the work will be engineers working in product development and validation of components and structures, which are subjected to mechanical loads. The scientific and technological relevance of this work applies not only to the early stage of design, but to a number of other applications areas in which benefits may accrue. A company may have needs for a rapid analysis and re-analysis tool for fatigue assessment of components manufactured slightly out of tolerance. Typically this needs to be carried out under a very restrictive time scale.

Table of Contents

Section	Page
Abstract	i
Table of Contents	ii
List of Figures	v
List of Tables	vii
List of Symbols	viii
Acknowledgement	ix
1. Introduction	1
1.1 Design	1
1.2 Machine Design	1
1.3 Design Process	1
1.4 Computer-Aided Engineering and Finite Element Analysis	5
1.5 Overview of Traditional Finite Element Analysis	6
1.6 Current Status of FEA in Design Process	6
1.7 Rapid Product Development Process	7
1.8 Early Analysis: The New Engineering Paradigm	12
1.9 Goal and Objectives	13
1.10 Significance of Work	14
2. Structural Reanalysis	15
2.1 Design Optimization	15
2.2 Design Variables	15
2.3 Structural Reanalysis	15
2.4 Combined Approximations Method and its Cost Analysis	22
2.4.1 Problem Formulation	22
2.4.2 Combined Approximation Reanalysis	23
2.5 Comments on Combined Approximation in Finite Element Analysis	27
3. ANSYS Interface and Supporting Routines	29
3.1 Introduction	29
3.2 ANSYS Interface	29
3.2.1 ANSYS Program Organization	29
3.2.2 Graphical User Interface	30
3.2.3 ANSYS Database and Files	32
3.2.4 ANSYS Parametric Design Language	33
3.3 Development Platform	33
3.3.1 Initial Design	34
3.3.2 Analysis and Post-processing	35
3.3.3 Re-modeling	35
3.3.4 Reanalysis	35
3.3.5 Repeated Analysis	38

4. Examples and Results	39
4.1 Overview	39
4.2 Case Study # 1: Plate with a Hole	39
4.2.1 Finite Element Model of Initial Problem	40
4.2.2 Redesign Option # 1: Plate with Circular Hole	43
4.2.3 Redesign Option # 2: Plate with Horizontal Elliptical Hole	50
4.2.4 Redesign Option # 2: Plate with Horizontal Vertical Hole	54
4.2.5 Conclusion of Problem # 1	58
4.3 Case Study # 2: Optimal Shape of Shoulder Fillet in Flat Plate under Tension	59
4.3.1 Initial Design	61
4.3.2 Redesign Option # 1: Plate with Free-form Fillet	64
4.3.3 Redesign Option # 2: Plate with Circular Arc Fillet	68
4.3.4 Redesign Option # 3: Plate with Two Circular Arc Fillet	70
4.3.5 Conclusion for Case Study # 2	71
4.4 Case Study # 3: Support Bracket Redesign	72
4.4.1 FEM Model and ANSYS Analysis	73
4.4.2 Redesign Option # 1: Optimum Thickness for Uniform Stress Distribution	75
4.4.3 Redesign Option # 2: Fillet Radius of 5 mm	77
4.4.4 Redesign Option # 3: Fillet Radius of 7.5 mm	79
4.4.5 Conclusion for Case Study # 3	81
5. Conclusion	83
6. Future Work	84
References	88
Appendices	
A ANSYS Result File (file.rst) Overview	98
A.1 Overview	98
A.2 Result File Structure	98
A.3 Accessing ANSYS Binary Files	102
B. ANSYS Parametric Design Language (APDL)	104
B.1 Introduction	104
B.2 Setting Material Properties	104
B.3 Changing Toolbar	105
C. Advantages of using Combined Approximation Reanalysis	110
C.1 Introduction	110
C.2 Comparison	111
C.2.1 Method # 1: Direct Analysis with Cholesky Decomposition Method	111
C.2.2 Method # 2: Combined Approximation Reanalysis Method	111

D. User Interface Design Language	114
D.1 Introduction	114
D.2 The Structure of UIDL	114
D.2.1 Control Files	114
D.2.1.1 Control File Header	115
D.2.1.2 Building Block	115
D.3 Overview of Building Block	116
D.3.1 Block Header Section	117
D.3.2 Data Control Section	117
D.3.3 Ending Line	117
D.4 The menulist57.ans File	117
E. Hand Calculations for Example Problems	119
E.1 Case Study # 1: Plate with a Hole	119
E.2 Case Study # 2: Circular Arc Fillet	123
F. Thesis Defense Presentation Slides	125

List of Figures

Figure	Page
1.1 Design Purpose	2
1.2 Design Process	4
1.3 Relative acceptance and age of three enabling technologies	8
1.4 Traditional product development process	9
1.5 Difficulties and cost in design changes	10
1.6 Cost spent versus product knowledge	10
1.7 Product development using early analysis	11
1.8 Improved cost spent versus product knowledge with early analysis	11
1.9 Product Development Cycle	13
2.1 Combined Approximation Reanalysis Flowchart	26
3.1 Organization of ANSYS 5.7	30
3.2 Regions of the ANSYS 5.7 Graphical User Interface	31
3.3 ANSYS PLANE42 Element Type	34
3.4 FEM Meshes	37
4.1 Initial Design Geometry	40
4.2 Quarter symmetry initial geometry	40
4.3 Initial design and three redesign options for hole	41
4.4 ANSYS Reanalysis Toolbar	41
4.5 ANSYS GUI for initial mesh	42
4.6 ANSYS Stress contour results of plate with square hole	42-43
4.7 Re-modeling prompts	44
4.8 Plate with a circular hole (Redesign Option # 1)	45
4.9 ANSYS Reanalysis Toolbar with result menu	45
4.10 Redesign Option # 1 contour plots for plate with circular hole	46
4.11(a) Maximum displacement (U_x) versus # of reduced basis vectors	48
4.11(b) % Error in maximum displacement versus # of reduced basis vectors	48
4.11(c) Maximum stress (σ_x) variation versus # of reduced basis vectors	49
4.11(d) % Error in maximum stress (σ_x) versus # of reduced basis vectors	49
4.12 Redesign Option # 2 contour results for plate with horizontal elliptical hole	50
4.13(a) Maximum displacement (U_x) variation versus # of reduced basis vectors	52
4.13(b) % Error in maximum displacement variation versus # of reduced basis vectors	52
4.13(c) Maximum stress (σ_x) variation versus # of reduced basis vectors	53
4.13(d) % Error in maximum stress (σ_x) variation versus # of reduced basis vectors	53
4.14 Redesign option # 3 contour results for plate with vertical elliptical hole	55
4.15(a) Maximum displacement (U_x) variation versus # of reduced basis vectors	56

4.15(b)	% Error in maximum displacement versus # of reduced basis vectors	57
4.15(c)	Maximum stress (σ_x) variation versus # of reduced basis vectors	57
4.15(d)	% Error in maximum stress (σ_x) variation versus # of reduced basis vectors	59
4.16	Geometry and notation for plate with fillet subjected to tension	60
4.17	Initial mesh used by Waldman	61
4.18(a)	Geometry for initial design and redesign cases	62
4.18(b)	FEM mesh for initial design	62
4.19	Contour plot of results for initial design	63
4.20	Contour plot of results for Redesign Option # 1	64
4.21(a)	Maximum displacement (U_x) variation versus # of reduced basis vectors	66
4.21(b)	% Error in Maximum displacement versus # of reduced basis vectors	66
4.21(c)	Maximum stress (σ_x) variation versus # of reduced basis vectors	67
4.21(d)	% Error in maximum stress (σ_x) variation versus # of reduced basis vectors	67
4.22	Contour plot of results for Redesign Option # 2	69
4.23	Contour Plot of results for Redesign Option # 3	70
4.24	Support Geometry	73
4.25	Initial Design and Redesign Options	73
4.26	FEM Mesh for Initial Design	74
4.27	Contour Plot of results	74
4.28	Contour Plots for Redesign Option # 1	76
4.29	Contour Plots for Redesign Option # 2	78
4.30	Contour Plots for Redesign Option # 3	80
B.1	ANSYS Toolbar before and after making a change	105
D.1	Control File with ANSYS Main Menu building block	116
E.1	Plate with a square hole	119
E.2	Cut Section	120
E.3	Plate with circular hole	120
E.4	Plate with a horizontal elliptical hole	121
E.5	Plate with a vertical elliptical hole	122
E.6	Circular arc Fillet	123

List of Tables

Table	Page
2.1 Comparison of Static Reanalysis Techniques	20
2.2 Combined Approximation Cost Analysis	27
4.1 Maximum Deflection (mm)	43
4.2 Minimum and Maximum stress components (N/mm ²)	43
4.3 Maximum Deflection (mm)	46
4.4 Minimum and Maximum stress components (N/mm ²)	46
4.5 Comparison of results for plate with circular hole	47
4.6 Maximum Deflection (mm)	51
4.7 Minimum and Maximum stress components (N/mm ²)	51
4.8 Comparison of results for plate with horizontal elliptical hole	51
4.9 Maximum Deflection (mm)	54
4.10 Minimum and Maximum stress components (N/mm ²)	54
4.11 Comparison of results for Redesign option # 3 plate with vertical elliptical hole	56
4.12 Comparison redesign options	59
4.13 Maximum Deflections (mm)	63
4.14 Minimum and Maximum stress components (N/mm ²)	63
4.15 Maximum Deflections (mm)	64
4.16 Minimum and Maximum stress components (N/mm ²)	65
4.17 Comparison of results for Redesign Option # 1	65
4.18 Maximum Deflections (mm)	68
4.19 Minimum and Maximum stress components (N/mm ²)	68
4.20 Comparison of results for Redesign option # 2	70
4.21 Maximum Deflections (mm)	71
4.22 Minimum and Maximum stress components (N/mm ²)	71
4.23 Comparison of results for Redesign Option # 3	71
4.24 Comparison of results for the three redesign options	72
4.25 Maximum Deflections (mm)	75
4.26 Minimum and Maximum stress components (N/mm ²)	75
4.27 Maximum Deflections (mm)	76
4.28 Minimum and Maximum stress components at fillet (N/mm ²)	76
4.29 Comparison of maximum results for Redesign Option # 1.	77
4.30 Maximum Deflections (mm)	77
4.31 Minimum and Maximum stress components (N/mm ²)	78
4.32 Comparison of maximum results at fillet for Redesign Option # 2.	79
4.33 Maximum Deflections (mm)	79
4.34 Minimum and Maximum stress components (N/mm ²)	79
4.35 Comparison of maximum results for Redesign Option # 3.	81
4.36 Comparison of results for the three redesign options.	82
C.1 Method 2 Cost Analysis	112

List of Symbols

n	Total Number of Degrees of Freedom for the Problem (with condition that the total number of degrees of freedom remains same in both designs)
F	External Nodal Force Vector
u_0	Displacement vector for initial design
K_0	Initial Stiffness Matrix
K	Modified Stiffness Matrix
u	Displacement vector for modified design
ΔK	Change in the Stiffness Matrix where, $K = K_0 + \Delta K$
	Upper Triangular Matrix where, $K_0 = U_0^T U_0$
m	Number of Rows Changed in the Stiffness Matrix
s	Number of Reduced Basis Vectors
ν	Poisson's ratio
E	Young's Modulus
U_x	Vector for X – directional displacement
U_Y	Vector for Y – directional displacement
σ_X	X – directional stress
σ_Y	Y – directional stress
σ_{VM}	vonMises stress
t	Thickness for the Plane Stress Problem
RBV	Number of reduced basis vectors

Acknowledgement

It gives me immense pleasure to thank all of those who have helped me, directly or indirectly in completion of this thesis. First of all I would like to thank Prof. Rencis for his extensive support as an advisor on this thesis, without which this thesis would have been nothing. Throughout these two years he was less like an advisor and more like a father. His office door was always open and he was always ready to help even the time when he was too busy in his work. I am extremely thankful for his support.

There are many people in ANSYS technical support whom I would like to thank for their extensive technical assistance in ANSYS 5.7. I really appreciate their efforts in answering my bombarding list of questions. Davis Rea, John Thompson, John Doyle, Dave Looman, Bill Baker, Jim Pasquerell are few names.

I would like to thank my roommates and my friends: Jayant, Gana, Praveen, Souvik, Murali, Viren, Rohit, Mandeep, Abhijeet, Sagar, Siju, Daniel for their help, directly or indirectly. I would also like to thank Mr. Sia Najafi for his help in using ANSYS in design studio. I would like to express my gratitude to my thesis committee Prof Hagglund, Prof. Hou and Prof. Sullivan for being in the committee and helping me to complete my thesis. I can't stop myself expressing my appreciation to ladies in ME office, Barbara Furhman, Pam and especially Janice and Barbara Edilberti. I would like to thank them all for their kindness and cooperation. Finally I would like to thank my family especially my mother and my brother for being an inspiration to me and their encouragement in whatever I do.

1. Introduction

1.1 Design

Design is defined as the process of applying various techniques and scientific principles for the purpose of defining a device, a process or a system in sufficient detail to permit its realization [1.1]. This is the broad definition of the design. *Engineering Design* is the process of devising a system, components, or a process to meet the desired needs. It is a decision making process (often iterative) in which the basic sciences, mathematics and engineering sciences are applied to convert the resources optimally to meet the stated objective [1.2].

1.2 Machine Design

In this work the focus is on *Machine Design*. A machine is a combination of mechanisms and other components that transforms, transmits, or uses energy, load, or motion for specific purpose. The critical concern is that machines create motion and develops forces. It is the engineer's task to define and calculate those motions, forces and changes in energy in order to determine the sizes, shapes, and materials needed for each of the interrelated parts in the machine. This is the essence of the machine design. A machine comprises several different machine elements properly designed and arranged to work together as a whole. Fundamental decisions regarding loading, kinematics and choice of materials must be made during the design of machine. Other factors such as strength, reliability, deformation, tribology (friction, wear and lubrication), cost, and space requirements also need to be considered [1.12]. The objective is to produce a machine that not only is sufficiently rugged to function properly for the reasonable time but is also economically feasible. Further, non-engineering decisions regarding marketability, product liability, ethics, politics, etc., must be integrated into the design process early. Since few people have the necessary tools to make all these decisions, machine design in practice is a discipline-blending human behavior. The ultimate goal in machine design is to size and shape the parts (machine elements) and choose appropriate materials and manufacturing processes so that the resulting machine can be expected to perform its intended function without failure. This requires that the engineer be able to calculate and predict the mode and conditions of failure for each element and then design it to prevent failure. This in turn requires that a *stress and deflection analysis* be done for each part. This is the part of the *design process* [1.1].

1.3 Design Process

A mechanical system is a synergistic collection of machine elements. It is synergistic because as a design it represents an idea or concept greater than the sum of the individual parts. For example, a wristwatch, although merely a collection of gears, springs, and cams, also represents the physical realization of a time-measuring device. Mechanical system design requires considerable flexibility and creativity to obtain good solutions. Creativity seems to be aided by familiarity with know successful designs, and

mechanical systems are often collections of well-designed components from a finite number of proven classes [1.12].

Machine design is a systematic process. Even if a new machine was conceived by invention, systematic machine design is needed to transform the invented concept into a working system that users will appreciate. The machine design process is subject to a large number of variations. In every text on the subject of engineering design, a different division of design process in distinct stages is proposed. They all make sense, although they seem very different from one another. This reflects the complex nature of the design process and the fact that every design problem requires a special treatment. This process cannot be exactly specified by an equation or an algorithm. A systematic approach is useful only to the extent that the designer is presented with a strategy that he can use as a basis for planning the required design strategy for the problem at hand [1.3].

The process of design is essentially an exercise in applied creativity. Various “*design processes*” have been defined to help solve “unstructured problems”, i.e., one from which the problem definition is vague and for which many possible solution exists. Some of these design process definitions contains only a few steps and others up to twenty-five detailed steps [1.1].

In simple terms, the “*design process*” can be defined as the interplay between “What we want to achieve?” and “How are we going to achieve it?” as shown in the Figure 1.1. The design approach begins with an explicit statement of “What we want to achieve?” and ends with clear description of “How we want to achieve it?” Once the customer needs are determined, they are transformed into a minimum set of specifications, which will be the Functional Requirements (FRs). The FRs adequately describe, “What we want to achieve?” to satisfy customer needs. The description of “How we are going to achieve it?” may be in the form of design parameters [1.4].

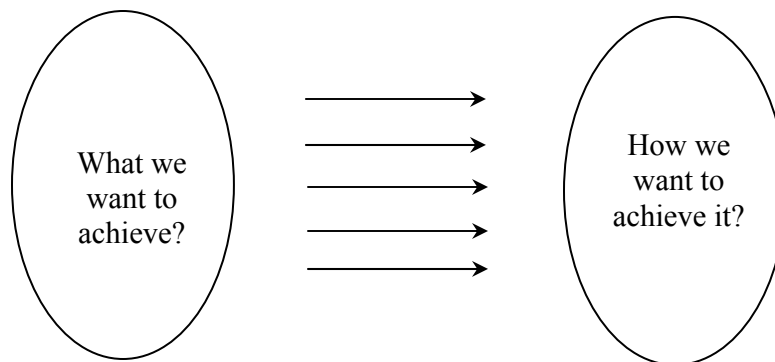


Figure 1.1 Design Purpose.

The design process can be more precisely illustrated in the flow chart as shown in Figure 1.2. The process can be essentially broken up into five steps and each step is as follows:

1. *Pre-design Process.* Sometimes, but not always, design begins when an engineer recognizes a need and decides to do something about it. Recognition of the need and phrasing the need often constitute a highly creative act, because the need may be only a vague discontent, a feeling of uneasiness, or a sensing that something is not right. The need is often not evident at all; recognition is usually triggered by a particular adverse circumstance or a set of random circumstances, which arise almost simultaneously. For example, the need to do something about a food-packaging machine may be indicated by the noise level, by the variation in package weight, and by slight but perceptible variations in the quality of the packaging or wrap. It is then followed by the definition of the problem. *Definition of the problem* must include all the specifications for the things to be designed. The specifications are the input and output quantities, the characteristics and dimensions of the space the thing must occupy, and all limitations on these quantities. We can regard the thing to be designed as something in a black box. In this case we must specify the inputs and outputs of the box, together with their characteristics and limitations. The specifications define the cost, the number to be manufactured the expected life, the range, the operating temperature and the reliability [1.13]. The problem definition also consists of the constraints, such as e.g. environmental constraints, dimensional constraints etc.
2. *Synthesis and Analysis.* The synthesis scheme connecting possible systems elements is sometimes called the invention of the concept. This is the first step in the synthesis task. In *Synthesis* as many alternative designs are sought, usually without regards (at this stage) for their value and quality [1.13]. This is also referred to as ideation and invention step in which as many creative solutions as possible are generated. Here creativity plays an important role. In the next step, analysis must be performed to assess whether the system performance is satisfactory or better and, if satisfactory, just how well it will perform. This is an analysis task. System schemes that do not survive analysis are revised, improved, or discarded. Those with potential are optimized to determine the best performance of which the scheme is capable. Competing schemes are compared so that the path leading to the most competitive product can be chosen. Synthesis draws heavily on talent. In this iteration the specification set is formed.
3. *Detailed Design and Design Analysis.* The intent of the detailed design phase of the design process is to develop a set of drawings, and geometric models that completely describes the design [1.2]. The proposed design needs to be analyzed and here the analysis techniques come into picture. In the past a stress analysis of individual components was carried out by either using mechanics of materials principles or experimentation [1.3]. The former is inadequate for the analysis of complex shapes, since it is too lengthy and costly. Experimentation requires too much time to make prototype parts and then test them individually. If the part fails then it is redesigned, manufactured and tested again. Finite element analysis plays an important role in this phase. Virtual models can be immediately analyzed for stresses. The process helps in design perfection so that a part may not be rejected in further testing. After the part is designed, it can be analyzed so that its

acceptability in that application is determined. The process takes very little time as compared to experimentation and can be used to analyze more complex shapes. We will discuss the use of Finite Element Analysis (FEM) in section 1.5.

4. *Prototype Testing.* The prototype parts are made from the final design; they are assembled and tested for various loading conditions, including the durability test. The prototype is tested in actual conditions and its failure mode is predicted. Making the prototype part is the most time consuming part in the entire design process. But, with the advent of tools like Rapid Prototyping has helped the design engineers to make the prototype parts rapidly and try them for assembly. Rapid Prototyping will be more discussed in the section 1.7.
5. *Production and Marketing.* After the part has passed the testing phase, the production parts are manufactured. The role of the design engineer does not necessarily end after beginning of the production. This is the most important process in the whole design process as the product is being sold to the customer and the engineer is the one who approves the final design.

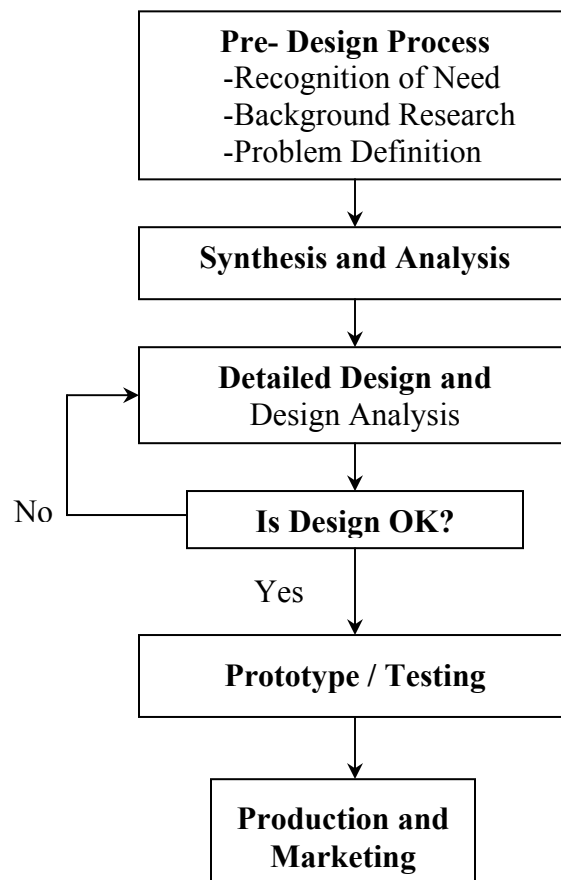


Figure 1.2 Design Process.

1.4 Computer-Aided Engineering and Finite Element Analysis

The computer has created a true revolution in engineering design and analysis. Problems whose solution methods have literally been known for centuries but that only a generation ago were practically unsolvable due to their high computational demands can now be solved in minutes on inexpensive microcomputers. One can no longer “do engineering” without using its latest and most powerful tool, the computer.

As the design progresses, the crude freehand sketches made at the earliest stages will be supplanted by formal drawings made either with conventional drafting equipment or as is increasingly common, with computer-aided design (CAD) and computer-aided drafting software. Present versions of CAD software packages allow (and sometimes require) that the geometry of the parts be encoded in a 3-D database as solid models. In the solid models the edges and the faces of the part are defined. From this 3-D information, the conventional 2-D orthographic views can be automatically generated if desired. Solid modeling systems usually provide an interface to one or more commercial Finite Element Analysis (FEA) programs and allows direct transfer of the model's geometry to the FEA package for stress, vibration, and heat transfer analyses.

The techniques referred above along with the CAD are a subset of the more general topic of Computer-Aided Engineering (CAE), which term implies that more than just the geometry of the parts is being dealt with [1.1]. However, the distinction between CAD and CAE continues to blur as more sophisticated software packages become available. In fact, the description of the use of solid modeling CAD system and an FEA package together is an example of CAE. When some analysis of forces, stresses, deflections, or other aspects of the physical behavior of the design is included, with or without the solid geometry aspects, the process is called CAE [1.1].

During the design process, the main concern of a design engineer is the stress analysis. Although Castigliano's method computes elastic deflections and forces for more difficult problems, the finite element method will solve problems when the component geometry and loading are complex and cannot be modeled accurately with standard strength of materials techniques. In these complex cases, the determination of stresses, strains, deformations, and loads favors the finite element method, an approach that has broad applicability to different types of analyses (deformations, stress, plasticity, stability, vibration, impact, fracture etc.), as well as to different classes of structures (shells, trusses, frames - and components - gears, bearings, and shafts, for example) [1.5].

In general, the finite element method is based on a theory whereby the body is viewed as an assembly of discrete building blocks. The application of the method involves dividing the body into an optimum number of blocks (elements) and using them as basis for computations; These blocks are considered severed from each other and joined only at specific points (nodes), forming a network. The number of elements is determined by two factors: the capabilities of the computer being used and the desired accuracy.

1.5 Overview of Traditional Finite Element Analysis

Traditionally, FEA is one of the most widely used engineering tools to determine deflection, stress and failure of mechanical parts under service loads. FEA can be thought of as an approximation technique for analyzing complex structures which, handled as a whole, would represent a mathematical model much too complicated to set up and solve. Instead, FEA uses a three-step approximation technique to tackle manageable pieces of the problem, and then combine the results into an overall solution. In the first step, called Pre-processing, a mathematical model is constructed by dividing the structure into elements connected at nodes to form mesh. Next, the solver performs the numerical analysis on a computer to determine the behavior of structure. This is referred as the Processing phase. In the last step, called Post-processing, the computer converts the analysis results from raw number into graphical form of display [1.7].

Earlier, FEA was used mainly a research tool, but was seldom used in daily engineering practice. It found acceptance primarily in the research center of large corporations, particularly in the aerospace industry. There, large, complex structures such as airplanes were analyzed to verify design performance [1.8].

In a workshop, a panel of leading users discussed the problem of computer-aided engineering (CAE) in the design cycle. Their consensus was that, due to time limitations, and lack of confidence in the results, FEA was not being used in the early stage of the design phase where it would be most beneficial. A similar situation exists in Japan: in a state-of-art report on Japanese Computer-Aided-Design (CAD) methodologies for mechanical products Whitney states, “Everyone I visit says it takes too long to prepare data for FEA. Even those who have ‘automatic meshers’ say so.”[1.9].

1.6 Current Status of FEA in Design Process

The design of machine part may be done in two different ways – either choosing a standard form and material that fits the requirements; or creating a new form, that is, planning the geometry and choosing the materials to fit the requirements. The first alternative is called the direct, or check problem, and the second alternative is called the inverse, or design problem. For simple parts, both check and design problems can be solved relatively easily using available strength formulas. With complex machine parts, seeking a solution is a more difficult process as the geometric variables become too numerous and stress computation becomes mathematically indeterminate. The design problem approach is therefore different from the direct problem [1.6].

Design is an iterative process of improvement. It starts with a certain assumption of the geometric form, dimensions, and materials. Through the computational process, arrives at a solution, finding the distribution and the magnitude of stresses, thus identifying the weakest spot for design changes. And then improves the assumption of form, dimensions and materials, and repeat the solution step-by-step until a satisfactory design is obtained. At times, the design may require several iterations involving geometry changes with repeated analyses. At other times, the first analysis is sufficient. Again, the

designer may use the same geometric form and simply revise the design by changing material [1.6].

As FEA began to enter in daily engineering activities, its scope was limited as far as the design is concerned. Analysis was done by the dedicated analyst with the knowledge and experience to properly apply the technology. Traditionally, engineers designs parts independently and then throw them “over the wall” to analyst, who assigns a priority to the project and then performs a stress analysis when they can. Engineers may provide CAD models from which analyst can build the FEA model. But in many cases, part geometry is conveyed as two-dimensional that must be interpreted and translated by the analyst. It may take days or even weeks before the analysis is completed [1.9].

In most organizations, this exchange is so inefficient that FEA typically is applied only in the final design phases. Often it happens that the part fails in the prototype-testing phase. The designer then redesigns the part and sends it back though testing analysis cycle. The design-test-redesign cycle adds considerable time and expense to the product development cycle.

1.7 Rapid Product Development Process

Three enabling technologies have emerged to provide the communication, visualization, and simulation capabilities required by Rapid Product Development (RPD). These technologies are 3D solid modeling, FEA, and rapid prototyping [1.14].

Solid models of the parts and assemblies, as discussed earlier, have allowed designers to quickly represent their ideas in an ambiguous manner (visualization and communication). Team members can qualify assembly techniques, manufacturability, and “look and feel” (simulation).

Rapid prototyping has bridged the virtual and physical worlds. The technology has progressed to the point where an engineer can literally make a “3-D print” of part in matter of hours. Engineering and marketing can test subtle variations of a concept and incorporate suggestions into prototypes in near “real time” (simulation). While the solid model can convey much data about a part using shaded, dynamic, on-screen manipulation, it is very difficult to pass a monitor and mouse around to meeting participants. In contrast, a physical part can answer many questions.

Although, the resultant deformations calculated by an analysis can often shed light on form and fit, FEA focuses on the function part of the form-fit-function equation. Understanding stress levels, deformation, temperatures, and response to vibration or fluid flow characteristics up-front in the design process is clearly the embodiment of simulation. Multiple design iterations on conceptual geometry can easily lead to a radical new design or a significant reduction in the number of prototypes. Today’s analysis tools also greatly enhance an engineer’s ability to visualize and communicate with rendered and animated color contour plots of parts under test.

Most engineers also have recognized the value of RPD and the importance of all the enabling technologies contributing to that process. However corporations have accepted these technologies to varying degrees. It is interesting to note that the acceptance of these technologies is not proportional to their maturity. The illustration in Figure 1.3 shows the relative age and acceptance level in product design of the core tools. Solid modeling tools were invented in mid 80s and it is used in 90% of the industries. Rapid prototyping concept was also invented in mid 80s and its use is 60%. But though invented in mid 60s and its use is in only 30 %.

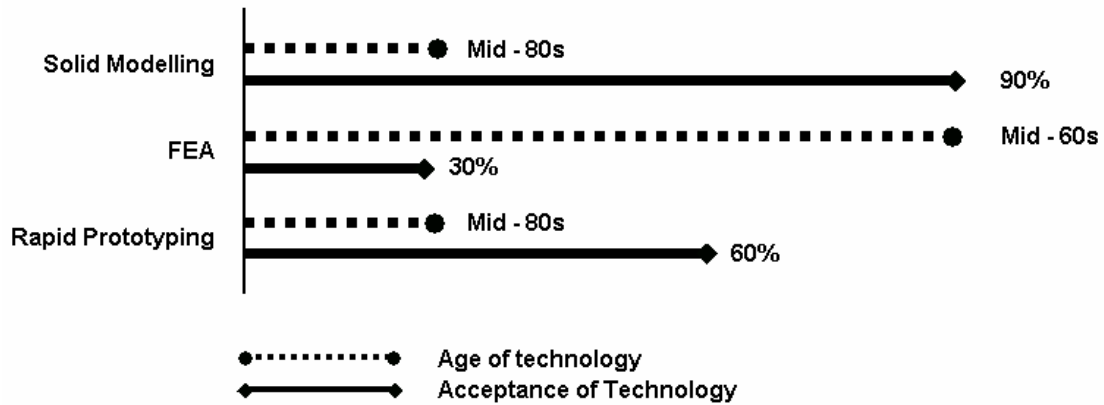


Figure 1.3 Relative acceptance and age of three enabling technologies [1.14].

The different level of acceptance of these tools sheds light on the reluctance of traditional design organizations to break away from familiar processes. Drawings and prototypes have been the mainstay of design groups throughout history while actual engineering has often been a small part of the overall process. In traditional product design process used at most companies, increasingly shorter time lines preclude lengthy engineering evaluations of the performance of chosen configurations. Even today, many engineering companies would prefer to take the chance that a “best guess” design will work, thereby risking possible redesign. This seems more attractive due to that instant gratification alluded to earlier than delaying the creation of initial prototypes through expanding early analysis in order to reduce testing and prototyping. Figure 1.4 depicts the traditional product design process used at most companies.

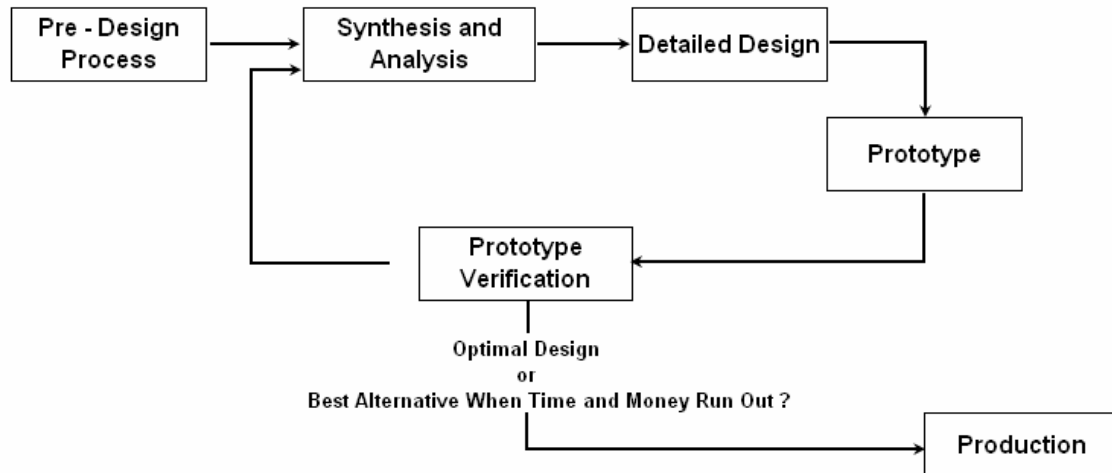


Figure 1.4 Traditional product development process [1.14].

Conceptual designs are rushed through the system. Here, the primary task of engineering is to develop layouts and drawings. When structural functionality is clearly an issue up-front, it may be addressed by calculations, analysis, or over-design during the drawing creation stage. The true performance of a part or system is typically not understood until the prototyping and testing phase. If no issue arises during these phases, the design is often deemed acceptable and considered finished. If time and budget permit, some degree of optimization is performed on a trial and error basis until schedule and costs dictate the end. If the part fails the testing phase, companies typically scramble to resolve the problem with as little change as possible. FEA is often brought in at this stage. However, the engineer's hands are somewhat tied by the design envelope dictated by other released and in-process components. True optimization is very difficult at this stage. And the changes required may not be the most cost effective due to these restrictions. Figure 1.5 indicates the relative cost and the difficulty in design changes at various stages of the design phases. The longer it takes to make these changes the more difficult it is to make modification and costs significantly increase [1.14].

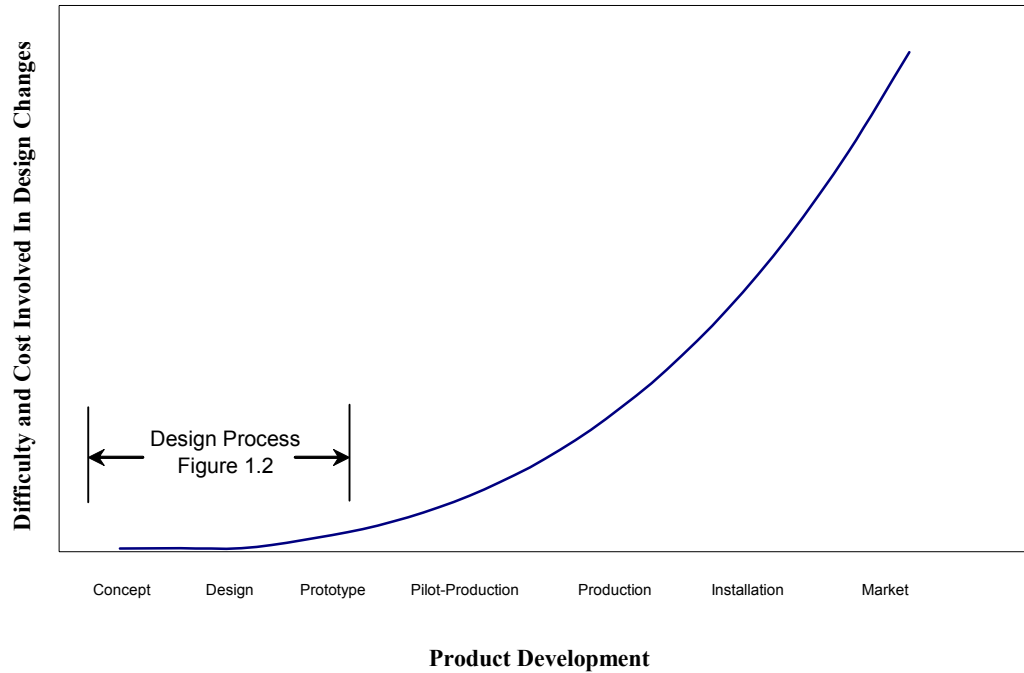


Figure 1.5 Difficulties and cost in design changes [1.11].

One of the reasons for the relative cost of change later in the process can be better understood by studying Figure 1.6, which indicates the disparity of a company's investment in a design compared to their level of understanding. The “build and break” cycle controls the area between the curves in Figure 1.6. The more cycles required, the greater the gap in knowledge versus cost. In fact, experienced manufacturers from different industries have shown that 90% of the project cost is determined at the initial stage of the design, where 10% of the total cost of the project is spent [1.1].

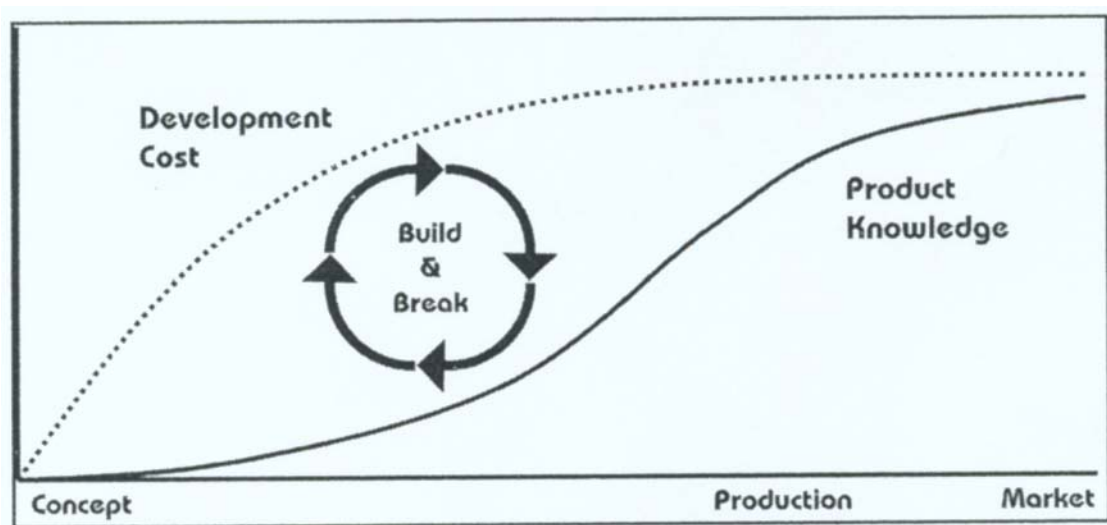


Figure 1.6 Cost spent versus product knowledge [1.14].

It should be clear that the value of the early analysis lies in the reduction of knowledge gap and in the potential for saving in later stages of the product development cycle. The next Figure (Figure 1.7) shows the ideal predictive engineering enabled design process where the test / redesign cycle is performed on software prototypes. Not only can planned testing then be done more quickly and with less cost, simulation can allow the engineer to explore design options or loading scenarios, which would be too costly to address in physical world. The revised design process results in rapid closure of the knowledge graph of the disparity between investment and understanding as shown in the Figure 1.8.

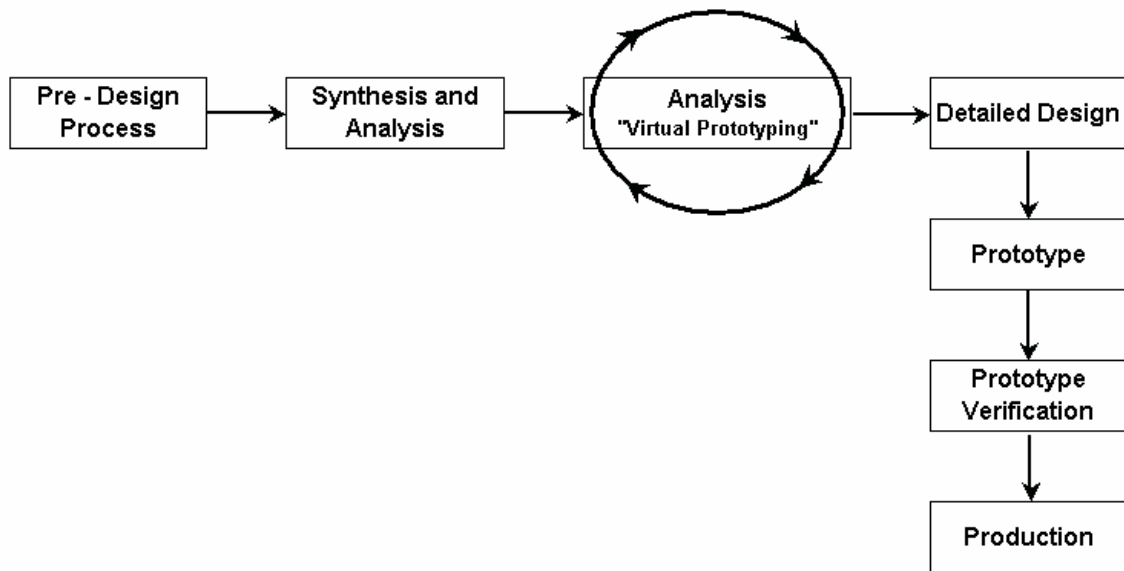


Figure 1.7 Product Development using early analysis [1.14].

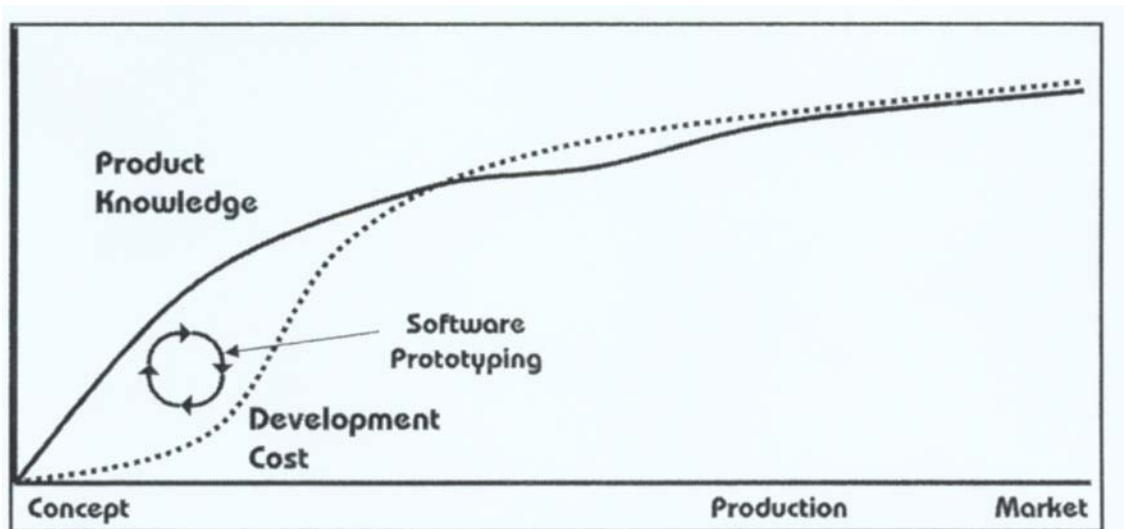


Figure 1.8 Improved Cost spent versus product knowledge with Early Analysis [1.14].

1.8 Early Analysis: The New Engineering Paradigm

Clearly, if analysis can be carried out earlier in the design process, the benefits will be significant, including shortened time to market, improved product design and reduced product development cost. The way to accomplish this is by re-orienting the process itself so that the analysis is performed much earlier in product development. This moves CAE forward into the conceptual phase. This step involves synthesis and analysis (Phase 2 in Figure 1.2), where changes are much easier and more economical to correct a poor design.

A major benefit of early analysis is the ability to perform a “what-if?” simulation. This helps the designer to consider and evaluate alternate approaches and to explore options in the early design cycle. Through this process, engineers and designers can quickly investigate many design variations and evaluate numerous ideas that would not be practical to test in hardware. Moreover, the computer analysis helps them find troubled spots that otherwise will be extremely difficult to isolate in the mess of complex interrelated variables. Also, “what-if?” studies can show engineer the effect of making a design modification to correct a problem in an isolated area, so that such changes do not adversely affect overall product performance [1.10].

Since more resources are focused in the initial design stages, costs during this phase will be higher than the traditional approach. Also design may take somewhat longer to release as concepts are being virtually proven upfront rather than later by repetitive and expensive testing. However this added time and cost is offset later through savings in prototype testing and fewer engineering changes.

In short, the use of analysis in the early design phases design phase supports the compression of the product develop cycle by changing the manner in which errors are found and the design is refined. Earlier without CAE, the design to get finalized it has to be gone through the repetitive stages of design, prototyping and testing. But now there is no need of this repetitive process when using CAE. This is summarized in Figure 1.9. In using analysis in early design phases, Computer Aided Design (CAD) and FEM are jointly conducted in the initial stages of the Product Development Cycle. As soon as a CAD model is configured, a preliminary FE analysis is run and the CAD model modified and reanalyzed until it performs optimally. Ideally, the resulting prototype design passes all qualifying tests the first time [1.10].

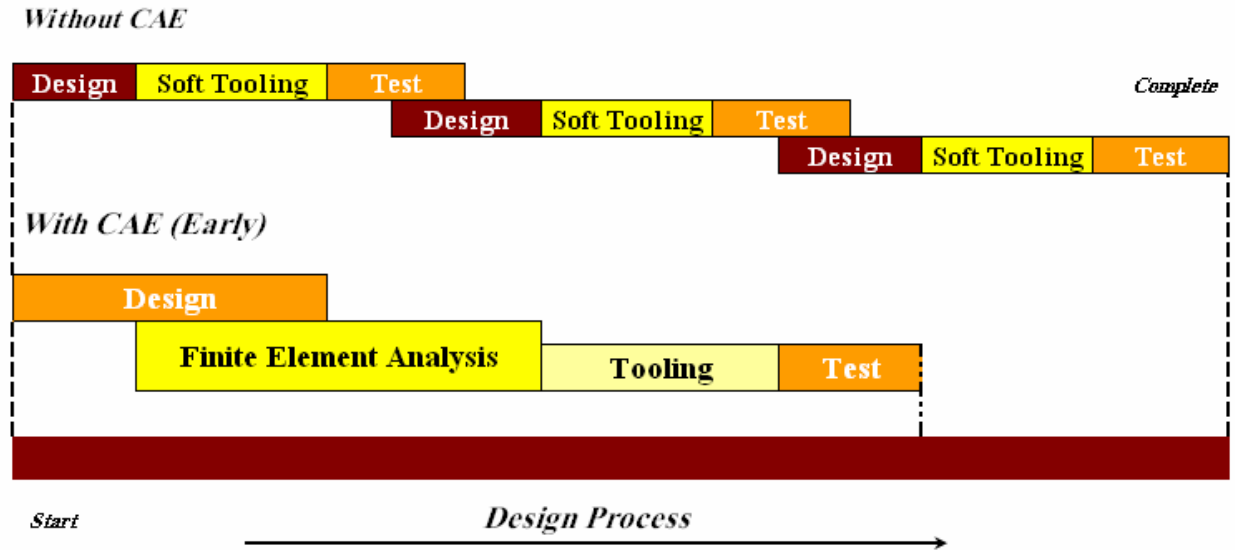


Figure 1.9 Product Development Cycle [1.10].

1.9 Goal and Objectives

The *goal* of this work is to develop a methodology to carry out finite element analysis in the early design stage to achieve the advantage of introducing early-analysis in the product development cycle. The approach is evolutionary in the sense that the design is evolving, being guided by the analyst and the analyst is responding at every stage during the evolution of the design. The four *objectives* of this work are as follows:

1. *Instantaneous Stress and Displacement Results.* This work will enable an engineer to obtain instantaneous stress and displacement information following a design change in a mechanical component. An engineer can first input an initial design of a component and then carry out a complete finite element analysis, i.e. pre-processing, processing and post-processing. If after post-processing it is felt that the stresses/displacements are too large, s/he can modify the component geometry graphically and the system will generate the results for the changed geometry based on the displacement results of the initial design (mesh). The work will allow an engineer to model a mechanical component using the commercial finite element code ANSYS 5.7, and will update the stress and displacement results with each geometric change. The process will continue until the engineer feels that the design is acceptable based on strength and stiffness requirements.
2. *Enhanced Computational Performance.* Various techniques were used to improve the computational performance; with the aim of producing results of acceptable accuracy in shorter period of time in order to emphasize the interactive nature of the design process. In this way a design may be optimized, though not in a mathematical sense. Instead, the optimization uses the experience of the engineer, who is very much aware of the possible effects of design changes on stress and displacement results.

Techniques of re-analysis for structural optimization will be used in this work. Significant research on re-analysis has been done from the early 60s until recently [1.15, 1.16].

3. *User Friendly*. The system will be developed using the commercial finite element code ANSYS 5.7. The reason why ANSYS is used is that its customizable features allow easy development of the system. Furthermore, the user-friendly features will help an engineer to carry out an analysis and reanalysis more easily.

This work is original and can be termed as evolutionary because it modifies the old trend and methodology of design process. Also the techniques used in this work to improve the computational effort such as, combined approximation reanalysis, were first developed only for structural optimization. During structural optimization the problem under consideration is repeatedly analyzed to assess changes in behavior due to geometric and structural modifications of the part. However, this method has never been applied to complex finite element types, though the concept is the same.

1.10 Significance of Work

The major beneficiaries of the work will be engineers working in product development and validation of components and structures, which are subjected to mechanical loads. It has long been accepted that the conceptual stage of mechanical product design development is of prime importance. It is at this stage that the fundamental geometry of a design is set, and as the evolution process continues it becomes significantly more expensive, more technically and organizationally challenging, to bring about a radical change to the design laid out at the conceptual stage. Conventional Finite Element software packages have also been found to have limited use to an engineer in the early design stage. The analysis model defined in a commercial software package is contrary to the idea process of conceptual design evolution since it forces the numerical model to be a detailed design. Furthermore, it is also well known that modifications to analysis models can become time-consuming even for simple geometric perturbations.

The scientific and technological relevance of this work applies not only to the early stage of design, but to a number of other applications areas in which benefits may accrue. A company may have needs for a rapid analysis and re-analysis tool to carry out fatigue assessment of components manufactured slightly out of tolerance. Typically this needs to be carried out under a very restrictive time scale. Furthermore, although the approach described here represents an engineer-driven optimization, it is clear that a rapid re-analysis solution would be valuable in a mathematical optimization procedure. Whether sensitivity information, hill climbing, or some more sophisticated scheme drives the optimization, it is clear that a stress analysis would often be performed on a model slightly perturbed from previous design iteration. Therefore, a solution of the type described in this work would have widespread relevance.

2. Structural Reanalysis

2.1 Design Optimization

The design process is divided in five distinct steps (shown in Figure 1.2) as discussed in the Section 1.3. The second step in the process is the Synthesis and Analysis. During the pre-design process within a selected concept there may be many possible designs that satisfy the functional requirements, and a “trial-and-error” procedure may be employed to choose the optimal design. Selection of best geometry or the cross-sections of the member are examples of the optimal design procedure. The procedure is referred to as the optimization process. Thus, optimization in the present context is an automated design procedure giving the optimal design values of certain design quantities, considering desired criteria and constraints.

2.2 Design Variables

A structural system can be described by a set of quantities, some of which are viewed as variables during the design optimization process. Those quantities defining a structural system that are fixed during the automated design are called pre-assigned parameters and they are not varied by the optimization algorithm. Those quantities that are not pre-assigned are called design variables. The pre-assigned parameters, together with the design variables, will completely describe a design. From a physical point of view, the design variables that are varied by the optimization procedure may represent the following structural properties [2.1]:

1. The mechanical and physical properties of the material.
2. The topography of the structure, i.e., the pattern of connection of the members or the number of the elements in the structure.
3. The configuration or the geometric layout of the structure.
4. The cross-sectional dimensions or member sizes.

Even though the properties described above are related to the Structural Optimization, they are more or less related to the properties in finite element analysis. In this work to be presented we will address the third property i.e. the geometric layout of the structure in context to finite element analysis. In structural system this property means the structural layout of the truss members to achieve certain support conditions. In finite element it means the nodal coordinates and element shapes.

2.3 Structural Reanalysis

Since design is an iterative process, the introduction of analysis in the design process, demands repetitive analysis of the design concepts. Typically a sequence of design and redesign is carried out until certain features such as weight, natural frequency, mode shape or stress magnitudes attain suitable values [2.2]. Therefore, the design optimization process becomes iterative and requires repeated analysis of structures obtained by progressive modification in design variable [2.3]. This operation, which

involves much computation effort, is one of the major obstacles when applying optimization methods to large systems. Because of the large number of analysis required, it is very important to develop efficient reanalysis techniques, especially for structures analyzed by finite element method, for only a small number of elements that are modified at each design step [2.4]. Reanalysis methods are intended to analyze efficiently modifications in a design using information from the previous design [2.3].

The definition of the structural static reanalysis is stated as follows: Find the response under the static load of a structure after modifications using the original response of the structure such that the computational time of reanalysis is less than the complete analysis time [2.4]. At the same time, reanalysis techniques allow one to efficiently compute the design sensitivity coefficients required for optimization methods. Reanalysis techniques are particularly important for large structures, especially in finite element analysis where only a small part of the structure / mesh is progressively modified. Such reanalysis techniques may be easily implemented in computer codes with minimal difficulty [2.6].

The finite element method in general requires the solution of the set of linear equilibrium equations,

$$F = K_0 u_0 \quad (2.1)$$

where, K_0 is the mesh stiffness matrix, u_0 is the column vector of unknown nodal displacements, and F is the column vector of externally applied loads. Consider a design problem in which the design variables represent only the geometry of the structure and the loadings are fixed. The elements of K_0 are the functions of the design variables, and the elements of F are assumed to be fixed.

This chapter deals with different types of reanalysis methods in which changes are made in the design variables. As a result, we have corresponding change in the stiffness matrix ΔK and in the displacement vector Δu . The objective is to find new displacement vector u .

$$u = u_0 + \Delta u$$

corresponding to new stiffness matrix K .

$$K = K_0 + \Delta K$$

One possibility is to analyze the new design by solving the new set of equations

$$F = Ku \quad (2.2)$$

this might be the best way in some cases where large modifications are made to a large part of the structure. However, in many cases when either a relatively small proportion of the structure is modified, or minor modifications are made to a large part of the structure, reanalysis methods might prove to be more efficient. Instead of performing a complete new analysis of the modified design by solving equations from a force-displacement relationship, it is often advantageous to use known values of u_0 from the previous analyses.

No single method of reanalysis is superior in all cases. To solve a particular problem, a method should be selected which is easy to apply and which requires a

relatively small computational effort. Furthermore, it might be sometimes more efficient to employ a combined technique which based on more than a single method.

Reanalysis techniques may be broadly classified as,

1. Direct (Exact)
2. Iterative
3. Approximate

These methods will now be discussed and are shown in Table 2.1.

Direct (Exact) methods are most efficient if the number of modified elements in the stiffness matrix is limited. This is the case, for example, if the coordinates of very small number of nodes are changed. The incremental stiffness matrix ΔK in this case could be compressed, by eliminating zero columns and rows, to form a reduced incremental matrix ΔK_R of size equal to the number of changed columns (or rows) in matrix K_0 . The relation between ΔK and ΔK_R is given by,

$$\Delta K = b^T \Delta K_R b$$

where b is a Boolean matrix with linearly independent rows, each of which contains all zeros except for one unit value, located at the column numbers where the change in K_0 occurs. For example, if ΔK is given by,

$$\Delta K = \begin{bmatrix} \Delta K_{11} & \Delta K_{12} & 0 & 0 & 0 \\ \Delta K_{21} & \Delta K_{22} & \Delta K_{23} & 0 & 0 \\ 0 & \Delta K_{32} & \Delta K_{33} & 0 & 0 \\ 0 & 0 & 0 & 0 & 0 \\ 0 & 0 & 0 & 0 & 0 \end{bmatrix}$$

we define matrix b by,

$$b = \begin{bmatrix} 1 & 0 & 0 & 0 & 0 \\ 0 & 1 & 0 & 0 & 0 \\ 0 & 0 & 1 & 0 & 0 \end{bmatrix}$$

and the reduced matrix, ΔK_R is,

$$\Delta K_R = \begin{bmatrix} \Delta K_{11} & \Delta K_{12} & 0 \\ \Delta K_{21} & \Delta K_{22} & \Delta K_{23} \\ 0 & \Delta K_{32} & \Delta K_{33} \end{bmatrix}$$

One direct method to reanalyze the structure is to compute the inverse of the modified stiffness matrix K^{-1} , using the known inverse of the original matrix. This algorithm is based on Sherman-Morrison identity [2.5] which can be written for the incremental matrix ΔK_R or, alternatively, for its single elements or columns. There are many Direct

Methods which can be used for reanalysis. Table 2.1 gives different types of the direct methods.

We can observe from the above illustration, Direct Method gives exact, closed-form solution that has the same effect of solving the modified system of equations from beginning without using any reanalysis technique. In general, direct methods are efficient if the number of modified elements is small, because for larger number of changes, the calculations become so high that solving the system with direct method becomes inefficient.

Iterative methods for reanalysis might be more suitable for minor modifications to a large part of a structure [2.1]. These methods apply successive correction to the initial solution and may converge to the most accurate solution for the modified structure. In these methods solution accuracy and rate of convergence are important. In iterative methods of reanalysis, the displacement vector u can be used as an initial solution for the iteration process [2.1]. One inherent drawback of these methods is that the entire process must be repeated for each loading condition. However, in view of the fact that stiffness matrices are banded and may possess a large number of zeros even within the band, an iterative scheme using only the nonzero elements of K and ΔK is advantageous from a storage point of view and may require less algebraic operations. One major difficulty which might be encountered during solution is concerned with convergence which is not always ensured, or might be slow. Computational effort and efficiency has to offset accuracy. These two factors can rarely be satisfied simultaneously, because to get near exact solution, the efficiency decreases and vice versa. Therefore some compromise must be made such that “run-time” is not excessive and that solution accuracy is sufficient [2.6].

For simple iteration techniques the force displacement relationship for the changed finite element model can be written as,

$$(K_0 + \Delta K)u = F \quad (2.2)$$

or

$$K_0 u^{(k)} = F - \Delta K u^{(k-1)} \quad (2.3)$$

where, $u^{(k)}$ is the value of u after the k^{th} iteration, and $u^{(0)}$ is the initial vector known from initial analysis.

$$u^{(0)} = u_0$$

Equation (2.3) represents simple iteration, similar to conventional matrix iterative methods for solving linear systems. For solving the equations, if Choleski decomposition is used, then only one triangularization of K_0 is needed for any specific modification. Successive cycles of iterations then require only forward and back substitution. Various iterative methods for reanalysis, such as, Jacobi, Gauss-Seidal etc. their efficiency and accuracy are listed in Table 2.1.

Approximate methods are generally sufficient to be employed for intermediate designs, which require less computational efforts. While approximate algorithms might be most efficient in many cases, the basic difficulty is usually associated with solution accuracy. Approximate methods are most efficient than direct (exact) methods, and are usually suitable for moderate changes in the whole structure. In general, the calculation efficiency and solution quality are conflicting factors that should be considered. Improved solution accuracy is often achieved at the expense of increased computational effort. Approximate methods can be divided into the following three classes (the details of which are given in Table 2.1):

- (a) *Global Approximations*. Global approximations are also called multipoint and are based on polynomial fitting or reduced basis methods [2.7-2.9]. These approximations are obtained by analyzing the structure at a number of design points, and they are valid for whole design space (or at least large portions of it). However, Global Approximations may require significant computational effort in problems with a large number of design modifications.
- (b) *Local Approximations*. Local approximations are also called single point approximations and are based on first order Taylor series expansion or binomial series expansion about a given design point. In other words Local approximations are based on information calculated at a single point. These methods are most efficient, but they are effective only in the case of small changes in design variables. For large changes in design, accuracy of approximations often deteriorates and they may become meaningless. That is, the approximations are valid only in vicinity of a design point. A possibility to improve the quality of the results is to consider second-order approximations [2.10], but this might increase considerably the computational effort.
- (c) *Combined Approximations (CA)*. Combined approximations attempts to give global qualities to local approximations. Similar to local approximations, the calculations are based on results of single exact analysis. Each subsequent reanalysis involves the solution of only a small system of equations. Thus, the computational effort is significantly reduced. Calculations of derivatives are not required, and the method can be used with general finite element program. Recently, it has been found that this method provides exact solution in certain cases [2.11 - 2.13]. This is reason why the method is used for this work.

The next section describes the Combined Approximation Method in-depth and shows the cost analysis of the method.

Table 2.1 Comparison of Static Reanalysis Techniques [2.6]

Method	Technique		References	Efficiency	Accuracy
Direct	Parallel Element Technique		[2.73, 2.74]	<ul style="list-style-type: none"> Very Efficient for a large number of modifications. More Efficient than Initial Strain. 	<ul style="list-style-type: none"> Accuracy is not affected by the magnitude of modifications.
	Initial Strain/Stress		[2.20, 2.22]	<ul style="list-style-type: none"> Found Inefficient when compared with the fresh analysis [2.86, 2.87]. 	<ul style="list-style-type: none"> Good.
	Modified Decomposed Matrices	Mathematical Approach	[2.24,2.33,2.35, 2.36,2.83]	<ul style="list-style-type: none"> Efficient only when the number of modifications is at minimum level. 	<ul style="list-style-type: none"> Good.
		Structural Analysis	[2.32,2.50,2.53, 2.54,2.71, 2.84]		
	Modified Inverse of Matrices	Mathematical Approach	[2.37,2.39,2.40, 2.41,2.21,2.52, 2.55,2.85]	<ul style="list-style-type: none"> Found to be efficient in comparison with Gauss Elimination when the modifications were are small. But overall found to be expensive in comparison with the other methods. 	<ul style="list-style-type: none"> Good.
		Modified Inverse of [K]	[2.46,2.47,2.65, 2.72]		
	Modified Displacement Vector		[2.21,2.23,2.46,2.47,2.79-2.82]	<ul style="list-style-type: none"> More efficient than the Modified Inverse method. Expensive in comparison with the complete reanalysis except for small modifications. 	<ul style="list-style-type: none"> Good.
	Superposition Technique	Linear Combination	[2.60-2.64]	<ul style="list-style-type: none"> Inefficient than the method of complete reanalysis. 	<ul style="list-style-type: none"> Good.
		Direct Superposition, Theorems of Structural and Geometric Variation	[2.29,2.56-2.59, 2.77,2.78]		

Method	Technique		References	Efficiency	Accuracy
Iterative	Simple Iterations		[2.25,2.30]	<ul style="list-style-type: none">Efficient when the modifications are kept to 10 %.Convergence is rapid for small changes.	<ul style="list-style-type: none">Error increase with more number of changes.
	Jacobi and Gauss Seidal Iteration		[2.48,2.70]	<ul style="list-style-type: none">Efficiency depends on the type and number of changes.Acceleration techniques can be easily implemented to improve efficiency.	<ul style="list-style-type: none">Depends on the nature of the problem.
	Combined Series-Iterative Technique		[2.49,2.66,2.68]	<ul style="list-style-type: none">For changes less than 20%, has same efficiency as modified reduced basis method.	<ul style="list-style-type: none">For changes less than 20%, gives same accuracy as modified reduced basis method.
Approximate	Series Expansion Techniques	Modified Inverse Matrices		[2.27,2.38,2.51] <ul style="list-style-type: none">Converges after first iteration when changes in the stiffness are less than 35%.For large changes it converges after four iterations. But, it is inefficient in working with inverses.	<ul style="list-style-type: none">Good.
		Modified Displacement	Power Series	[2.65] <ul style="list-style-type: none">Unsuitable even for small number of changes.	<ul style="list-style-type: none">Unsuitable even for small number of changes.
			Taylor Series	[2.26,2.43,2.44, 2.45,2.68,2.69, 2.75,2.76] <ul style="list-style-type: none">Even though the Second -Order Taylor expansion was more accurate but at the expense of more computational and storage requirements.	<ul style="list-style-type: none">Inaccurate after the one iteration for changes in stiffness matrix more than 20%. The error can in reduced after first iteration.Second-order Taylor expansion was the more accurate technique.
	Reduced Basis Techniques		[2.31,2.34,2.42, 2.60-2.64] <ul style="list-style-type: none">Found to be efficient compared with computational effort for a new analysis	<ul style="list-style-type: none">Performs best for global changes rather than local ones.	
	Modified Reduced Basis Techniques		[2.67-2.69] <ul style="list-style-type: none">Offers the highest potential in terms of accuracy and efficiency.	<ul style="list-style-type: none">Higher Accuracy	
	Combined Approximation Method		[2.11, 2.12, 2.14, 2.17] <ul style="list-style-type: none">Calculation of Derivative is not required. Computational effort is considerably reduced	<ul style="list-style-type: none">Very good. Recently, it has been found that the method provided exact solution in certain cases.	

2.4 Combined Approximations (CA) Method and its Cost Analysis

We have seen in the previous section that, for the Combined Approximation method the calculations that are based on results of a single exact analysis. Because of reduced computation effort, the method can be applied to a general finite element program. Several studies in early eighties have shown [2.14] that combined approximations can be introduced by scaling the initial stiffness matrix such that the changes related to the scaled design are reduced. The advantage of this approach is that the solution is based on results of a single exact analysis. It has been demonstrated that the scaling procedure is useful for various types of design variables and behavior functions. Several criteria for selecting the scaling multiplier have been proposed, based on geometrical and mathematical considerations [2.13]. In early nineties, it has been found [2.15, 2.16] that scaling both the designs and the modified approximate displacements can be expressed in reduced basis form. Extending the concept of scaling to include also the approximate displacements significantly improved the results. It has been shown also that high quality approximations can be achieved for very large changes in the design variables by considering only two basis vectors.

2.4.1 Problem Formulation

The reanalysis problem considered for this study can be stated as follows [2.14]:

- a) We start with given initial design. For FEA we construct a mesh and find corresponding square stiffness matrix K_0 , and the column vector for nodal forces F , the corresponding displacement column vector u_0 are computed by solving the force-displacement relationship of the mesh:

$$F = K_0 u_0 \quad (2.4)$$

It is assumed the mesh stiffness matrix K_0 is given from the initial analysis in the decomposed form:

$$K_0 = U_0^T U_0 \quad (2.5)$$

where U_0 is upper triangular matrix.

- b) Assume changes in the geometry (coordinates of nodes) so that the modified square stiffness matrix K is given by

$$K = K_0 + \Delta K \quad (2.6)$$

where ΔK is the change in the stiffness, due to changes in the geometry.

- c) The goal is to find efficient and accurate approximations of the modified displacements u due to various changes in the geometry, without solving the complete set of modified analysis equations.

$$Ku = (K_0 + \Delta K)u = F \quad (2.7)$$

Once the displacements u are evaluated, the explicit stress-displacement relations can be used to determine the stresses. Thus, the presented approximations of u are intended only to replace the set of implicit analysis Equation (2.7).

The above formulation is general and can be applied to different types of design variables and structures. For illustrative purposes, discrete structures are considered in this study, but the approach presented is suitable for the shape changes in continuum structures.

2.4.2 Combined Approximation Reanalysis

In Combined Approximation Reanalysis (CA), the computed terms of the binomial series expansion are used as high quality basis vectors in reduced basis approximations. The unknown coefficients of the reduced basis expression are determined by solving a reduced set of analysis equations. For completeness of presentation, evaluation of the displacements by the combined approximation method is briefly described in this section.

Given the initial stiffness matrix K_0 in the decomposed form of Equation (2.5), the initial loads F_0 and the initial displacements u_0 , calculation of the modified displacements u for any assumed changes ΔK , ΔF , in the stiffness matrix and in the load vector, respectively involves the following steps:

- a) The modified stiffness matrix K and the modified load vector F are first introduced. Since K_0 and F_0 are given, this step involves only introduction of ΔK and ΔF .
- b) The basis vector u_i is calculated. Define square matrix B as

$$B = K_0^{-1} \Delta K \quad (2.8)$$

Pre-multiplying Equation (2.7) by K_0^{-1} , substituting Equations (2.4) and (2.8) and pre-multiplying the resulting equation by $(I + B)^{-1}$, yields the following expression for the displacements:

$$u = (I + B)^{-1} u_0 \quad (2.9)$$

For small changes in ΔK , this expression can be approximated by the binomial series,

$$u = (I - B + B^2 - \dots + B^{s-1})u_0 \quad (2.10)$$

Equation (2.10) in the series of basis vectors, defined as

$$u_1 = K_0^{-1}F \quad (2.11)$$

$$u_i = -Bu_{i-1} \quad i = 2, \dots, s \quad (2.12)$$

where s is the number of vectors considered (it is assumed that $s \ll$ number of degrees of freedom), the matrix of the basis vectors u_B is defined by

$$u_B = [u_1 \quad u_2 \quad \dots \quad u_s] \quad (2.13)$$

In the case where $\Delta F = 0$, the first basis vector is simply $u_1 = u_0$. Calculation of the basis vectors by Equation (2.12) involves only forward and backward substitutions in cases where K_0 is available in the form of Equation (2.5) from the initial analysis of the structure. For example, assuming that u_1 is given, the column vector u_2 is calculated by

$$K_0 u_2 = -\Delta K u_1 \quad (2.14)$$

We solve first for the vector of unknowns t by the forward substitution

$$U_0^T t = -\Delta K u_1 \quad (2.15)$$

The vector u_2 is then calculated by the backward substitution

$$U_0 u_2 = t \quad (2.16)$$

Similarly, u_3 is calculated by

$$K_0 u_3 = -\Delta K u_2 \quad (2.17)$$

- c) The reduced square matrix K_R and the reduced column vector F_R , are calculated by

$$K_R = u_B^T K u_B \quad F_R = u_B^T F \quad (2.18)$$

- d) The column vector of unknown coefficients y is calculated by solving the set of $(s \times s)$ equations [2.17],

$$K_R y = F_R \quad (2.19)$$

e) The modified displacements u are evaluated by

$$u = y_1 \cdot u_1 + y_2 \cdot u_2 + \dots + y_s \cdot u_s = y \cdot u_B \quad (2.20)$$

The flowchart in Figure 2.1 outlines this entire process of the combined approximation reanalysis. Table 2.2 shows the cost analysis of the algorithm used.

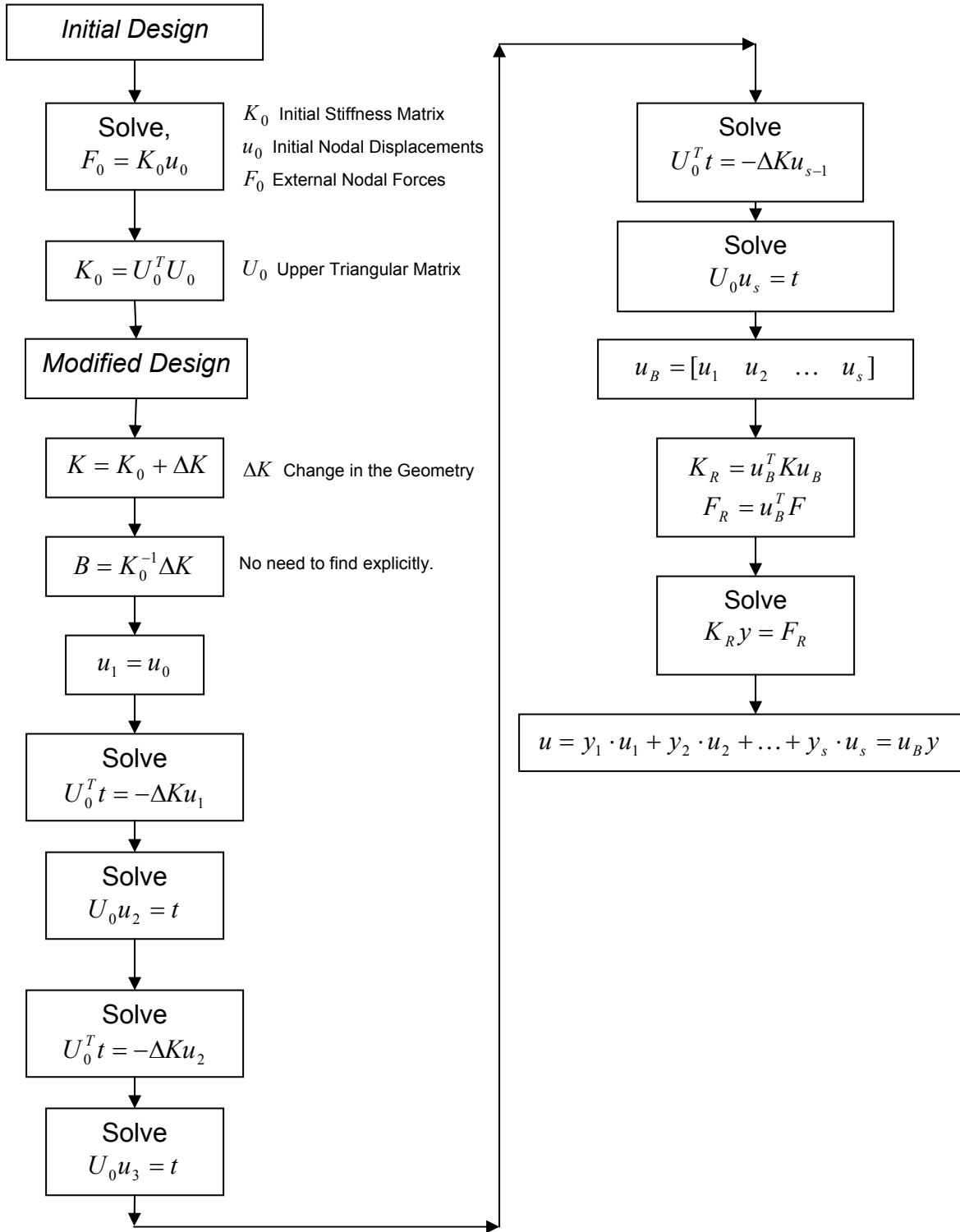


Figure 2.1 Combined Approximation Reanalysis Flowchart

Table 2.2 Combined Approximation Cost Analysis

Step No.	Operation	Approximate Multiplications	Comments
<i>Initial Design</i>			
1	Solve $F = K_0 u_0$	$\left(\frac{n^3}{6} + n^2\right)$ [2.18]	Solution based on Cholesky decomposition.
<i>Modified Design</i>			
2	Find $\Delta K = K_0 - K$	n (subtractions)	
3	$u_1 = u_0$	-	
4	$-\Delta K u_1$	m^3	m is the number of rows changed in K_0 because of change in geometry.
5	Solve $U_0^T t = -\Delta K u_1$	n^2	Forward Substitution.
6	Solve $U_0 u_2 = t$	n^2	Backward Substitution.
7	$-\Delta K u_2$	m^3	
8	Solve $U_0^T t = -\Delta K u_2$	n^2	Forward Substitution.
9	Solve $U_0 u_3 = t$	n^2	Backward Substitution.
\vdots	\vdots	\vdots	Continue till finding u_s .
10	$u_B = [u_1 \quad u_2 \quad \dots \quad u_s]$	-	$n \times s$ matrix (only m non-zero terms)
11	$u_B^T K$	sm^2	$(s \times n)(n \times n)$
12	$(u_B^T K) u_B = K_R$	$s^2 m$	$(s \times n)(n \times s) = (s \times s)$
13	$F_R = u_B^T F$	sm	$(s \times 1) = (s \times n)(n \times 1)$
14	Solve $K_R y = F_R$	$\frac{s^3}{3} + s^2$	Based on Gauss elimination with partial pivoting.
15	$u = u_B y$	sn	

Note: Assume the stiffness matrix K_0 contains $n \times n$ terms. For the changed geometry, only $m \times m$ elements in the stiffness matrix K_0 out of $n \times n$ are changed. Generally for good accuracy, $s = 3$ so 3×3 matrix has to be solved [2.19].

2.5 Comments on Combined Approximation in Finite Element Analysis

The Combined Approximation procedure discussed in Section 2.4 is used in this work for analyzing a plane stress problem using four-node quadrilateral elements. Kirsch [2.3,2.11,2.12,2.14,2.17] introduced the Combined Approximation method by coupling

the accuracy of Global Approximation (GA) with the efficiency of Single Point Approximations (SA). This has been mainly used in the past for structural optimization. Very few research efforts have been carried out using CA with more complex element types other than the truss and beam. Gullickson and Averill [2.19] used the CA method to show its use with general finite element procedures. The accuracy and efficiency of CA was demonstrated with a one-dimensional bar element for stress analysis and the two-dimensional four-node quadrilateral element for heat transfer. The authors found that as the number of basis vectors (shown as 's' in Table 2.2) is increased; the CA reanalysis method results converge quickly to the reference solution for all problems tested. The relative number of basis vectors necessary for an accurate approximation decreases as the number of degrees of freedom in the problem increases.

3. ANSYS Interface and Supporting Routine

3.1 Introduction

The previous chapter discussed the combined approximations (CA) method that is used for reanalysis. In this work CA was integrated into the commercial finite element code ANSYS 5.7. A mechanical component can be developed by creating the two-dimension model in ANSYS using four-node quadrilateral elements. The analysis problem is then solved using the ANSYS solver. If the engineer decides that the stress and displacement results are not acceptable, then ANSYS can be used to change the geometry of the component. The modified problem is solved using the combined approximation reanalysis method in this work.

ANSYS was used in this work due to its open architecture since routines and subroutines can be written in C or FORTRAN and either linked to ANSYS or used with external commands. In fact, some of the ANSYS features seen today as “standard” offerings originated as *user programmable features (UPFs)*. The user programmable feature is an ANSYS capability where one can write his/her own routines. Even a design optimization algorithm can be written that calls the entire ANSYS program as a subroutine. UPFs provide the following capabilities [3.1]:

- To read or retrieve information from the ANSYS database. One can create subroutines and either links them to the ANSYS program or use them as external command features.
- ANSYS provides a set of routines that can be used to specify loading types that include body forces, pressures, etc.

In this work the finite element problem is solved using reanalysis methods, the user programmable features and other ANSYS features. UPFs are mainly used to read files generated by ANSYS, details of which are discussed later in this chapter. Although, UPFs allows programming in C and FORTRAN, FORTRAN is used. FORTRAN can interact with ANSYS directly as ANSYS itself uses FORTRAN to solve finite element problem. Many readymade FORTRAN subroutines are provided by ANSYS to obtain information from the database. Using C requires a converter to access those subroutines as functions in C.

3.2 ANSYS Interface

ANSYS 5.7 is used to develop the platform for solving the reanalysis problem. Before discussing details of the development platform, some ANSYS basics and its GUI will be first discussed.

3.2.1 ANSYS Program Organization

Before introducing the Graphical User Interface (GUI), some basic concepts of ANSYS program will be discussed. The ANSYS program is organized into two levels:

1) the *BEGIN Level* and (2) the *PROCESSOR Level*. Upon first entering the program, the user starts in the BEGIN level and can then enter the ANSYS processors shown in Figure 3.1.

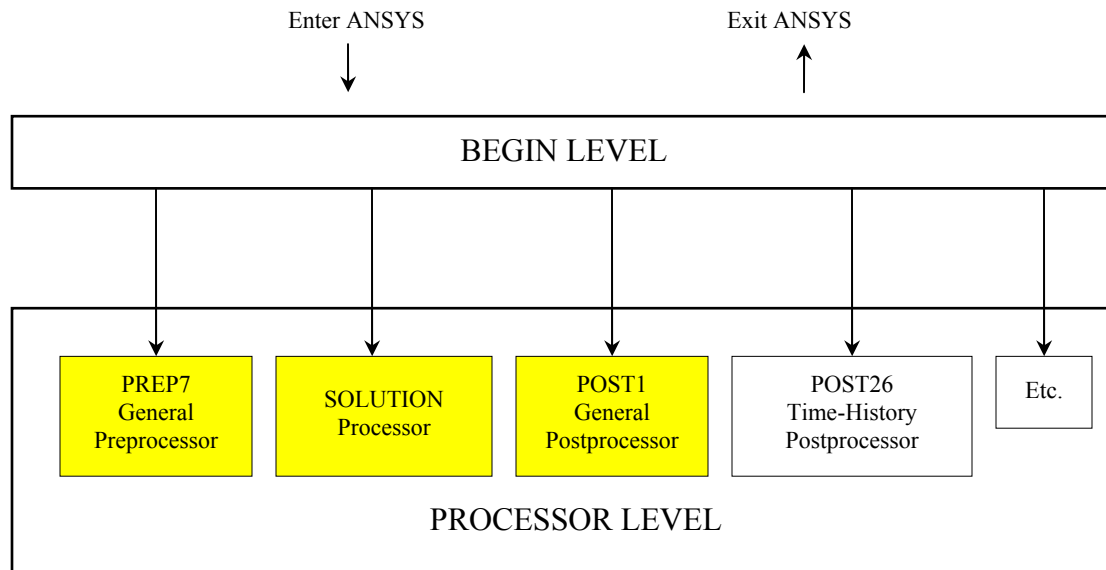


Figure 3.1 Organization of ANSYS 5.7 [3.2].

One may have more or fewer processors available than those shown in Figure 3.1. The actual processors available depend on the particular ANSYS product you have. The Begin level acts as a gateway into and out of ANSYS. It is also used to access certain global program controls. At the PROCESSOR level, several routines (processors) are available; each accomplishes a specific task. Most analyses will be done at the PROCESSOR level. A typical analysis in ANSYS involves the following three steps [3.2]:

1. *Preprocessing*. The PREP7 processor is where the user defines geometric, materials, and element types to ANSYS.
2. *Solution*. The SOLUTION processor is used to define the analysis type, set boundary conditions, apply loads, and initiate the finite element solution.
3. *Postprocessing*. POST1 (for static or steady-state problems) or POST26 (for transient problems), can be used to review the analysis results in the graphical user interface and tabular listings.

Only PREP7, SOLUTION and POST1 processors will be used in this work since static stress analysis considered. These processors are denoted by the shaded boxes in Figure 3.1. The next section presents a brief overview of the Graphical User Interface.

3.2.2 Graphical User Interface

The simplest way to communicate with ANSYS is by using the ANSYS menu system, called the Graphical User Interface (GUI). The GUI provides an interface

between the user and ANSYS. The program is internally driven by ANSYS commands. However, by using the GUI, an analysis with little or no knowledge of ANSYS commands can be performed. This process works because each GUI function ultimately produces one or more ANSYS commands that are automatically executed by the program.

The ANSYS GUI consists of the following six main regions [3.3] as shown in Figure 3.2:

- A** *Utility Menu.* This menu contains utility functions that are available throughout the ANSYS session, such as file controls, selecting and graphic controls. One can exit ANSYS through this menu.
- B** *Main Menu.* This menu contains the primary ANSYS functions organized by processors. These functions include preprocessor, solution, general postprocessor, design optimizer, etc.

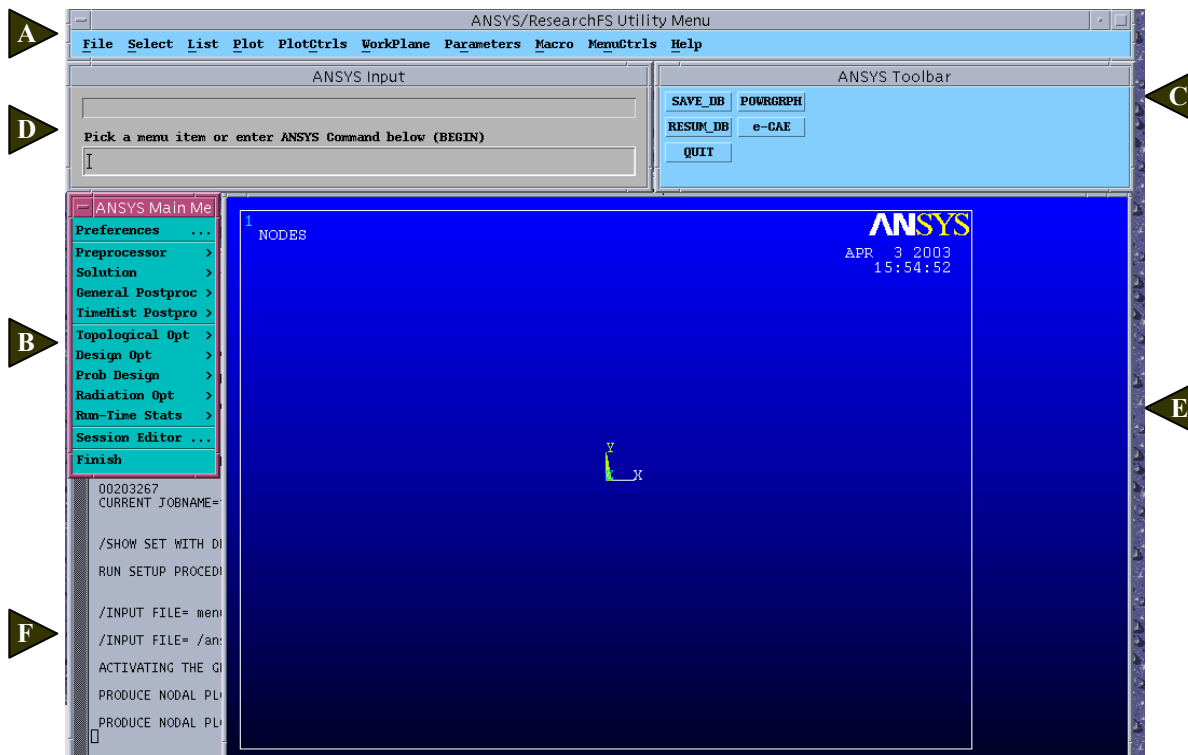


Figure 3.2 Regions of the ANSYS 5.7 Graphical User Interface

- C** *Toolbar.* The toolbar contains push buttons that execute commonly used ANSYS commands and functions. The user can add his/her own pushbuttons by defining abbreviations.
- D** *Input Window.* The input window displays program prompt messages and allows one to type in commands directly. All previously typed-in commands also appear in this window for easy reference and access.
- E** *Graphics Window.* The graphic window is where graphics displays are drawn.
- F** *Output Window.* This window receives text output from the program. It is usually positioned behind the other windows.

The User Interface Design Language (UIDL) can be used to modify the Main Menu. Furthermore, user specific Menu Items can be added by using the UIDL. UIDL and how it was used in this work will be discussed later in Appendix D. Furthermore, ANSYS customization features allow changing the Toolbar as per the user's requirements.

3.2.3 ANSYS Database and Files

The previous section explained how ANSYS is organized. This section discusses the ANSYS database and how ANSYS reads and writes various file types during a typical analysis. The information the user inputs when modeling a problem, e.g., element type, material property, dimensions, geometry, etc. is stored as *input data*. During the solution phase ANSYS computes various results, such as displacements, stresses, etc. and this information is stored as *results data*. The input data and results data are stored in the ANSYS database. The database can be accessed from anywhere in the ANSYS program. The database resides in memory (RAM of the computer) until the user saves the database to a database file *Jobname.DB*, where *Jobname* is the file name.

The input and output files that ANSYS reads and writes, respectively, are of the form *Jobname.Ext*, where the default jobname is *file*. Files used in this work include the following [3.5]:

- *Log File (Jobname.LOG).* This file is opened when ANSYS is first entered. Every command issued in ANSYS is copied to a log file. This is very helpful when creating the APDL code for processes which need to be repeated.
- *Database File (Jobname.DB).* This file is one of the most important ANSYS files because it contains all input data and some results. This is a file where the ANSYS analysis model is stored.
- *Output File (Jobname.OUT).* This file is opened when the user first enters ANSYS. This file saves responses given by ANSYS to every command executed by the user. It also records warning and error messages and some results.

- *Structural Analysis Results File (Jobname.RST)*. This file gets created when the finite element solution is determined. This file is created after the Solution stage (Section 3.2.1). This file stores the results of the finite element solution, e.g., displacement, stresses and geometry data. This file, its structure and procedure to read it are discussed in-depth in Appendix A.

3.2.4 ANSYS Parametric Design Language

APDL stands for ANSYS Parametric Design Language, and is a scripting language that can be used to automate common tasks or even build a model in terms of parameters (variables) [3.4]. Parameters are APDL variables and they are more similar to FORTRAN variables than to FORTRAN parameters. You don't need to explicitly declare the parameter type. All numerical values whether integer or real, are stored as double precision values. ANSYS uses two types of parameters: scalar and array.

APDL also encompasses a wide range of other features such as repeating a command, macros, if-then-else branching, do-loops, and scalar, vector and matrix operations. While APDL is the foundation for sophisticated features such as design optimization and adaptive meshing, it also offers many conveniences that can be used in common analysis problems. The applications of APDL are limited only by the user's imagination.

A macro is defined as a series of the APDL commands. Users can record a frequently used sequence of ANSYS commands in a macro file (this is sometimes referred to as command files). Creating macro enables the user, in effect, to create his/her own custom ANSYS command. For example, calculating power loss due to eddy currents in a magnetic analysis would require a series of ANSYS commands in the postprocessor. By recording this set of commands in a macro, a user can have a new, single command that executes all the commands required for that calculation. Furthermore, to executing a series of ANSYS commands, a macro can call GUI functions or pass values into arguments. Macros can also be nested, i.e., one macro can call a second macro; the second macro can call the third, and so on. A macro can be created either in ANSYS or using a text editor, e.g. emacs, vi, or wordpad.

3.3 Development Platform

APDL and macros along with the output files generated by ANSYS will be used in the work for solving a reanalysis problem. The five basic steps used to solve the problem are as follows:

1. *Initial Design*
2. *Analysis and Post-processing*
3. *Re-modeling*
4. *Reanalysis*
5. *Repeated Analysis*

3.3.1 Initial Design

During the design process, the designer comes up with some fundamental geometric changes in the component to satisfy design requirements. As discussed in the previous chapter, the methodology generated in ANSYS will allow a designer to check the feasibility of his/her design concept in terms of allowable displacements and stresses. The problem in this work will be limited to two-dimensions in ANSYS.

The *element type* must be defined before starting the analysis problem in ANSYS. The ANSYS element library contains more than 150 different types. Each element type has a unique number and a prefix that identifies the element category. The element type determines, among other things [3.6]:

- The degree-of-freedom set (which in turn implies the discipline – structural, thermal, magnetic, electric, quadrilateral, brick, etc.)
- Whether the element lies in two-dimensional or three-dimensional space.

The plane stress/strain four node quadrilateral elements will be used as discussed in previous sections. This element type is referred as PLANE42 in the ANSYS material type library. PLANE42 is used for 2-D modeling of solid structures. The element is defined by four nodes having two degrees of freedom at each node: translations in the cartesian X and Y directions. The geometry, node locations, and the coordinate system for this element are shown in Figure 3.3.

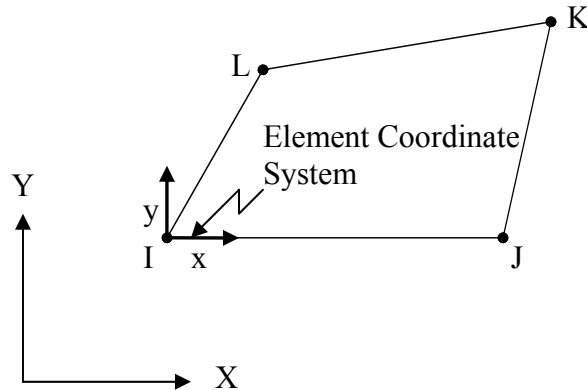


Figure 3.3 ANSYS PLANE42 Element Type

The element input data includes four nodes, a thickness (for the plane stress option only) and orthotropic material properties. Orthotropic material directions correspond to the element coordinate system. The element type is defined using the command [3.6, 3.7].

ET, ITYPE, Ename, KOP1, KOP2, KOP3, KOP4, KOP5, KOP6, INOPR

where, ET is the command which defines element type, ITYPE is arbitrary element type number and it starts with 1, Ename - actual element type given in element library, e.g., PLANE42, and *KOPn* are element option keys. These keys (referred to as KEYOPT (*n*)) are used to turn on certain options for this element. This is used to change many options for the element type. Only the following options will be considered:

KEYOPT (2)

1 -- Suppress extra displacement shapes.

KEYOPT (3)

0 -- Plain stress.

2 -- Plain strain (Z strain = 0.0).

3 -- Plain stress with thickness input.

The next step is to define *real constants* are properties of the element type and depend on the element type and option key selected. If the option key for the PLANE42 is set to a Plain Stress with thickness input, then real constant asks for the element thickness. Also *material properties* for the element type needs to be defined and include Young's Modulus and Poisson's ratio. All element type and material property definition are written in a form of an APDL code. In this code the program will select the element type as PLAN42 with the above required option keys. Then it will ask the user to enter the element thickness and other material properties.

3.3.2 Analysis and Post-processing

The designer will then mesh the model using the finite element mesher in ANSYS 5.7 and solve the two-dimension problem using the ANSYS solver. ANSYS generates the displacement and stress results for the solved analysis problem. The next step, post-processing, involves analyzing the displacement and stress results generated by ANSYS for known acceptability.

3.3.3 Re-modeling

If the stresses (or displacements) are not acceptable the designer can make changes to the mesh boundary geometry. In this work APDL is used which allows the user to make changes in the mesh geometry interactively on the screen. The user can select nodes graphically and change the nodal location. A loop is created so that user can change the node coordinates until the desired geometry is achieved. The changed geometric data is stored in a separate file using APDL.

3.3.4 Reanalysis

After the mesh geometry is changed, instead of using the ANSYS solver, the user can use the reanalysis approach developed in this work. Section 2.4.2 and Appendix C demonstrated that the combined approximation reanalysis approach is more cost effective compared with solving the problem again. In absence of reanalysis, the designer would

have to remodel the whole problem, mesh it and then solve the problem again. This is very time consuming whereas, the reanalysis approach will yield very accurate results in a shorter period of time. At this stage of reanalysis the displacement results generated by the analysis of initial design mesh will be used. The solution files generated by ANSYS (discussed in Section 3.2.2) for the initial design will be used.

The important thing in combined reanalysis is to determine the change in the mesh stiffness matrix due to the change in nodal locations. The changes in mesh stiffness matrix ΔK is defined (Equation 2.6 in Chapter 2) as,

$$\Delta K = K - K_0 \quad (3.1)$$

where K_0 is the stiffness matrix for the initial mesh (design) and K is the stiffness matrix for the modified mesh (design). Now to find ΔK by Equation 3.1, the modified stiffness matrix K must be found. But finding the stiffness matrix K will require determining the element stiffness matrix of all the elements and then adding them to obtain the global stiffness matrix. This is not different than creating and solving another analysis problem, and we don't want to do that. Furthermore the problem types we are dealing with, the changes in geometry are relatively in small area.. This means not all nodes are undergoing changes in coordinates. And subsequently few elements and their corresponding element stiffness matrices undergoing change. Therefore, the modified stiffness matrix does not have to be calculated explicitly. Using this idea a methodology was developed to find out the change in the global stiffness matrix.

Consider a finite element four node quadrilateral mesh for the initial design as shown in Figure 3.4(a). The numbers in the figure shows the node numbers and the circled numbers denote element numbers. Consider a mesh consisting of 9 quadrilateral elements shown in Figure 3.4. The global stiffness matrix for the original design can be constructed by adding the element stiffness matrices. If $K_{e_0}^1, K_{e_0}^2, K_{e_0}^3, \dots, K_{e_0}^9$ represents the element stiffness matrices for the original design corresponding to the elements 1, 2, 3, ..., 9 respectively, where the matrix elements in the element stiffness matrix are arranged according to their positions in the global stiffness matrix. The global stiffness matrix is obtained by adding the element stiffness matrices in accordance to the direct assembly procedure as follows,

$$K_0 = K_{e_0}^1 + K_{e_0}^2 + K_{e_0}^3 + \dots + K_{e_0}^9$$

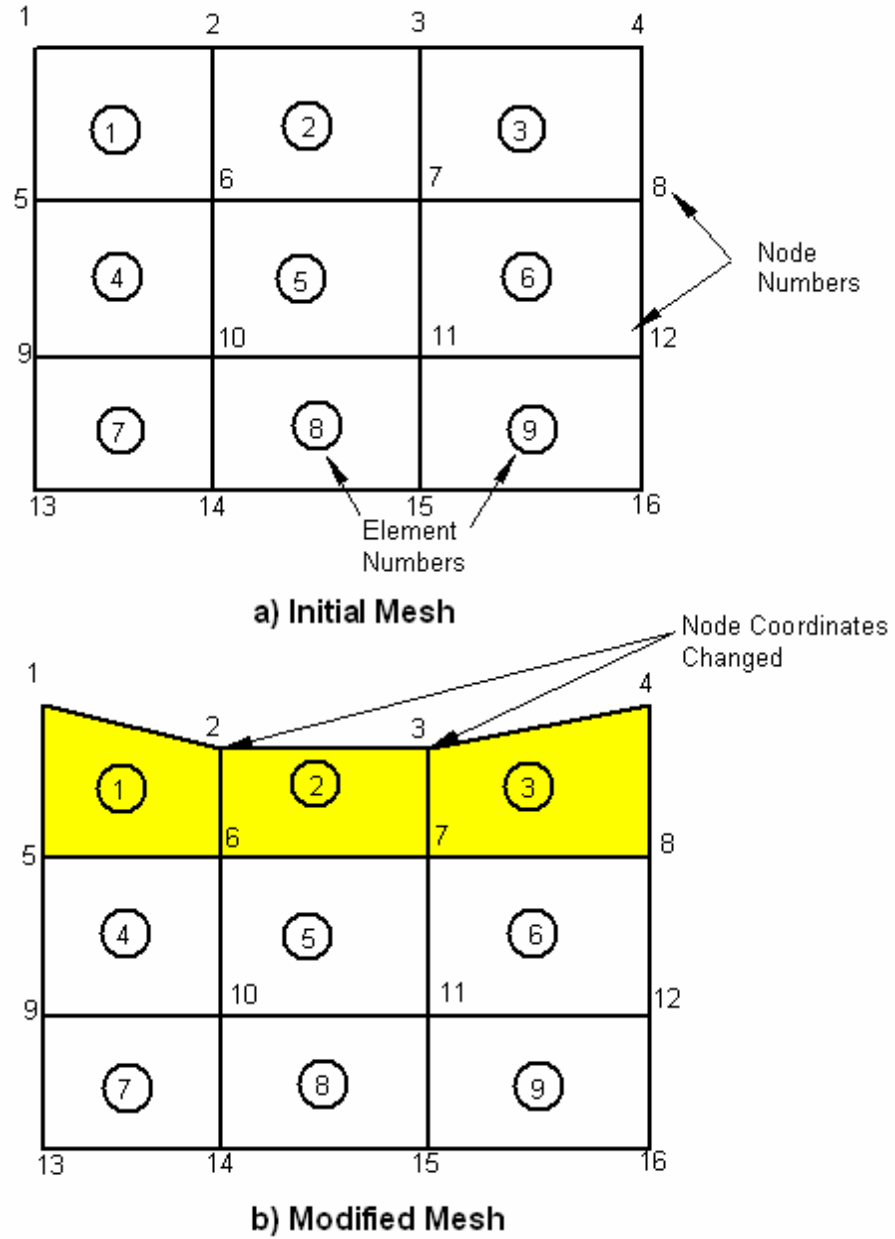


Figure 3.4 FEM Meshes

Now consider Figure 3.4(b) where geometric locations of nodes 2 and 3 are modified. This modification causes changes in elements ①, ② and ③. Due to the modification in coordinates the element stiffness matrix for these elements changes. The global stiffness matrix of the changed geometry is given by,

$$K = K_e^1 + K_e^2 + K_e^3 + K_e^4 + K_{e_0}^5 + \dots + K_{e_0}^9$$

The change in the global stiffness matrix is given by,

$$\Delta K = K - K_0$$

Thus yielding,

$$\Delta K = (K_e^1 - K_{e_0}^1) + (K_e^2 - K_{e_0}^2) + (K_e^3 - K_{e_0}^3)$$

where,

$$\Delta K = \left[\begin{array}{l} \text{Sum of the differences in} \\ \text{element stiffness matrices of} \\ \text{those elements whose at least} \\ \text{one node has undergone a} \\ \text{change in coordinates.} \end{array} \right]$$

By using this methodology, the change in the global stiffness matrix ΔK is generated. Using this ΔK and the above mentioned information, an algorithm was developed applying the Combined Approximation reanalysis method to obtain the stress and displacement results of the changed design.

3.3.5 Repeated Analysis.

The process will continue until the acceptable stress (or displacement) results are obtained.

4. Case Studies and Results

4.1 Overview

The system developed in this work is used by a designer as discussed in Section 1.8. When the designer is in the early design phase, stress analysis of the concept needs to be done time to time until s/he finalizes a particular idea and go into detail design phase. Using the work discussed here, designer can consider various design option and analyze them. S/he can modify the concept graphically and check the new design options for acceptable values of stress and displacements. The main objective of this chapter is to demonstrate how this reanalysis algorithm can be used to solve a redesign problem. Three case studies are considered here and their complexity increases. The chapter also explains the steps used to solve each redesign case study. The first case study explores the optimum number of reduced basis vectors that can be used for the reanalysis.

4.2 Case Study # 1: Plate with a Hole

Figure 4.1 shows a rectangular plate with a hole. The plate has dimensions 100 mm \times 50 mm with a square central hole 8 mm \times 8 mm with a fillet of radius 1 mm at its corners. The design decision is to determine what type of hole will yield the smallest stress concentration factor? Initially the designer selects a square hole with some radius at the four corners.

Using the reanalysis tool developed in this work, the problem is modified with circular and elliptical holes. It is good practice before starting any finite element analysis to carry out a hand analysis. Hand analysis for the initial and redesign problems are performed to determine the maximum stress in the plate and is discussed in Appendix E. The problem with sharp corners for the rectangular hole is not considered since the stress at the sharp corner is infinite according to the theory of elasticity. Though finite element analysis gives some finite value of the final stress at these corners, the results will not converge. Furthermore, a rectangular plate with sharp corner is practically impossible to manufacture and there will always be a small radius at the corners. The problem is considered with a radius at the corners.

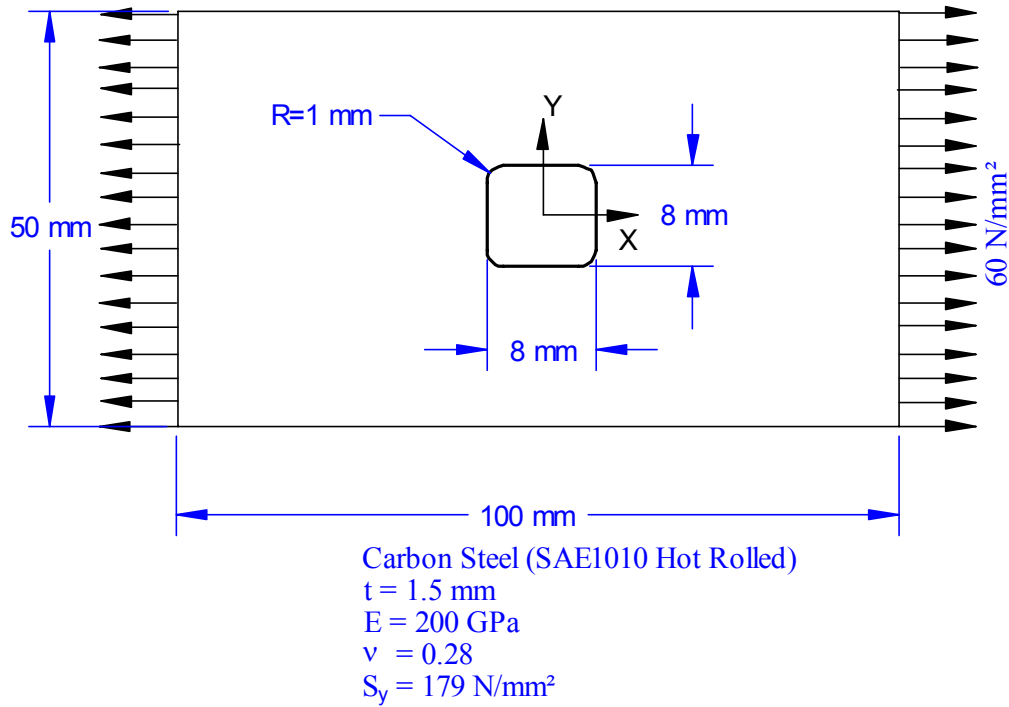


Figure 4.1 Initial design geometry.

4.2.1 Finite Element Model of Initial Problem

A quarter symmetry of the problem was used as shown in Figure 4.2. To apply a pressure of 60 N/mm^2 , work equivalent nodal forces are calculated based on the number of the elements at that face.

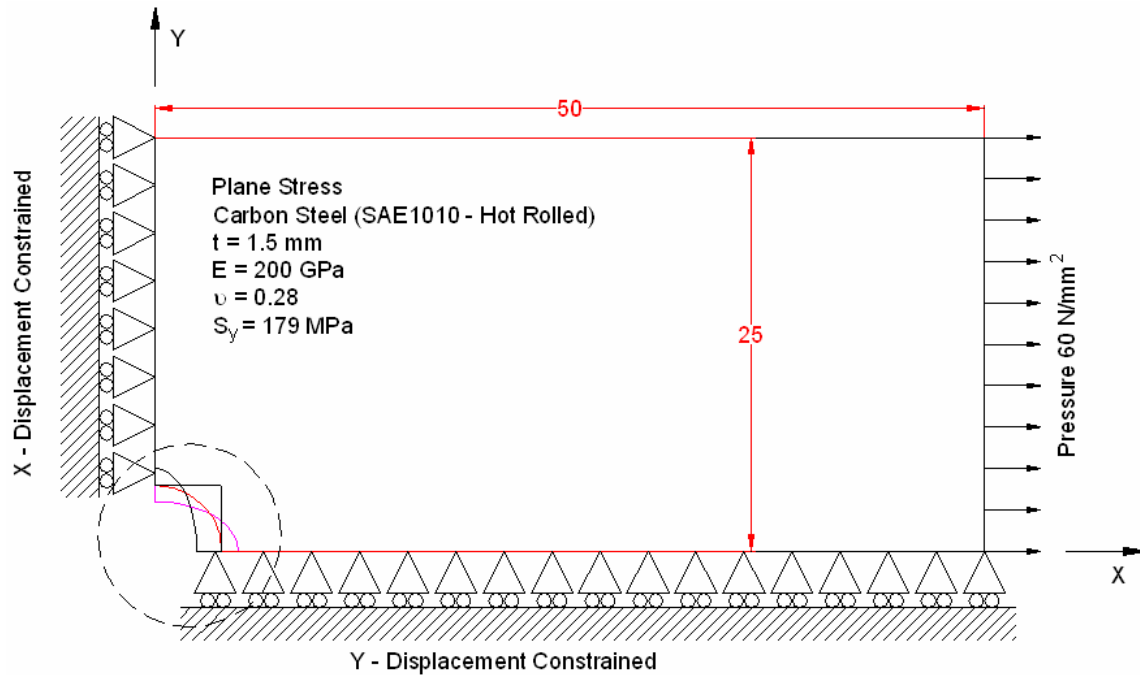


Figure 4.2 Quarter symmetry initial geometry.

Figure 4.3 shows the hole geometry for the initial design and each redesign case study. In each case, the hole-geometry is modified to explore the change in stress and displacement. The hole that minimizes stresses will be selected. As discussed earlier, the problem of plate with the square hole will be analyzed first and is denoted as the ‘Initial Design’ in Figure 4.3. Procedure for solving this problem will be discussed in details hereafter.

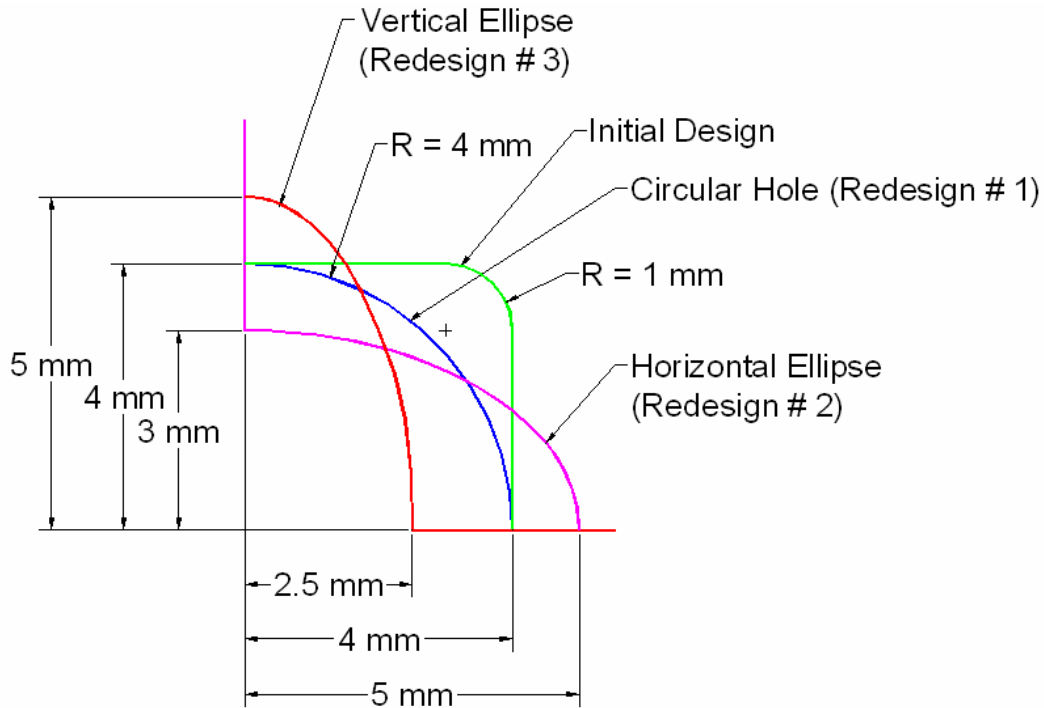


Figure 4.3 Initial design and three redesign options for hole.

Before starting to make the finite element model, it is required to define the problem type to be solved, e.g., what is the element type? Whether the problem is plane stress or plane strain, etc. The above mentioned problem is solved with plane stress element type. As described in Appendix A, an APDL code is written to set the element type and element type properties. Figure 4.4 shows the ANSYS toolbar modified for reanalysis.



Figure 4.4 ANSYS Reanalysis Toolbar

By clicking on ELM_PROP the element type will be set as PLANE42 a four-node quadrilateral element, plane stress with thickness problem. This will ensure that the user always uses the element type as PLANE42 since the algorithm developed only allows solving reanalysis problem for element type PLANE42. A window will open asking the user to enter the thickness for the plane stress problem. Thickness is set as 1.5 mm. Subsequent windows will prompt the user to input the material properties such as Young’s Modulus and Poisson’s ratio as shown in Figure 4.1. The next step is modeling

the geometry. This is done by choosing ANSYS main menu options for modeling. The modeling procedure is not discussed here. The mesh considered is coarse except in the vicinity of the fillet due to the stress concentration. Figure 4.5 shows a snapshot of ANSYS GUI, displays the mesh and the mesh characteristics. The boundary conditions are set such that the Y – DOF for the nodes on the bottom line surface is constrained to zero, and for the nodes on the left line surface X – DOF is constrained. After applying the boundary conditions and the nodal forces, this problem is first solved using ANSYS solver. Figure 4.6 shows contour plots of displacement and stress results using ANSYS with no reanalysis.

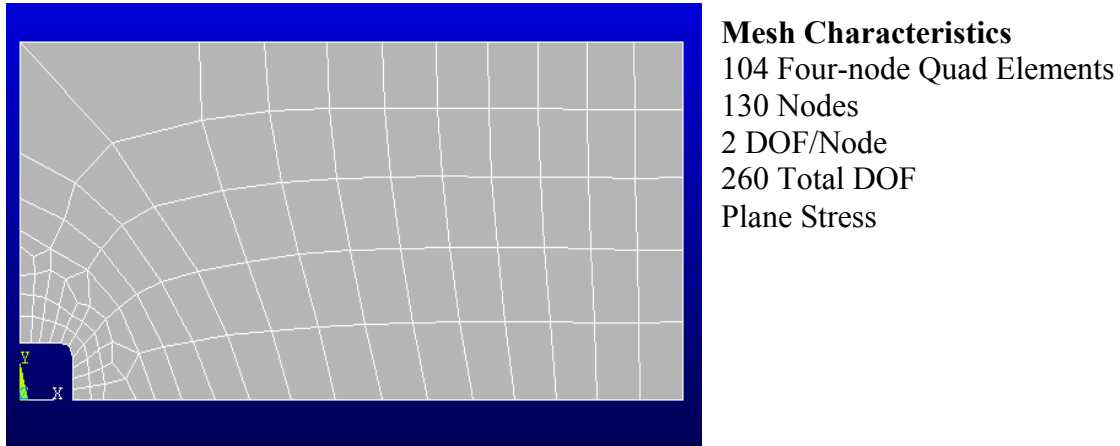


Figure 4.5 ANSYS GUI for initial mesh.

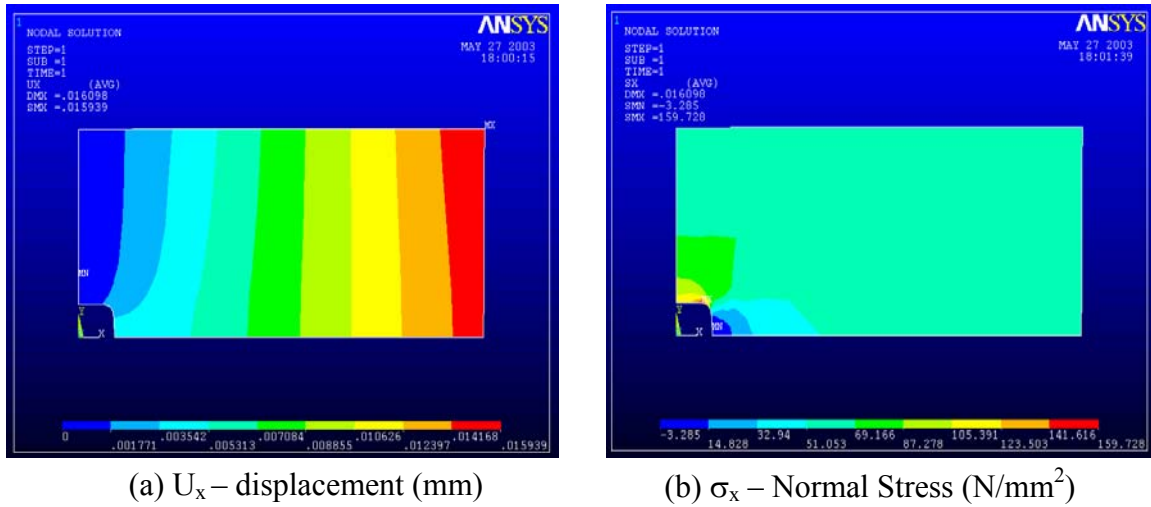
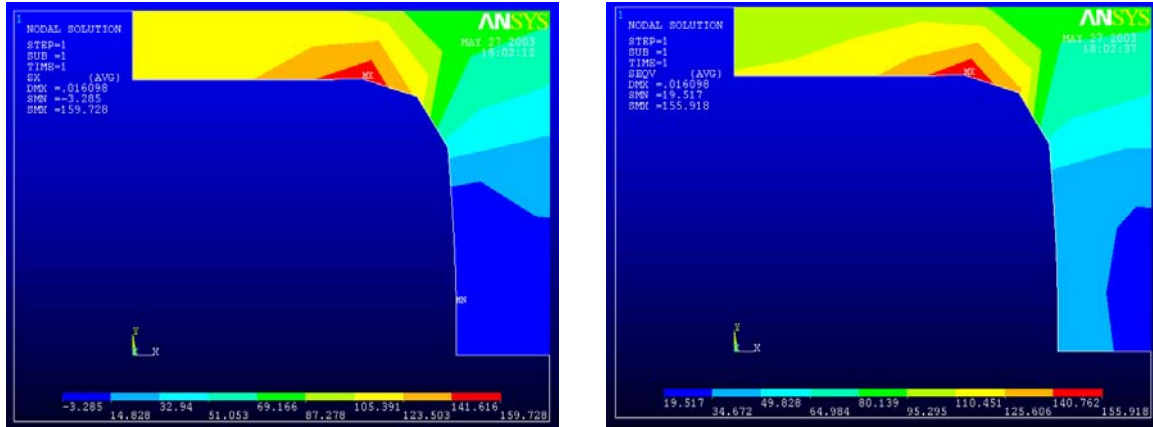


Figure 4.6 ANSYS stress contour results of plate with square hole.



(c) σ_x – Normal stress at fillet (N/mm²). (d) σ_{VM} – von Mises stress at fillet (N/mm²).

Figure 4.6 ANSYS stress contour results of plate with square hole.

As expected the maximum normal stress σ_x was observed to be near the fillet. The FEA result of maximum stress was found to be 159.73 N/mm² compared to analytical value of 158.57 N/mm² (Appendix E) and a maximum deflection of 0.15939×10^{-1} mm. The stresses are very high yielding a factor of safety of 1.12. The resultant absolute maximum values are shown in Tables 4.1 and 4.2 for deflection and stress, respectively.

Table 4.1 Maximum Deflection (mm)

	U_x	U_y
Node #	17	22
Value	0.15939×10^{-1}	-0.2634×10^{-2}

Table 4.2 Minimum and Maximum stress components (N/mm²)

		σ_x	σ_y	σ_{xy}	σ_{VM}
Minimum	Node #	40	1	102	4
	Value	-3.2847	-50.418	-39.466	19.517
Maximum	Node #	37	37	52	37
	Value	159.73	29.524	2.3933	155.92

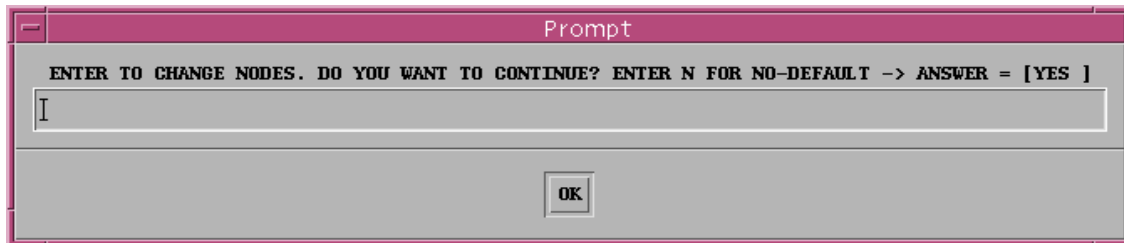
4.2.2 Redesign Option # 1: Plate with Circular Hole

The initial square hole geometry is modified to a circular hole as shown in Figure 4.3. Instead of creating the new geometry, nodes of the earlier finite element model (Section 4.2.1) are moved to create a circular hole. This can be achieved by clicking the RE_MODEL button on the ANSYS toolbar shown in Figure 4.7(a), as discussed in Appendix Section B.3. This creates a prompt to the user asking “Enter to change node. Do you want to continue? Press ‘N’ for No, DEFAULT – YES” as shown in Figure 4.7(b). Upon entering, the ANSYS pick-up menu appears as shown in Figure 4.7(c). This menu allows graphical selection of the node to be moved and then prompts the user to choose the final nodal location. The loop of changing the node coordinates until the user

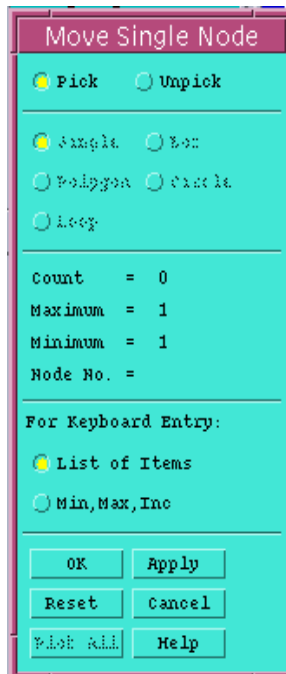
is satisfied with the geometry. By entering N in the prompt as shown in Figure 4.7(b), the RE_MODEL stage is completed. This entire procedure is written in APDL (Appendix A). After finishing the modeling, a required circular geometry is achieved as shown in Figure 4.8. To determine the exact dimension for the radius, a temporary arc with the required radius is drawn and the nodes are moved to that line.



(a) ANSYS Reanalysis Toolbar

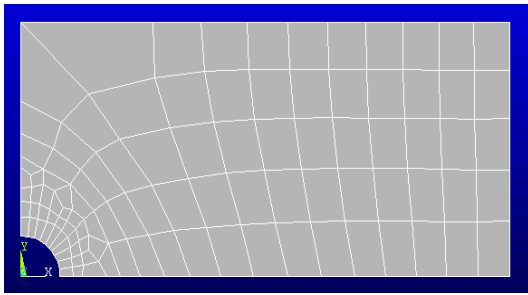


(b) Prompt for re-modeling



(c) Pick-up Menu

Figure 4.7 Re-modeling prompts.



Mesh Characteristics

104 Four – Node Quad Elements
130 Nodes
2 DOF/Node
260 Total DOF
Plane Stress

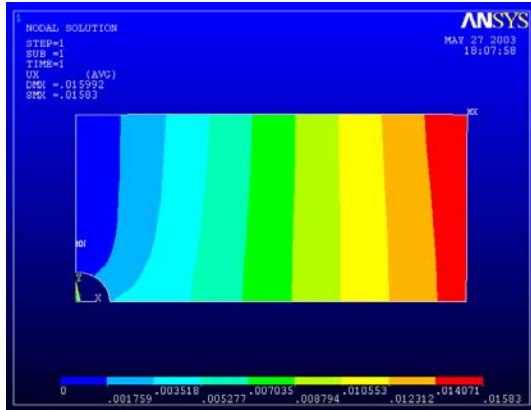
Figure 4.8 Plate with a circular hole (Redesign Option # 1).

After re-modeling, the next step is to solve the redesigned finite element model in Figure 4.8 using the reanalysis method. This is done by clicking on the RUN_REAN button on the toolbar shown in Figure 4.7(a). This will run the combined approximation reanalysis algorithm to solve the modified finite element problem (plate with circular hole). The results of reanalysis can be seen by clicking on the RESULT button shown in Figure 4.7(a). This creates a new menu as shown in Figure 4.9

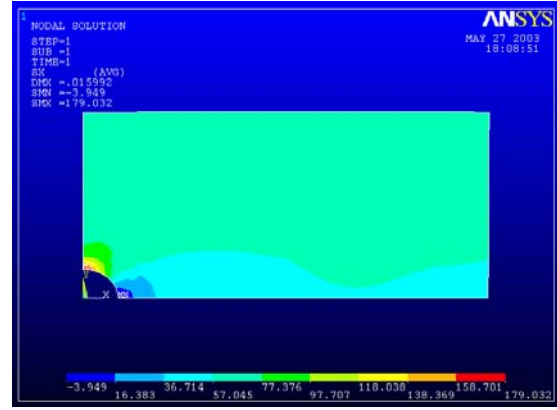


Figure 4.9 ANSYS Reanalysis Toolbar with result menu.

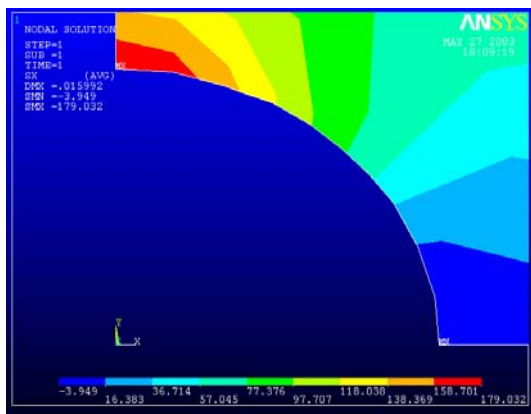
Each button whose name begins with “PLT” creates a contour plot of results on the screen, whereas “LIST” produces a text list of the results. Figure 4.10 shows contour plots of results produced by reanalysis of design option # 1. The stress is maximum at the top left-hand corner of circular arc. The maximum stress and displacement results are as shown in Tables 4.3 and 4.4, respectively. Table 4.3 shows the deflection results U_X and U_Y . The table shows exactly at which node the deflection is maximum. Table 4.4 shows the maximum and minimum normal stress in X – direction (σ_x), in Y – direction (σ_y), σ_{xy} and von Mises stress (σ_{VM}) with the node number. It can be seen that σ_x is 179.03 N/mm^2 which is higher than the case when the plate with square hole and circular fillets (initial design). The factor of safety is less than one.



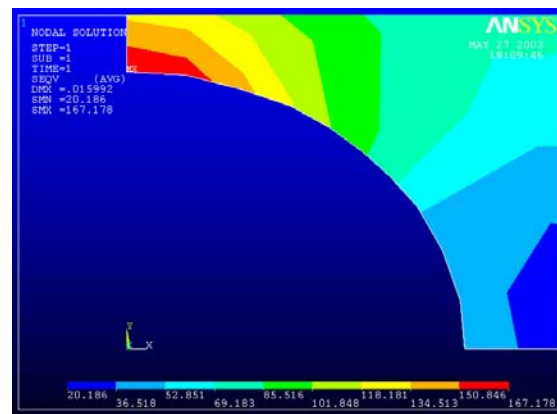
(a) U_x – Displacement (mm)



(b) σ_x – Normal Stress (N/mm²)



(c) σ_x – Normal stress at circular hole (N/mm²)



(d) σ_{VM} – von Mises stress at circular hole (N/mm²)

Figure 4.10 Redesign Option # 1 contour results for plate with circular hole.

Table 4.3 Maximum Deflection (mm)

	U_x	U_y
Node #	17	22
Value	0.1583×10^{-1}	-0.25617×10^{-2}

Table 4.4 Minimum and Maximum stress components (N/mm²)

		σ_x	σ_y	σ_{xy}	σ_{VM}
Minimum	Node #	1	1	1	3
	Value	-3.9486	-54.329	-24.293	20.186
Maximum	Node #	32	32	108	32
	Value	179.03	27.045	4.0545	167.18

As discussed in Chapter 2, the number of reduced basis vectors determines the accuracy of the displacement results based on the combined approximation reanalysis method. Good accuracy is obtained by setting the number of reduced basis vectors to three [4.1]. In this problem, a study is carried out to analyze the stress and displacement

result by varying the number of reduced basis vectors from 1 to 5. The same problem was also solved using ANSYS directly (without using reanalysis) to produce displacement and stress results as denoted by the ANSYS Direct Analysis column in Table 4.5. Table 4.5 provides a comparison for stress and displacements varying the number of reduced basis vectors and the theoretical result.

Table 4.5 Comparison of maximum results for plate with circular hole.

Maximum Quantities		Theoretical	ANSYS Direct Analysis	Reanalysis Reduced Basis Vectors				
				1	2	3	4	5
σ_x N/mm ²	Value	183.584	176.33	200.25	169.19	179.03	180.25	180
	Node #	-	32	37	32	32	32	32
σ_{VM} N/mm ²	Value	183.584	164.40	196.58	159.11	167.18	167.92	167.61
	Node #	-	32	37	32	32	32	32
U_x $\times 10^{-1}$ mm	Value	0.15518*	0.15829	0.15744	0.15824	0.1583	0.15830	0.15829
	Node #	-	17	17	17	17	17	17

Note:

* - Theoretical value of displacement, is based on a very fine mesh of four – node quadrilateral elements. (# of Elements = 13800, # of Nodes = 14043).

Since the combined approximation reanalysis method only calculates displacement values, it can be observed that as the number of reduced basis vectors increases, the maximum displacement values approaches the ANSYS direct analysis result. This demonstrates that as the number of reduced basis vectors is increased the accuracy of the reanalysis method increases. However, increasing the number of reduced basis vectors increases computational effort. Figure 4.11 shows the variation in maximum displacement when the number of reduced basis vectors is increased. A comparison is made with respect to the ANSYS direct analysis. The theoretical value of the maximum displacement results of very fine mesh (# of Elements = 13800 and # of Nodes = 14043) are presented since there is no known analytical method to find the displacement results for the plate with a circular hole.

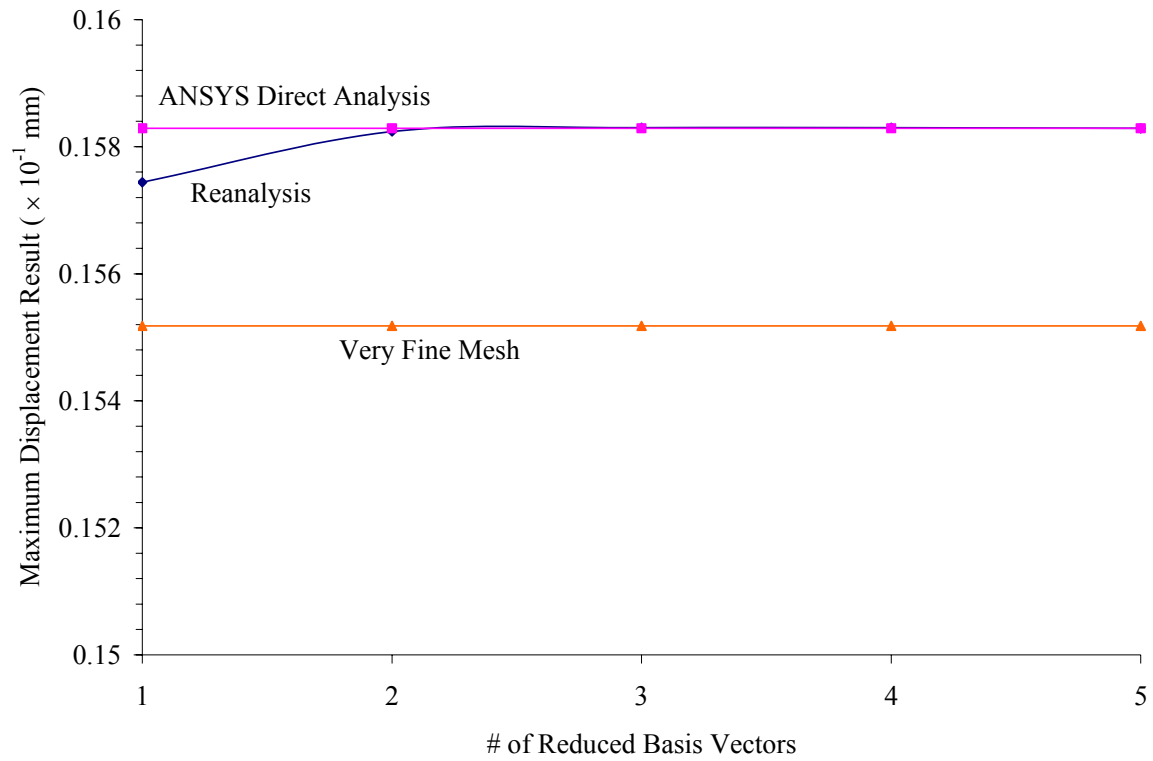


Figure 4.11 (a) Maximum displacement (U_x) versus # of reduced basis vectors.

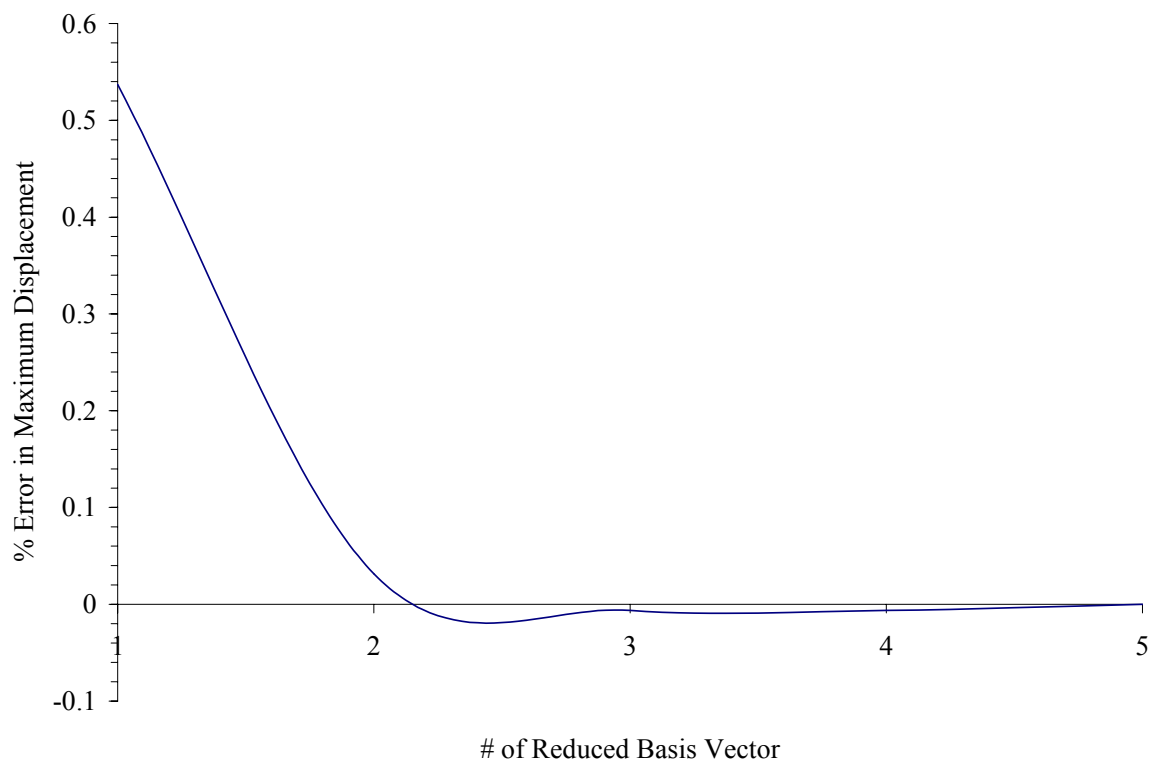


Figure 4.11 (b) % Error in maximum displacement versus # of reduced basis vectors.

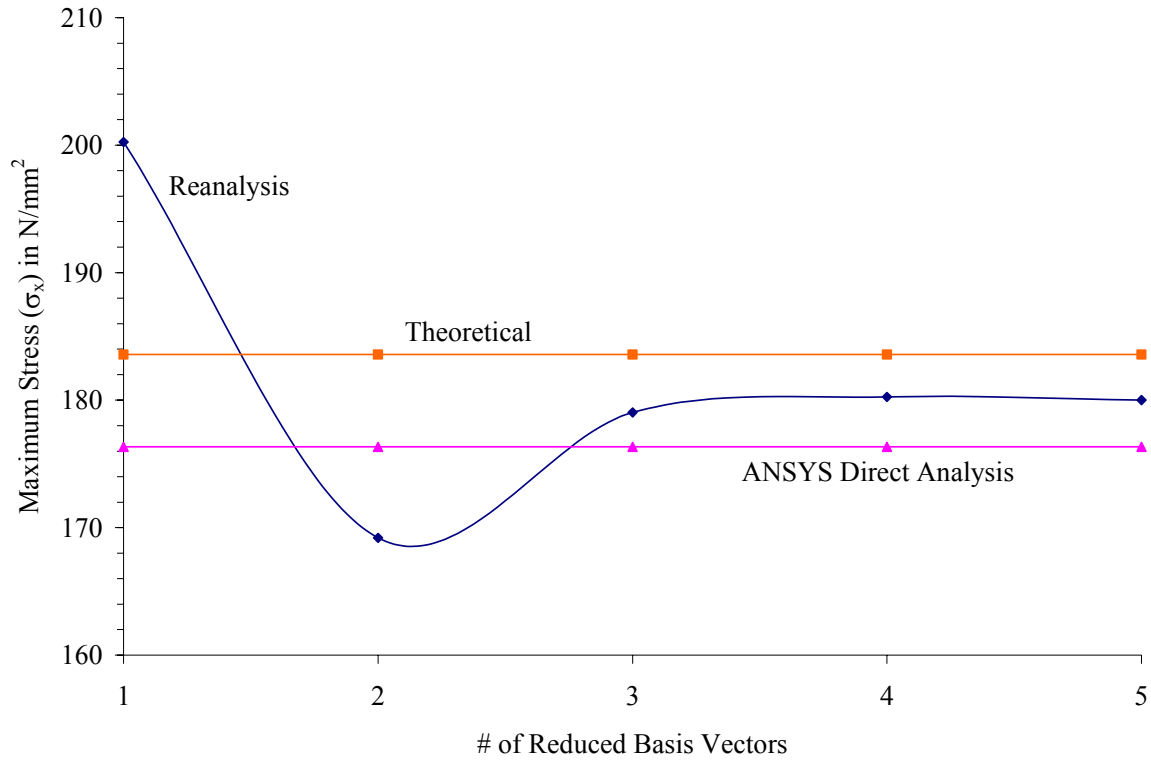


Figure 4.11 (c) Maximum stress (σ_x) variation versus # of reduced basis vectors.

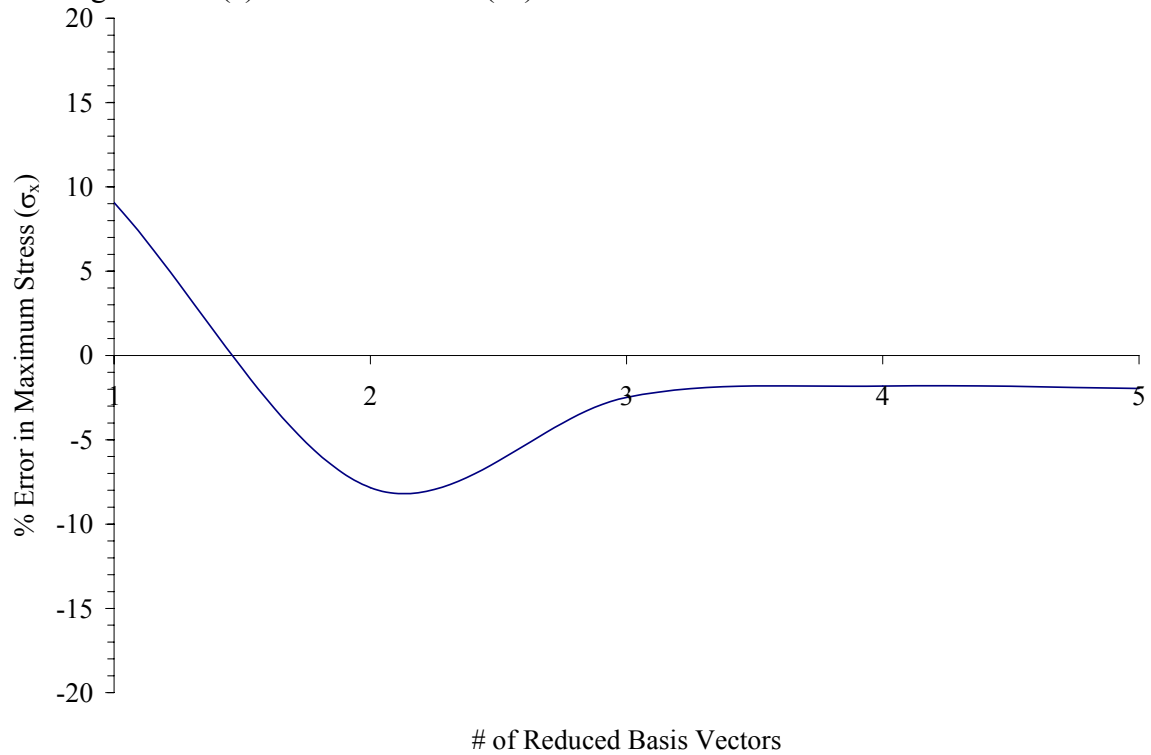


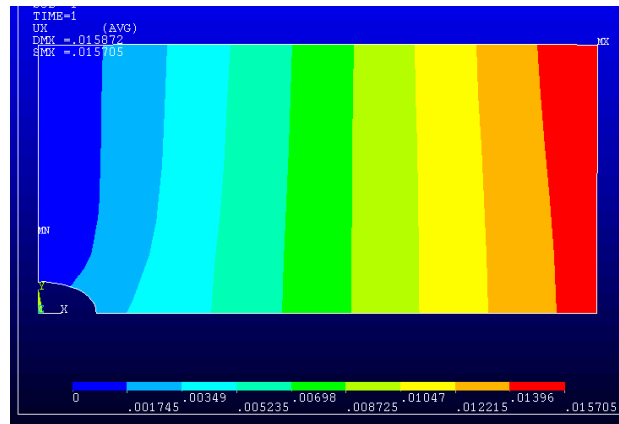
Figure 4.11 (d) % Error in maximum stress (σ_x) versus # of reduced basis vectors.

From Figure 4.11 (b) it can be observed that the % error in displacement with three reduced basis vectors is only 0.006% and is considered negligible. Therefore, per

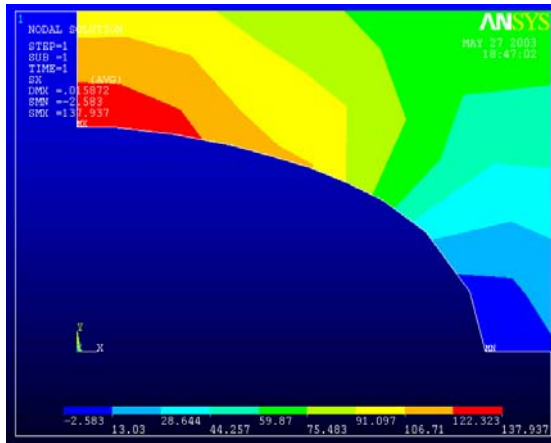
Gullickson [4.1] the number of reduced basis vector can be set at three for all reanalysis in this work. This reanalysis method also yields very good accuracy with regards to stress. When the number of RBV is three, the error in stress σ_x with respect to ANSYS direct analysis is only 1.53% whereas, with respect to the theoretical value the error is 2.48%, as shown in Figure 4.11(d).

4.2.3 Redesign Option # 2: Plate with Horizontal Elliptical Hole

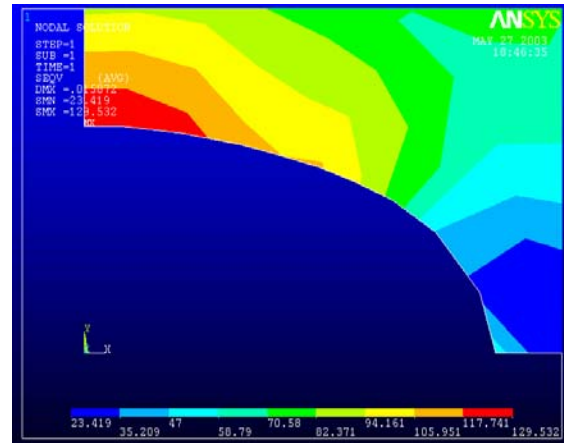
Redesign Option # 2 changes Redesign Option # 1 from a plate with a circular hole to horizontal elliptical hole as shown in Figure 4.3. Similar to # 1, the nodes near the circular arc are moved graphically to form a horizontal elliptical arc. A horizontal elliptical arc is first drawn and then the nodes are moved to match the geometry. The result contour plots for displacement and stress are shown in the Figure 4.12. This figure shows the X – directional displacement and von Mises stresses at the elliptical arc. In this case the maximum stress occurs at the top corner of the elliptical arc. Maximum displacement and stress results are shown in Tables 4.6 and 4.7, respectively. It is found that the maximum stress is 137.94 yielding the factor of safety of 1.3.



(a) U_x – Displacement (mm).



(b) σ_x – Normal Stress at fillet (N/mm²).



(c) σ_{VM} – von Mises Stress at fillet (N/mm²).

Figure 4.12 Redesign Option # 2 contour results for plate with horizontal elliptical hole.

Table 4.6 Maximum Deflection (mm)

	U_X	U_Y
Node #	17	22
Value	0.15705×10^{-1}	-0.2466×10^{-2}

Table 4.7 Minimum and Maximum stress components (N/mm²)

		σ_x	σ_y	σ_{xy}	σ_{VM}
Minimum	Node #	1	1	39	4
	Value	-2.5830	-52.199	-26.364	23.419
Maximum	Node #	32	99	108	32
	Value	137.94	19.435	2.8567	129.53

The stress and displacement result variation for reduced basis vectors was also considered. As discussed in Appendix E, the theoretical solution for stress is known. The same problem is solved varying with different number of reduced basis vectors from 1 to 5. An ANSYS solution is also obtained by solving the same problem in ANSYS using the ANSYS solver. Table 4.8 compares the stress and displacement results versus the number of degrees of freedom.

Table 4.8 Comparison of results for plate with horizontal elliptical hole

Maximum Quantities		Theoretical	ANSYS Direct Analysis	Reanalysis Reduced Basis Vectors				
				1	2	3	4	5
σ_x N/mm ²	Value	132.273	134.28	232.47	161.23	137.94	139.74	142.43
	Node #	-	32	102	32	32	32	32
σ_{VM} N/mm ²	Value	132.273	126.44	230.36	150.51	129.53	131.24	133.62
	Node #	-	32	102	32	32	32	32
U_X $\times 10^{-1}$ mm	Value	0.15359*	0.15704	0.15542	0.15693	0.15705	0.15705	0.15704
	Node #	-	17	17	17	17	17	17

Note:

* Theoretical value of displacement, is based on a very fine mesh of four – node quadrilateral elements (# of Elements – 13500, # of Nodes – 13741).

It can be seen from Table 4.6 that the variation in displacement results are similar to Redesign Option # 1. Based on three or greater reduced basis vectors, the results exactly match the ANSYS direct analysis results. The theoretical value of displacement is based on the results of very fine mesh (# of Elements = 13500, # of Nodes = 13741) are presented since there is no known theoretical method to find the displacement results for the plate with an elliptical hole. Figure 4.13 (c) shows a comparison of the stress results with the theoretical and ANSYS direct analysis results.

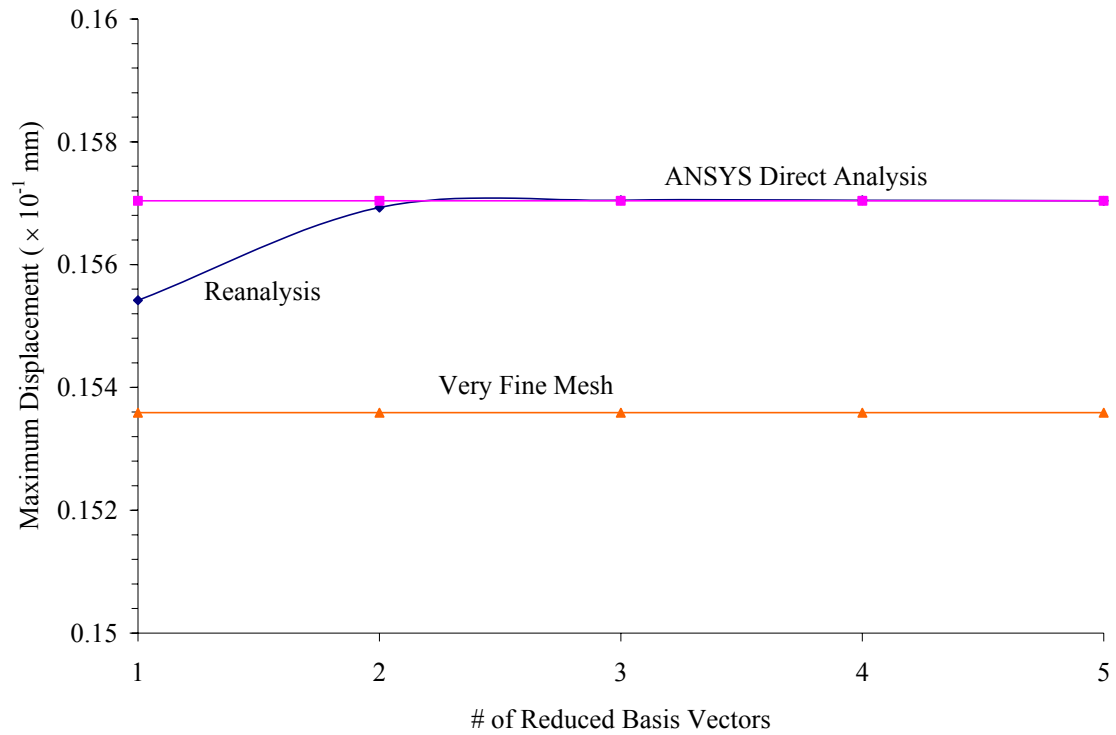


Figure 4.13 (a) Maximum displacement (U_X) variation versus # of reduced basis vectors.

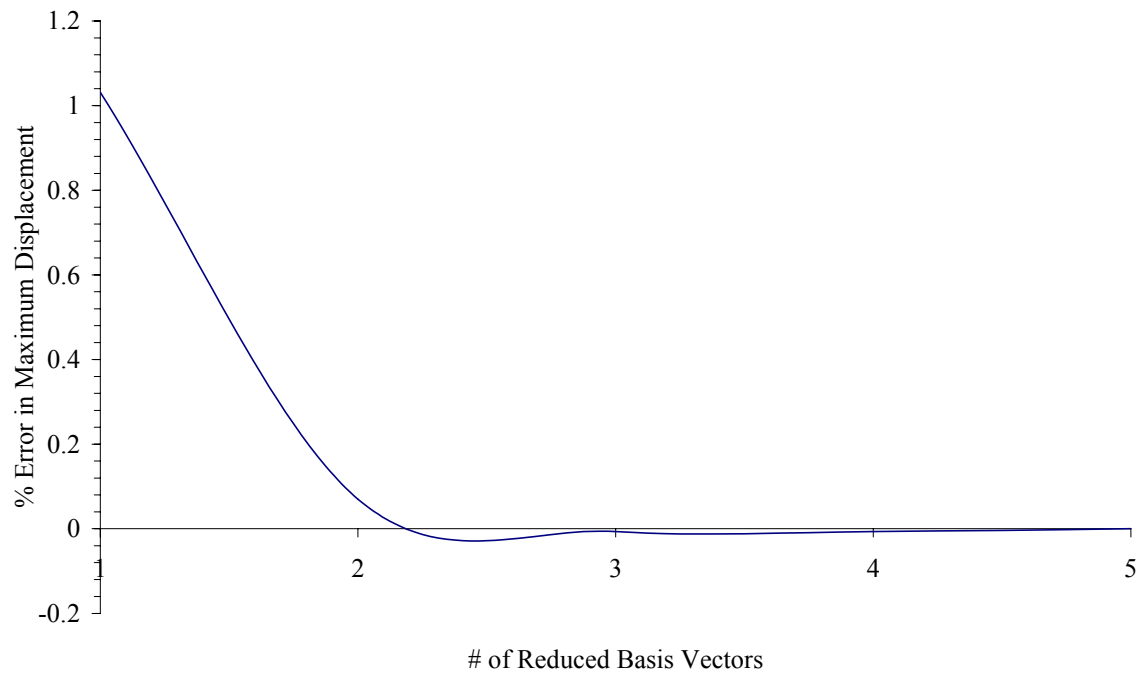


Figure 4.13 (b) % Error in maximum displacement variation versus # of reduced basis vectors.

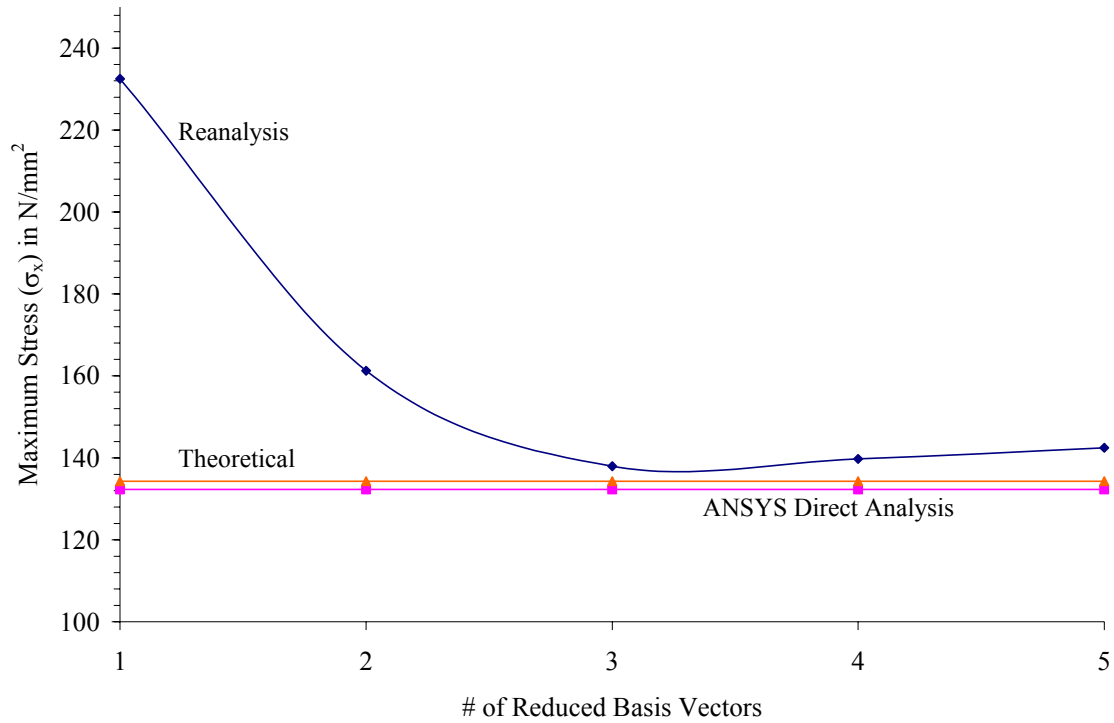


Figure 4.13 (c) Maximum stress (σ_x) variation versus # of reduced basis vectors.

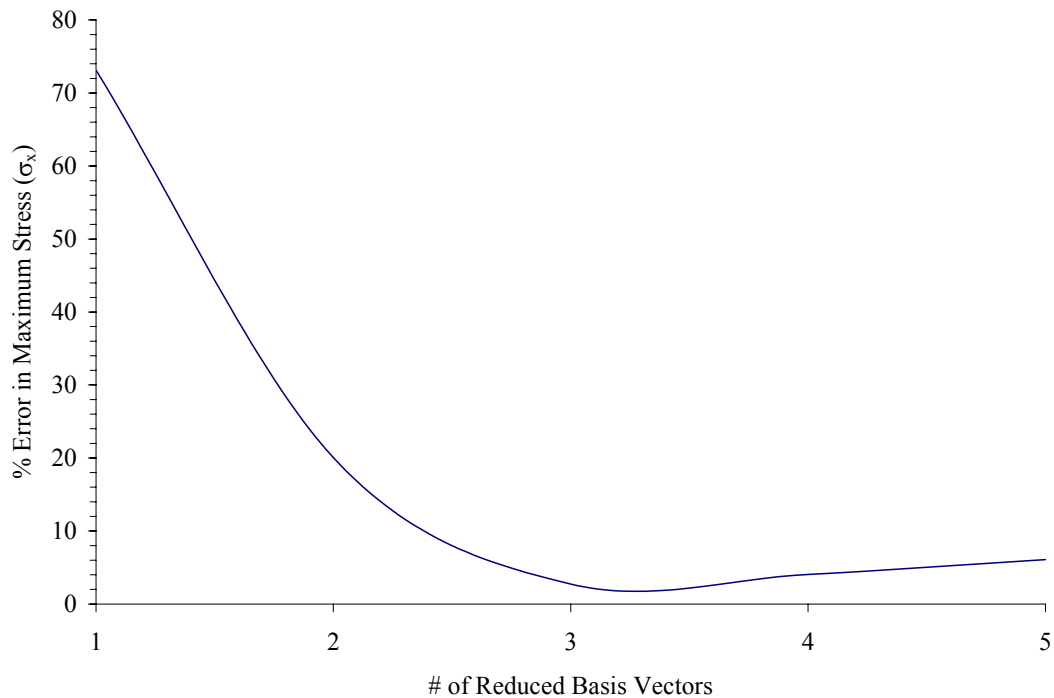


Figure 4.13 (d) % Error in maximum stress (σ_x) variation versus # of reduced basis vectors.

It can be observed that there is almost zero % error in displacement when the number of reduced basis vectors equals three as shown in Figure 4.13(b). However, the %

error in stress is 4.28 % when compared with the theoretical solution and is 2.73 % when compared with the ANSYS direct results. In Section 4.2.3 it is observed that the stress results converge to a value for a large number of reduced basis vectors. However, it did not converge to the theoretical value. This may be due to the following reasons:

1. The mesh is not fine enough in the vicinity of the hole to yield accurate results.
2. The exact value of theoretical stress concentration factor, which is the basis of comparison here, is not known.

4.2.4 Redesign Option # 3: Plate with Vertical Elliptical Hole

It is seen from Redesign Option # 2 that with the horizontal elliptical hole yield a smaller stress concentration compared to the plate with square and circular holes. However, for elliptical hole only one case was considered where the major axis of the ellipse is parallel to the direction of application of the load (horizontal ellipse). In Redesign Option # 3 the case when major axis is perpendicular to the direction of application of force (vertical ellipse) will now be considered.

In Redesign Option # 3 the major axis of the elliptical hole is perpendicular to the direction of application of the force. Values for theoretical stress concentration factor are also known. The FEM model for this problem is compared to the other geometries discussed above and is shown in Figure 4.3. This figure only shows the enlarged view of all alternate geometries used for the hole.

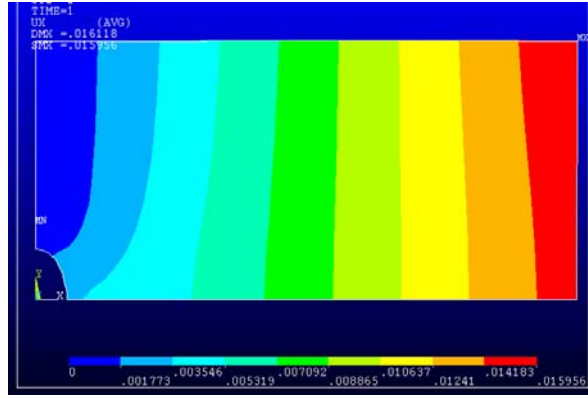
Similar to the discussion in Section 4.2.3, a reanalysis is carried out for this problem. Figure 4.14 shows the contour plot of the displacement U_x , stress σ_x and von Mises stress result σ_{VM} at an elliptical arc. As seen in Figure 4.14, maximum stress occurs at the top of the vertical elliptical hole. The results of displacement and stress are given in Tables 4.9 and 4.10, respectively. It is seen that the maximum stress is 314.27 yielding a factor of safety of 0.5 and therefore resulting in a poor design.

Table 4.9 Maximum Deflection (mm)

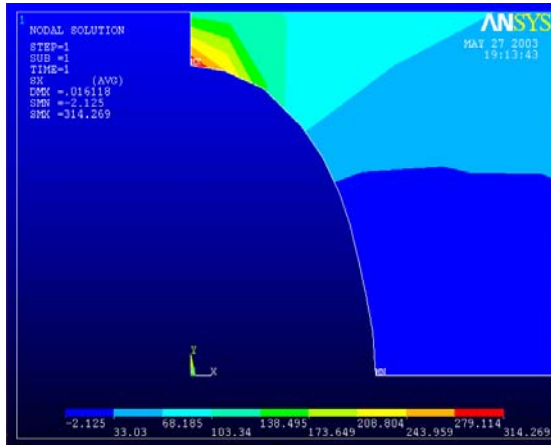
	U_x	U_y
Node #	17	22
Value	0.15956×10^{-1}	-0.25558×10^{-2}

Table 4.10 Minimum and Maximum stress components (N/mm²).

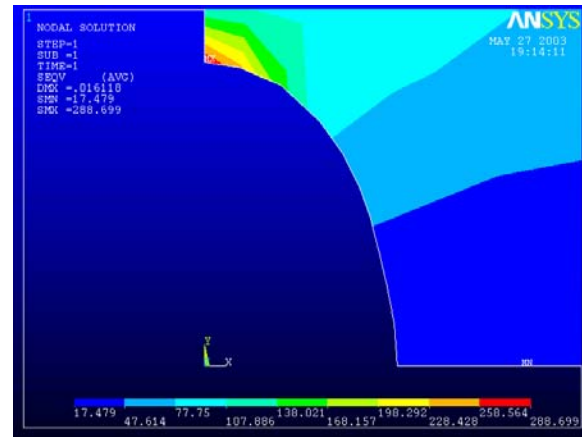
		σ_x	σ_y	σ_{xy}	σ_{VM}
Minimum	Node #	1	1	101	3
	Value	-2.1249	-47.029	-38.598	17.479
Maximum	Node #	32	32	33	32
	Value	314.27	61.198	9.4840	288.70



(a) Displacement U_x (mm).



(b) σ_x (N/mm²) at elliptical arc.



(c) σ_{VM} (N/mm²) at elliptical arc.

Figure 4.14 Redesign option # 3 contour results for plate with vertical elliptical hole.

The stress and displacement result variation for the reduced basis vectors was also considered in this problem. As discussed in Appendix E, the theoretical solution is known. The same is solved varying the number of reduced basis vectors from 1 to 5. An ANSYS solution is also obtained by solving the same problem in ANSYS using ANSYS solver, i.e., no reanalysis. Table 4.11 shows the results in tabular form. The table shows the results of the theoretical solution. The theoretical stress is found in Appendix E. Very fine mesh was used to find displacement since no theoretical solution exists. The fourth column in Table 4.11 shows the ANSYS direct analysis results. The fifth column onwards, results as the number of reduced basis vectors varies from 1 to 5. These variations are then plotted similar to Redesign Options # 1 and 2.

Table 4.11 Comparison of maximum results for Redesign Option # 3.

Maximum Quantities		Theoretical	ANSYS Direct Analysis	Reanalysis Reduced Basis Vectors				
				1	2	3	4	5
σ_x N/mm ²	Value	309.9	298.75	191.98	294.29	314.27	315.91	312.55
	Node #	-	32	32	32	32	32	32
σ_{VM} N/mm ²	Value	309.9	274.29	194.36	274.13	288.70	289.19	286.39
	Node #	-	32	32	32	32	32	32
U_x $\times 10^{-1}$ mm	Value	0.15661*	0.15958	0.15808	0.1594	0.15956	0.15958	0.15958
	Node #	-	17	17	17	17	17	17

Note:

* - For Theoretical value of displacement, is based on a very fine mesh of four – node quadrilateral elements (# of elements = 14250, # of nodes = 14496).

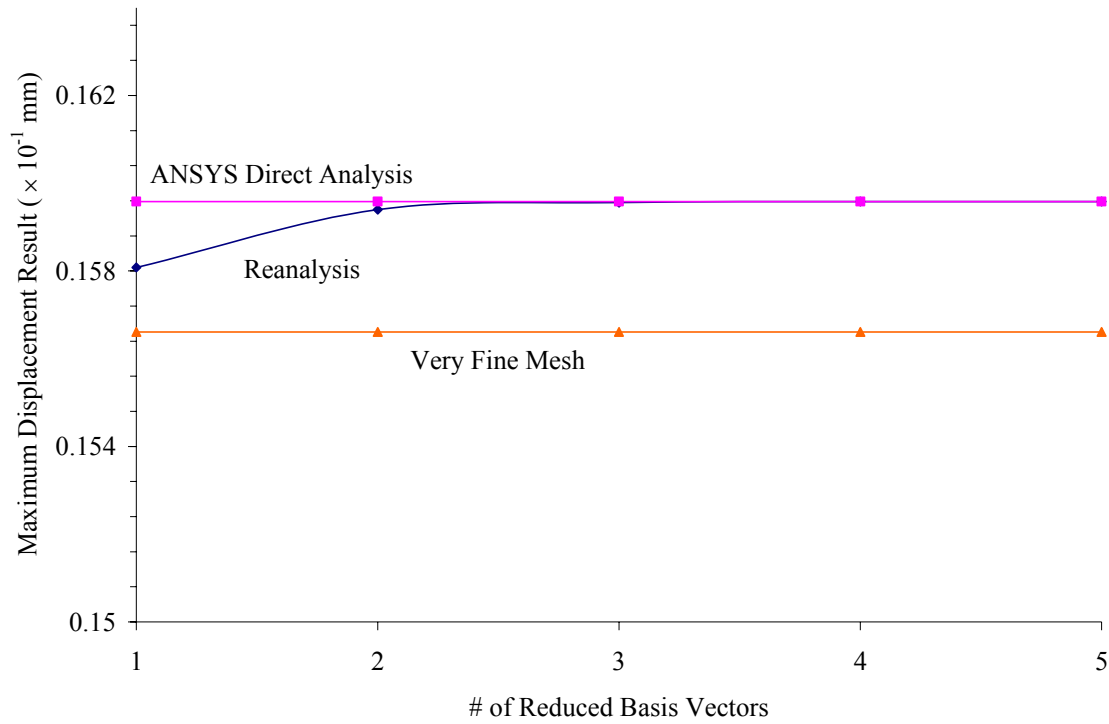


Figure 4.15 (a) Maximum displacement (U_x) variation versus # of reduced basis vectors.

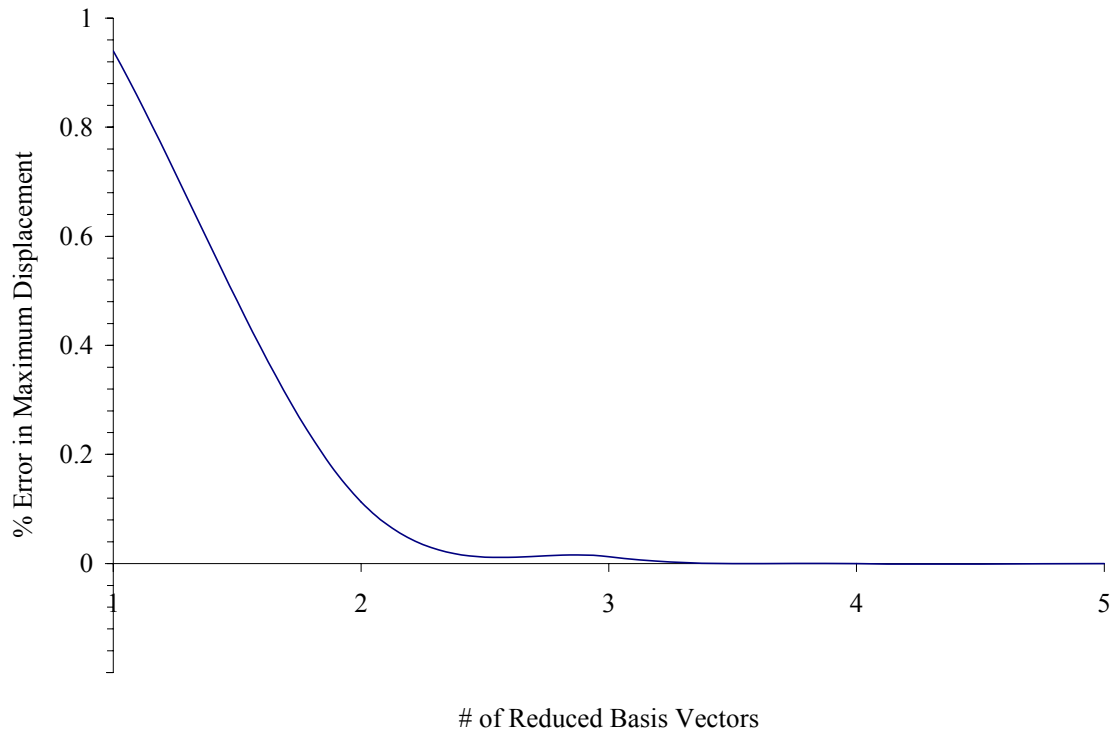


Figure 4.15 (b) % Error in maximum displacement versus # of reduced basis vectors.

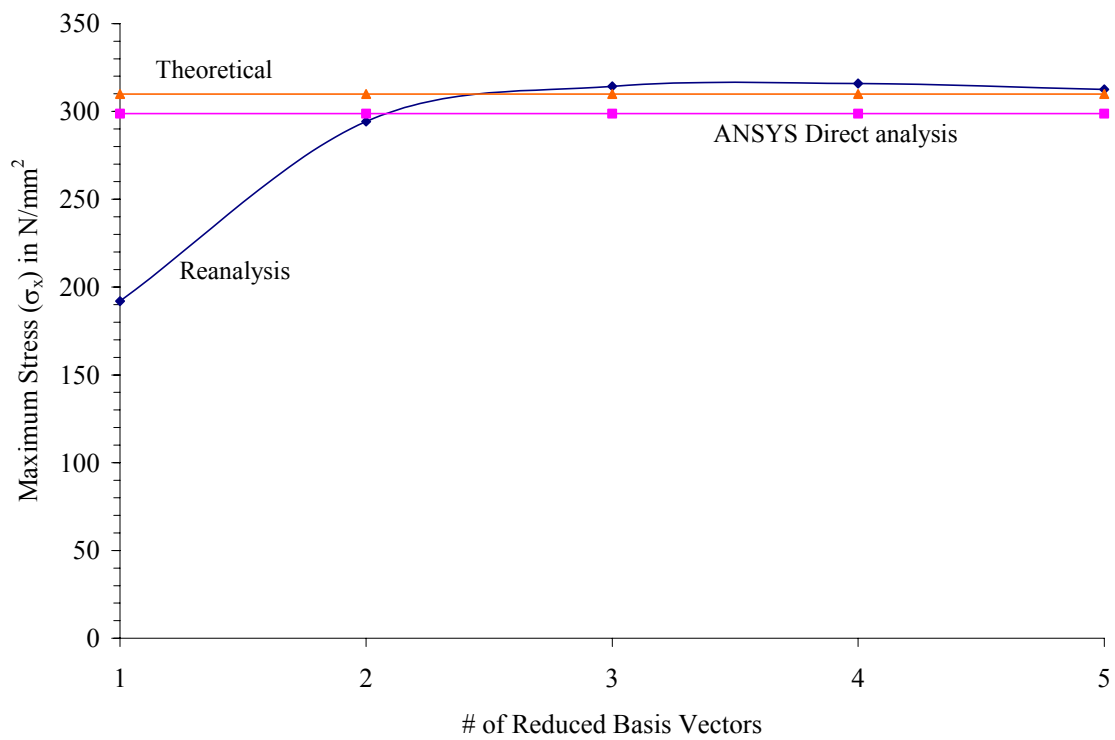


Figure 4.15 (c) Maximum stress (σ_x) variation versus # of reduced basis vectors.

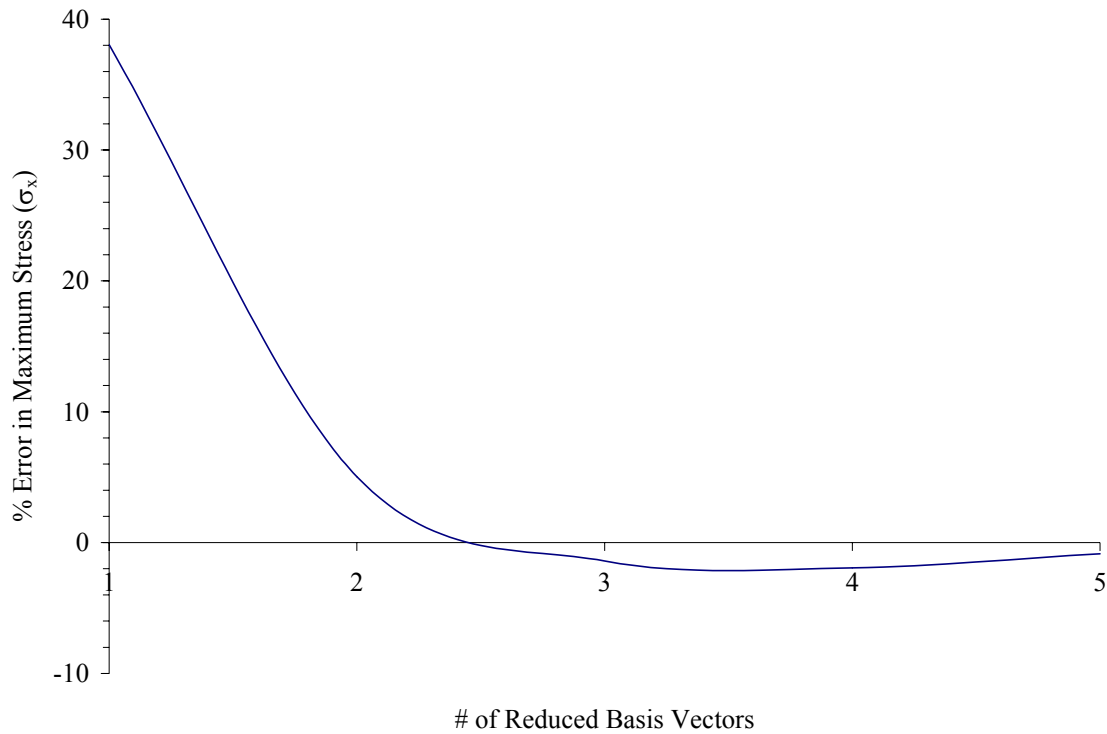


Figure 4.15 (d) % Error in maximum stress (σ_x) variation versus # of reduced basis vectors.

It can be observed that there is 0.0125% error in displacement for three reduced basis vectors. However, the % error in stress is 1.41% for three number of reduced basis vectors when compared with the ANSYS Direct solution and it is 5.19% when compared with theoretical solution. By changing the ellipse orientation such that the major axis is perpendicular to the direction of application of force, the stress concentration increases significantly. The displacement results were obtained based on very fine mesh (# of Elements = 14250, # of Nodes = 14496) since there is no known analytical method.

4.2.5 Conclusion for Case Study # 1

For the design problem solved in Case Study # 1 different hole types were explored and they include the square, circle, and ellipse. The result shows that the stresses were higher in circular hole when compared with a square hole with circular fillet. Furthermore, it is observed that the stresses are still lower in the case of a horizontal elliptical hole. Whereas, stresses increase when vertical elliptical hole is used. Reanalysis methodology can be used very conveniently to change the geometries easily and can be used to explore how stress results vary with each change. Table 4.12 shows the comparison of stress, safety factor and displacement results for all geometric shapes. These are the results when the number of reduced basis vectors is three. The comparison shows for each geometric shape, the ANSYS Direct Analysis result and the Reanalysis algorithm results.

Table 4.12 Comparison redesign options for plate with hole.

Maximum Quantities	Redesign Options					
	# 1: Circular Hole		# 2: Horizontal Ellipse		# 3: Vertical Ellipse	
	ANSYS Direct Analysis	Reanalysis ⁺	ANSYS Direct Analysis	Reanalysis ⁺	ANSYS Direct Analysis	Reanalysis ⁺
σ_x N/mm ²	176.33	179.03	134.28	137.94	298.75	314.27
σ_{VM} N/mm ²	164.40	167.18	126.44	129.53	274.29	288.70
Safety Factor	1.01	1	1.335	1.317	0.599	0.57
U_x ($\times 10^{-1}$ mm)	0.15829	0.15830	0.15704	0.15705	0.15958	0.15956

⁺ Based on three reduced basis vectors

One more observation is in regard to the number of reduced basis vectors used. As discussed by Gullickson [4.1], the displacement results are accurate when the number of reduced basis vectors is three. No past work has considered the stress results. This problem demonstrates that with three reduced basis vectors the stress results are near accurate (less than 2 % of error). The accuracy of results increases when the number of reduced basis vectors is increased. More test cases need to be considered to obtain the optimum number of reduced basis vectors to be used to obtain accurate stresses.

4.3 Case Study # 2: Optimal Shape of Shoulder Fillet in Flat Plate under Tension

Filletts are common features of many load bearing structural components, and as a result, the analysis of stress concentrations at the fillets has been of particular interest. The general geometry and the notation for symmetric flat plate with shoulder fillets, subjected to uniaxial tension loading is shown in Figure 4.16 [4.2]. Here the transition length of the fillet is given as l , the maximum plate width is $2a$, over a length l_a , and the minimum plate width is $2b$ over a length l_b . Therefore the height of the shoulder fillet is $h=a-b$.

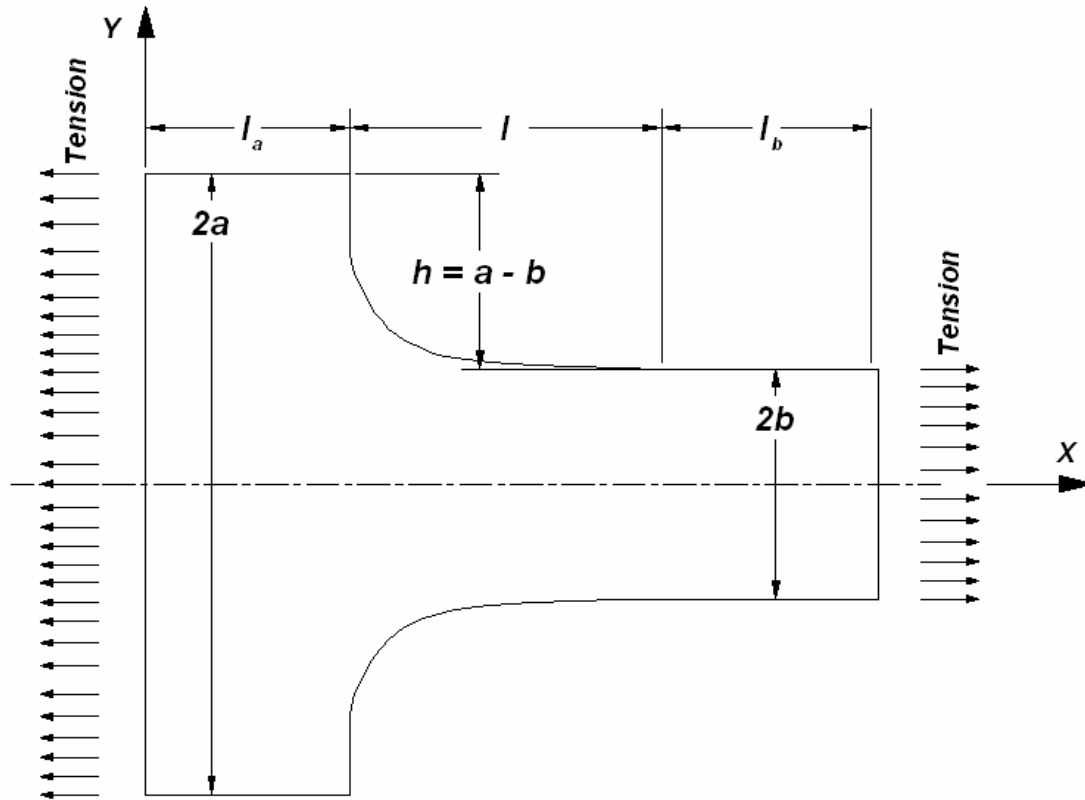


Figure 4.16 Geometry and notation for plate with fillet subjected to tension.

When selecting a suitable fillet, designers often rely on circular or elliptical shapes, for which the stress concentration factors, K_t , are given for some standardized geometries [4.3]. However, as compared to optimal fillet geometry, such circular profiles can be poor in terms of associated K_t , since optimal fillet profiles minimize the peak stress along the fillet contour resulting in large increases in fatigue life for cyclically loaded components. Nevertheless, there have been a number of reasons why circular fillets have historically continued to be common: (i) ease of visualization, drawing and manufacture; (ii) no analytical solutions for true optimal shapes of shoulder fillets in tension available in literature; and (iii) accurate numerical and or experimental methods are needed to determine optimal fillet profiles [4.2].

In the paper by Waldman [4.2], finite element solutions are presented for free-form shapes tension fillets, for a range of constrained shapes. The general approach that is used here is based on an analogy with the growth behavior of biological structures [4.4], where material is added at the region of high stress and removed where the stresses are low. The typical finite element mesh for initial analysis used by Waldman [4.2] is shown in Figure 4.17. Eight-node quadrilateral elements under the plane stress condition were used. The material considered was aluminium alloy with Young's Modulus $E = 72.4$ GPa and Poisson's ratio $\nu = 0.33$. Since the geometry shown in Figure 4.16 is symmetric, half-symmetry was used to construct the finite element model.

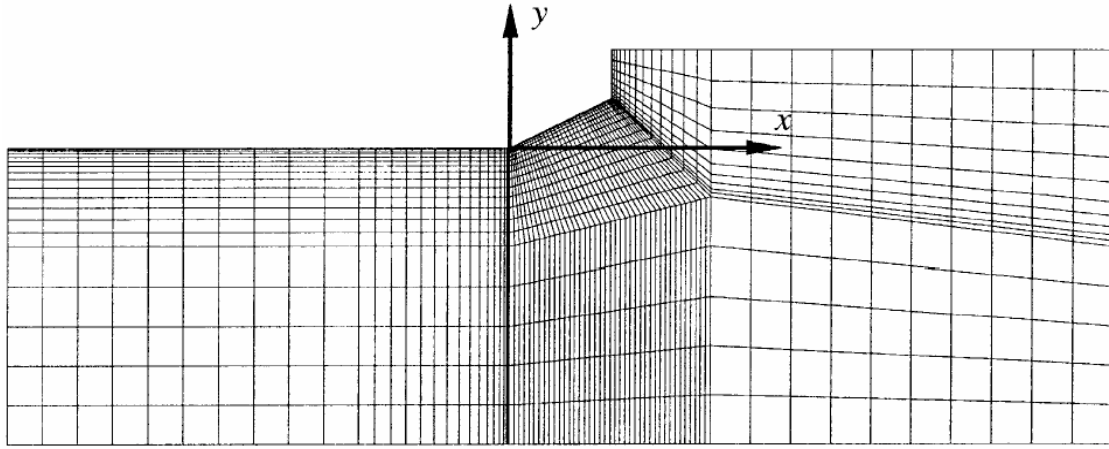


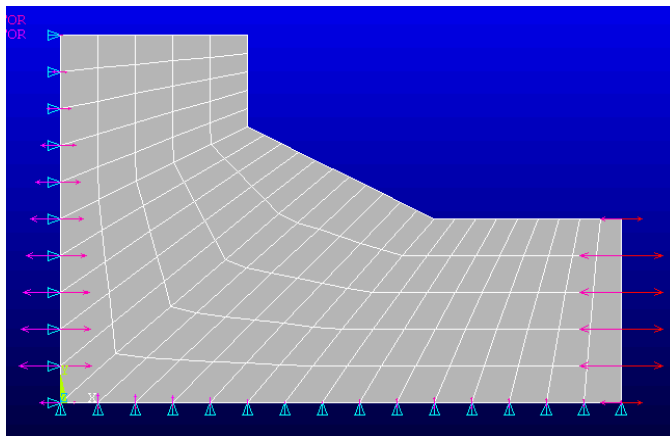
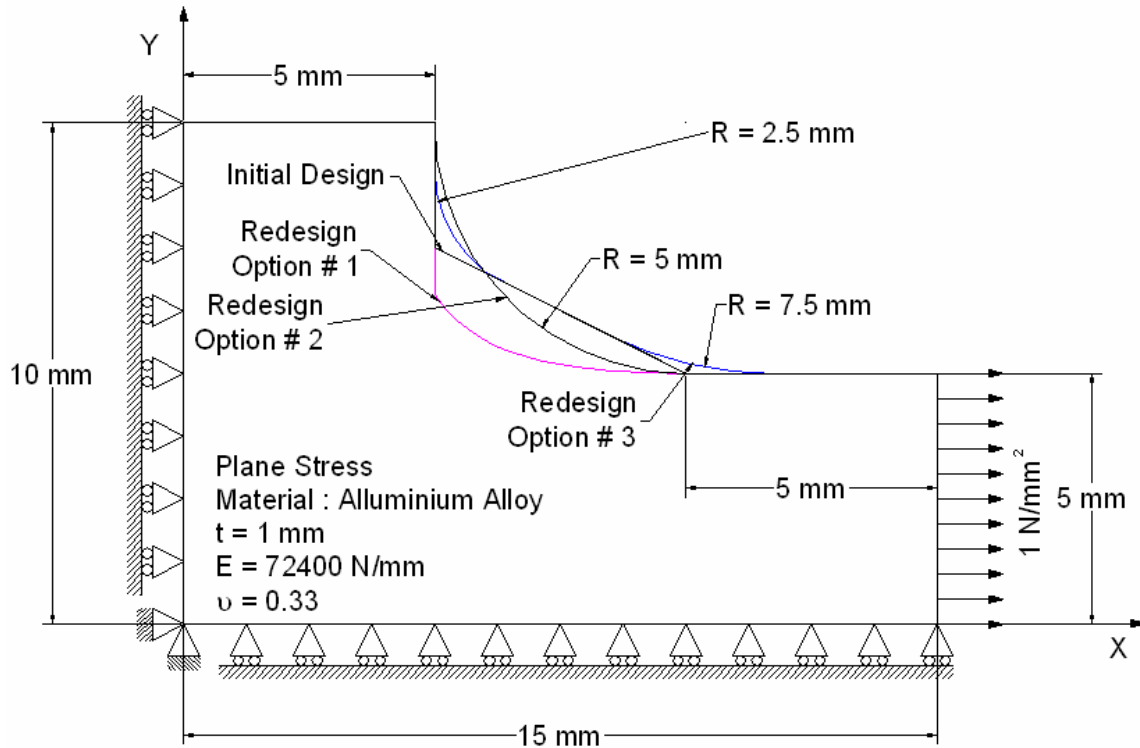
Figure 4.17 Initial mesh used by Waldman [4.2]

Using the mesh shown in Figure 4.17 a finite element analysis is used to solve the problem. Using the tangential stress results generated and using the approach described above, adding material at highly stressed area and removing material from low stress region, the FEM problem is solved repeatedly. The results are produced in the paper including the final geometry for the fillet. It gives the optimal free form shape of the fillets which produces the lower stress concentration factor. The fact that the optimal fillet profile needs to be reproduced accurately in order to deliver the full optimal K_t value is not considered to be a problem, as the modern machining techniques can readily meet the precision requirement.

The work considered by Waldman [4.2] was used as the Case Study # 2 for evaluating the reanalysis methodology developed in this work. The same problem of the flat plate with fillet is solved using the reanalysis techniques. The process is started using the initial geometry used by Waldman [4.2] and Figure 4.18 (b) shows the FEM mesh used for the initial problem. The results of the above work are compared with the result using reanalysis. For reanalysis the fillet geometry is modified to the geometry obtained by Waldman [4.2]. Alternative fillet geometries are also considered which includes, (i) the circular arc fillet and (ii) two circular arcs at two locations. These geometries are described further in Sections 4.3.3 and 4.3.4, respectively.

4.3.1 Initial Design

Figure 4.18 (a) shows the geometries used for the initial design and three redesign options. Figure 4.18 (b) shows the FEM mesh used to solve the initial design. Since the half symmetry of the entire model is used, the displacement U_x of the left vertical face is restrained and displacement U_y is restrained for the bottom horizontal face. The stress applied at the end is kept as 1 N/mm^2 so that assuming it to be the nominal stress, the maximum stress value obtained will be the stress concentration factor for the particular geometry.

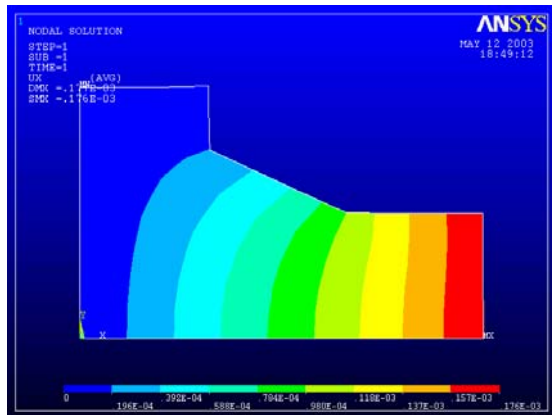


Mesh Characteristics

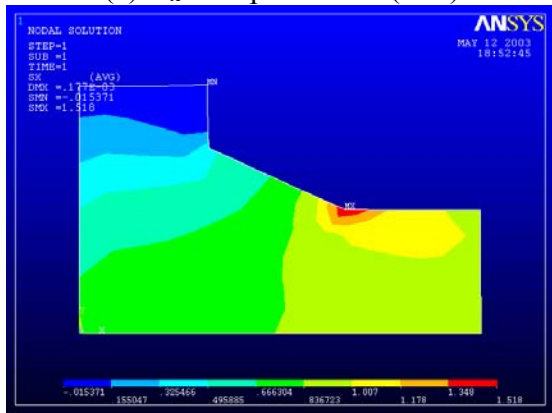
125 # Four-node Quad Elements
 156 Nodes
 2 DOF/Node
 312 Total DOF
 Plane Stress

Figure 4.18 (b) FEM mesh for initial design.

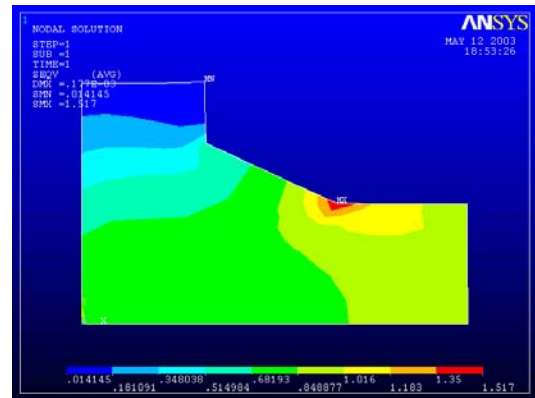
Similar to the Case Study # 1, first the analysis of the initial design is carried out using the ANSYS solver. Figure 4.19 shows the contour plot for the stress and the displacement results. The maximum values of displacement and the stress results are presented in Tables 4.13 and 4.14, respectively. As expected the maximum stress is observed to be at the bottom part of the notch.



(a) U_x – displacement (mm)



(b) σ_x – Normal Stress (N/mm²)



(c) σ_{VM} – von Mises Stress (N/mm²)

Figure 4.19 Contour plot of results for initial design.

Table 4.13 Maximum Deflections (mm)

	U_x	U_y
Node #	12	1
Value	0.17647×10^{-3}	-0.36526×10^{-4}

Table 4.14 Minimum and Maximum stress components (N/mm²)

		σ_x	σ_y	σ_{xy}	σ_{VM}
Minimum	Node #	52	11	51	52
	Value	-0.1537×10^{-1}	-0.17352	-0.36426	0.1414×10^{-1}
Maximum	Node #	32	32	1	32
	Value	1.5184	0.29364	0.1044×10^{-1}	1.5167

It is observed that the maximum value of displacement U_x is 0.176×10^{-3} mm. But the point of concern here is the stress σ_x . Since the nominal stress is 1 N/mm², the solution is the stress concentration factor for this geometry. The stress concentration factor is found to be $K_t = 1.5184$. There is no way to check this value therefore, no hand analysis was performed. The focus in this case study is the stress concentration factor for

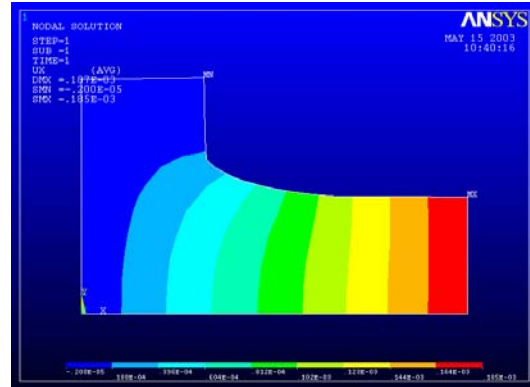
the modified geometry. Furthermore, reanalysis methods are applied and the above geometry is changed to different shape to check the accuracy of the reanalysis algorithm.

4.3.2 Redesign Option # 1: Plate with Free-form Fillet

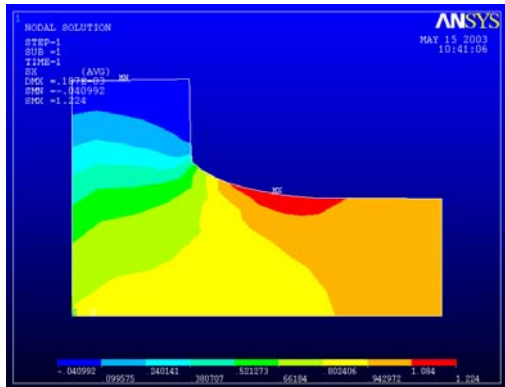
A similar process as discussed in Section 4.2.2 (Redesign Option # 1 of Case Study # 1) is applied for solving the reanalysis of this problem. Here the geometry is changed to optimum shape geometry as quoted by Waldman [4.2]. His paper gives the coordinates of the optimum shape for the free-form fillet. The coordinates are used to create the “Key-points” in the above geometry. A “Spline” is generated which goes through these points. This “Spline” is used as the reference to create the modified geometry. During the “RE_MODEL” (Section B.3), the boundary nodes at the fillet are repositioned to the “Spline” such that the final geometry obtained is the free-form optimum fillet. Figure 4.20 shows contour plots of the displacement and stress.

Mesh Characteristics

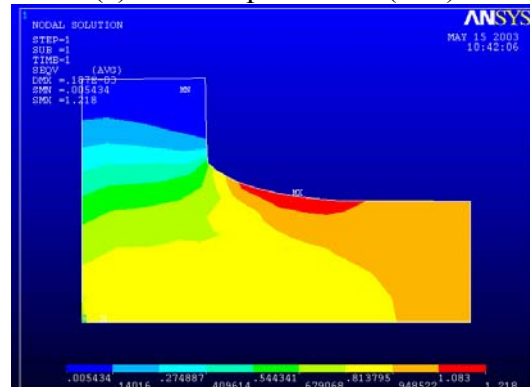
125 Four-node Quad Elements
156 Nodes
2 DOF/Node
312 Total DOF



(a) U_x – Displacement (mm)



(b) σ_x – Normal Stress (N/mm²)



(c) σ_{VM} – von Mises Stress (N/mm²)

Figure 4.20 Contour plot of results for Redesign Option # 1.

Table 4.15 Maximum Deflections (mm)

	U_x	U_y
Node #	27	1
Value	0.18524×10^{-3}	-0.35971×10^{-4}

Table 4.16 Minimum and Maximum Stress Components (N/mm²)

		σ_x	σ_y	σ_{xy}	σ_{VM}
Minimum	Node #	58	10	46	64
	Value	-0.40992×10^{-1}	-0.18609	-0.37165	0.54336×10^{-2}
Maximum	Node #	49	46	1	49
	Value	1.2241	0.31196	0.14363×10^{-1}	1.2180

In this case the maximum stress concentration was found to be at the bottom of the fillet. The value of stress concentration factor is much less than the initial design. After the reanalysis, when keeping the number of reduced basis vectors to be three, the stress concentration factor is $K_t = 1.224$. Whereas, Waldman [4.2] has commented on it to be $K_t = 1.242$. Thus there is 1.44% difference in the result. The obtained value of K_t after reanalysis is less. Since, the mesh used in this work is not as fine as used by Waldman.

Furthermore, to check the variation of the stresses and the displacements, additional reanalysis were carried out by changing the number of reduce basis vectors. For checking purpose the number of reduced basis vectors varied form 1 to 5. The results are presented in Table 4.17.

Table 4.17 Comparison of maximum results for Redesign Option # 1.

Maximum Quantities		Theoretical	ANSYS Direct Analysis	Reanalysis Reduced Basis Vectors				
				1	2	3	4	5
σ_x N/mm ²	Value	1.242 [†]	1.214	1.520	1.197	1.224	1.205	1.201
	Node #	-	51	32	33	49	51	51
σ_{VM} N/mm ²	Value	1.242 [†]	1.213	1.521	1.203	1.218	1.211	1.198
	Node #	-	49	32	46	49	49	49
U_x $\times 10^{-3}$ mm	Value	0.1861 [*]	0.1856	0.1823	0.1848	0.1852	0.1852	0.1852
	Node #	-	27	12	12	27	27	27

Note:

* Theoretical value of displacement, is based on very fine mesh of four-node quadrilateral elements (# of Elements = 12500, # of Nodes = 12801).

† Stress results from Waldman's [4.2].

Table 4.17 summarizes the results obtained by reanalysis. The three different rows shows the (i) the maximum value of the stress in X – direction, i.e., σ_x in N/mm², (ii) maximum value of von Mises stress, i.e., σ_{VM} in N/mm² and (iii) maximum value of displacement in X – direction, i.e. U_x in $\times 10^{-3}$ mm. The first column shows the theoretical value, however for stress and displacements theoretical value is not known. The stresses the values provided by Waldman [4.2] were used as a reference. The theoretical value for displacement was obtained using a fine mesh and the results are compared to the reanalysis solutions. The column with heading ANSYS shows the ANSYS direct analysis solution. The same mesh that is used in the reanalysis was solved by the ANSYS solver i.e., no reanalysis solver was used for comparing the results. Next five columns show the reanalysis results with the number of reduced basis vectors

varying from 1 to 5. Figure 4.21 shows the variation of the results when increasing the number of reduced basis vectors.

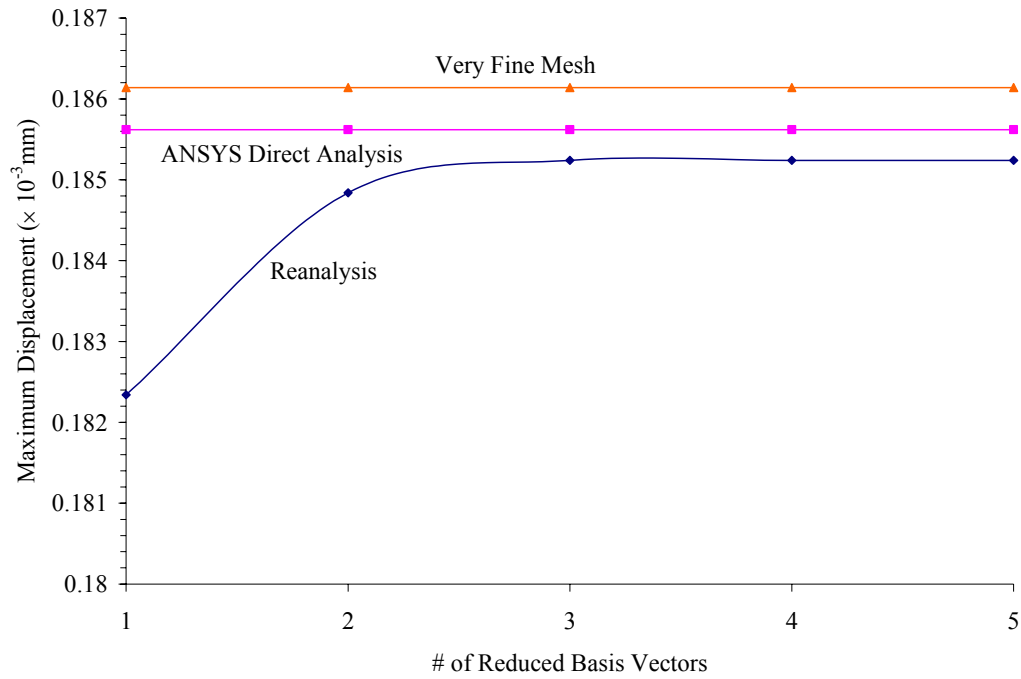


Figure 4.21 (a) Maximum displacement (U_x) variation versus # of reduced basis vectors.

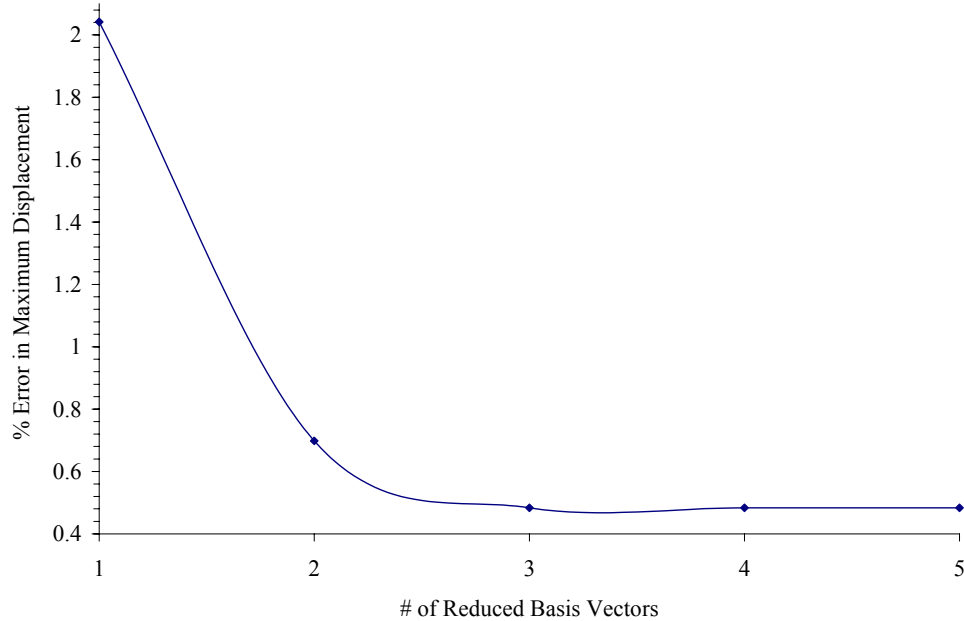


Figure 4.21 (b) % Error in Maximum displacement versus # of reduced basis vectors.

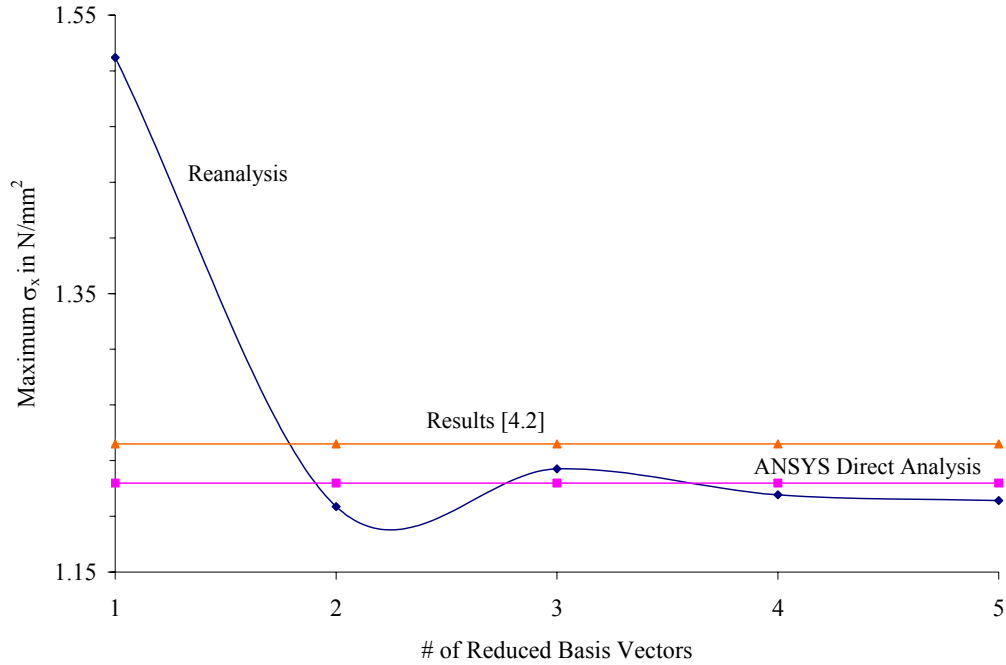


Figure 4.21 (c) Maximum stress (σ_x) variation versus # of reduced basis vectors.

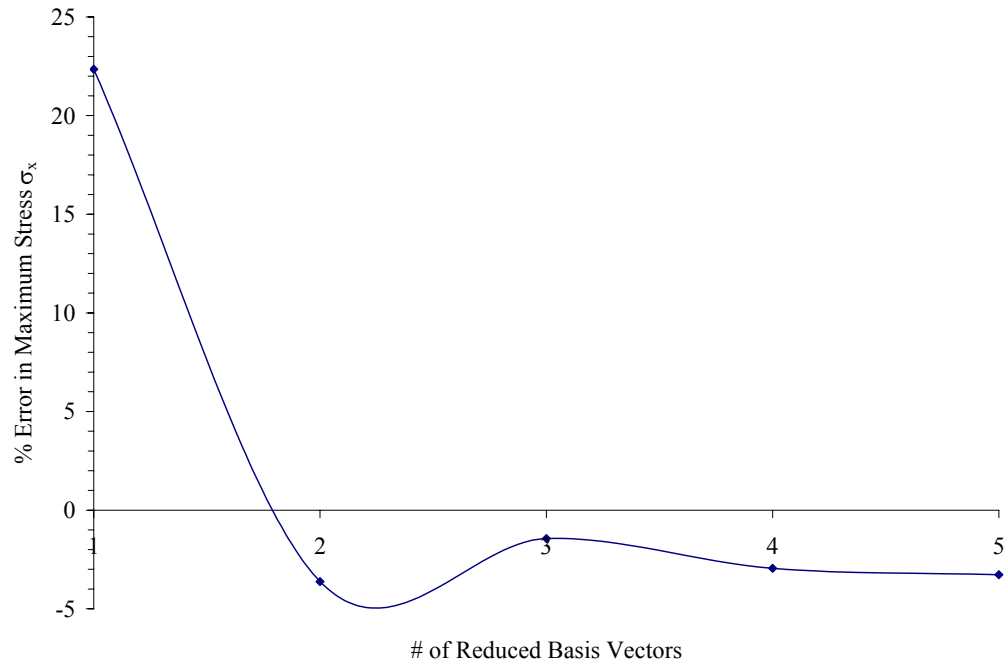


Figure 4.21 (d) % Error in maximum stress (σ_x) variation versus # of reduced basis vectors.

Figure 4.21 (a) shows the variation of the displacement results with increase in the number of reduced basis vectors. The displacement values are not observed to exactly match the reference value (which is the value obtained after carrying out the analysis with extremely fine mesh) in this case. However, the % error in the displacement results is observed to be very low, i.e., 0.48% (Figure 4.21(b)) using three reduced basis vectors.

Thus the results are acceptable. As far as the stress results are concerned, the % error in the stress when compared with the theoretical value (values given by Waldman [4.2] in his paper) is only 3.2 % with five reduced basis vectors. However, when the number of reduced basis vector equals to three the % error in the stress value is 1.44 %. This value of reduced basis vectors will be used in this work. As discussed by Gullickson [4.1], for fairly good accuracy and less computational efforts the number of reduced basis vectors should be kept as three.

4.3.3 Redesign Option # 2: Plate with Circular Arc Fillet

In this Redesign Option and the next, even though it is observed that the stress concentration factor in Option # 1 is found to be lower, different geometric options for the fillet are explored to check the stress concentration factor. In this case the geometry is changed to a circular fillet at the corner as shown in Figure 4.18. Here a circular arc is added to reduce the stress concentration. A similar method of reanalysis is used and Figure 4.22 shows the contour plot of the stress and displacement results. The reanalysis will use the solution for the initial design discussed in Section 4.3.1 as the base for generating results for the new design option. The results are also presented in tabular form for displacement and stress in Tables 4.18 and 4.19, respectively.

Table 4.18 Maximum Deflections (mm)

	U_x	U_y
Node #	27	1
Value	0.18024×10^{-3}	-0.36539×10^{-4}

Table 4.19 Minimum and Maximum stress components (N/mm²)

		σ_x	σ_y	σ_{xy}	σ_{VM}
Minimum	Node #	52	10	48	60
	Value	-0.81206×10^{-2}	0.18712	-0.4085	0.10157×10^{-1}
Maximum	Node #	50	49	1	50
	Value	1.3890	0.30406	0.1×10^{-1}	1.4096

Mesh Characteristics

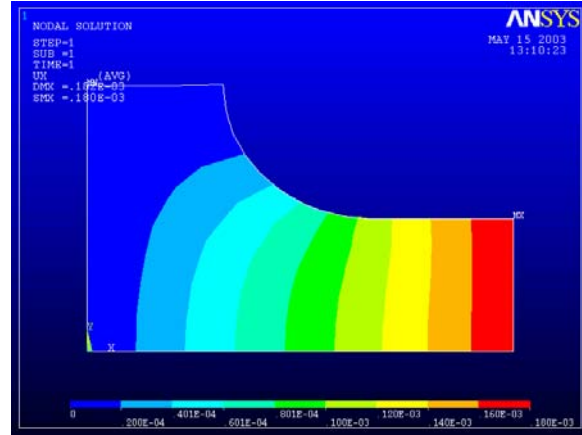
125 Four-node Quad Elements

156 Nodes

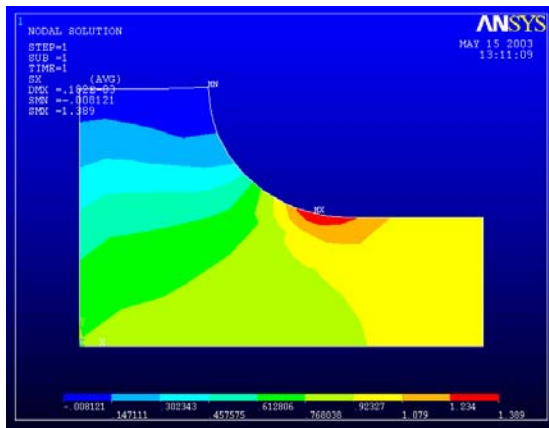
2 DOF/Node

312 Total DOF

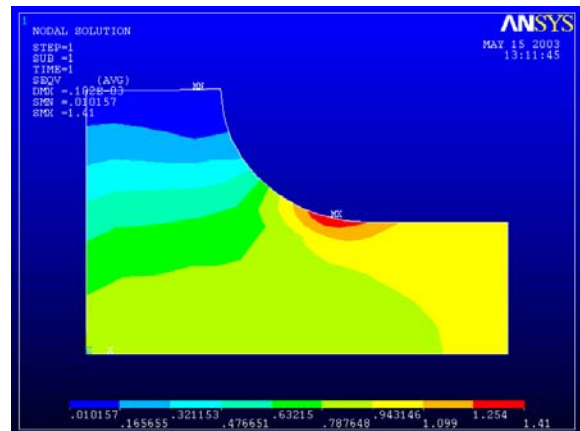
Plane Stress



(a) U_x – Displacement (mm)



(b) σ_x – Normal Stress (N/mm²)



(c) σ_{VM} – von Mises Stress (N/mm²)

Figure 4.22 Contour plot of results for Redesign Option # 2.

In this problem, the number of reduced basis vectors is equal to three. The analysis for varying the number of reduced basis vectors is not considered. Table 4.20 shows a comparison of these results with respect to the theoretical answer and also with respect to ANSYS solution when the same problem is solved using the ANSYS solver.

The results in Table 4.20 show that for displacements, % error is 0.68 % when compared with the theoretical value. The theoretical value is based on the ANSYS solution for a very fine mesh (# of elements = 12500 and # of nodes = 12801). If the same is compared with the ANSYS direct analysis solution for the same mesh, then the % error is found to be 0.19%. For comparing stresses, (i.e., the stress concentration factor in this problem) when compared with the theoretical value, the % error is found to be 1.1%. The theoretical value is calculated in Appendix E. When compared with ANSYS direct analysis result for the same mesh yields 0.27 %.

Table 4.20 Comparison of results for Redesign Option # 2

Maximum Quantities		Theoretical	ANSYS Direct Analysis	Reanalysis ⁺
σ_x N/mm ²	Value	1.3734	1.3852	1.3890
	Node #	-	51	50
σ_{VM} N/mm ²	Value	1.3734	1.3932	1.4096
	Node #	-	50	50
U_x $\times 10^{-3}$ mm	Value	0.18148*	0.18058	0.18024
	Node #	-	27	27

Note:

* Theoretical value of displacement is based on very fine mesh of four-node quadrilateral elements (# of elements = 12500, # of nodes = 12801).

⁺ Reanalysis based on initial design using three basis vectors.

4.3.4 Redesign Option # 3: Plate with Two Circular Arc Fillets

Redesign Option # 3 considers a small circular arc that is added at the two corners of the fillet. The dimensions of the arcs can be found in Figure 4.18. The reanalysis results are shown in Figure 4.23 as contour plots and Tables 4.21 and 4.22 shows the displacement and stress results, respectively.

Mesh Characteristics

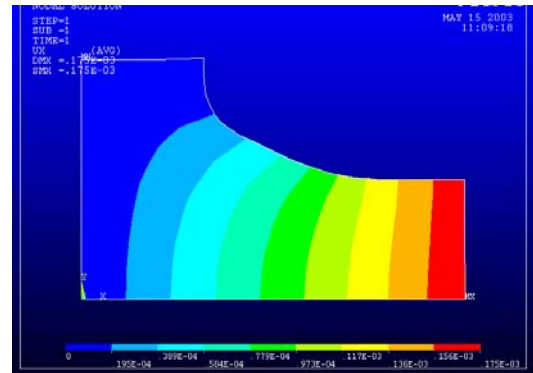
125 Four-node quadrilateral Elements

156 Nodes

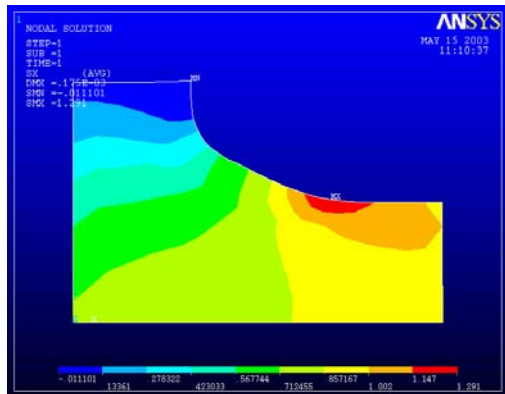
2 DOF/Node

312 Total DOF

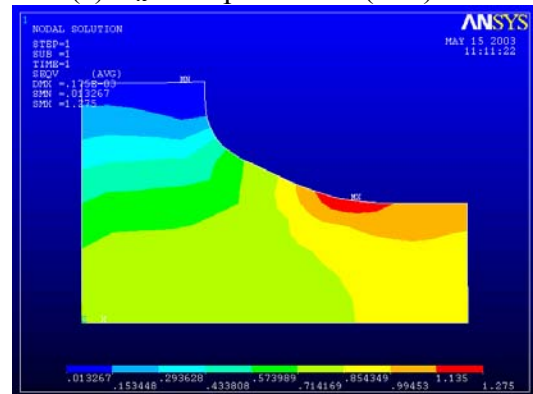
Plane Stress



(a) U_x – Displacement (mm)



(b) σ_x – Normal Stress (N/mm²)



(c) σ_{vM} – von Mises Stress (N/mm²)

Figure 4.23 Contour Plot of results for Redesign Option # 3.

Table 4.21 Maximum Deflections (mm)

	U_x	U_y
Node #	12	1
Value	0.17517×10^{-3}	-0.36403×10^{-4}

Table 4.22 Minimum and Maximum stress components (N/mm²)

		σ_x	σ_y	σ_{xy}	σ_{VM}
Minimum	Node #	52	11	50	60
	Value	-0.111×10^{-1}	0.1759	-0.31285	0.13267×10^{-1}
Maximum	Node #	33	32	11	33
	Value	1.2913	0.20431	0.10479	1.2749

The number of reduced basis vectors is equal to three in this redesign option. The analysis for varying the number of reduced basis vectors from one to five is not considered. Table 4.23 shows the comparison of these results with respect to the theoretical answer and also with respect to ANSYS solution when the same problem is solved using the ANSYS solver. The theoretical value of stress concentration factor for this geometry is not available therefore, a very fine mesh was used.

Table 4.23 Comparison of maximum results for Redesign Option # 3.

Maximum Quantities		Theoretical	ANSYS	Reanalysis ⁺
σ_x N/mm ²	Value	1.3224*	1.288	1.2913
	Node #	-	33	33
σ_{VM} N/mm ²	Value	1.3408*	1.2727	1.2749
	Node #		33	33
U_x $\times 10^{-3}$ mm	Value	0.17591*	0.17543	0.17517
	Node #	-	12	12

Note:

* Theoretical value of displacement is based on a very fine mesh of four-node quadrilateral elements (# of elements = 12500, # of nodes = 12801)

⁺ Reanalysis based on initial design using three basis vectors.

The results in Table 4.23 show that for displacements, % error is 0.42 % when compared with the theoretical value and is 0.15 % when compared with the ANSYS direct analysis solution for the same mesh. When comparing stresses (i.e., the stress concentration factor in this problem) with the theoretical value, the % error is found to be 2.35% whereas, when compared with ANSYS direct analysis result for the same mesh it is found to be 0.26 %.

4.3.5 Conclusion for Case Study # 2

The main objective in this problem was to use the reanalysis method to verify whether the same results are obtained for K_t using the free-form geometry of the fillet as discussed by Waldman [4.2]. The stress concentration factor values obtained by

reanalysis for the free-form geometry were observed to be consistent with the values obtained by Waldman resulting in an error of 1.44%. By keeping the number of reduced basis vectors to be equal to three, fairly accurate results were obtained for stresses. Therefore, in future case studies only three reduced basis vectors will be used. Table 4.24 provides a comparison of results for all fillet shapes.

Table 4.24 Comparison of maximum results for the three redesign options.

Maximum Quantities	Redesign Options					
	# 1: Free-form Fillet		# 2: Circular Arc Fillet		# 3: Two Circular Arcs	
	ANSYS Direct Analysis	Reanalysis ⁺	ANSYS Direct Analysis	Reanalysis ⁺	ANSYS Direct Analysis	Reanalysis ⁺
σ_x N/mm ²	1.2138	1.2241	1.3852	1.3892	1.288	1.2913
σ_{VM} N/mm ²	1.2127	1.2180	1.3932	1.4096	1.2727	1.2749
U_x ($\times 10^{-3}$ mm)	0.18562	0.18524	0.18058	0.18024	0.17543	0.17517

⁺ Reanalysis results are based on three reduced basis vectors.

4.4 Case Study # 3: Support Bracket Redesign

Case Study # 3 considers the redesign of support. The idea is to design a support which will act as a cantilever beam, will support a load at the end and will be fixed on two pin holes. Figure 4.24 shows the geometry of the initial design and three redesign options considered. Figure 4.25 shows the dimensions for the initial design and the three redesign options. The finite element models have the same geometry. The pins are represented by nodes lying on the circle that are constrained in X and Y translational DOFs. A point load of 50 N is applied at the free end. The following items are considered by the engineer in the redesign process:

1. The support shown in Figure 4.24 is loaded such that the maximum stress will be at the fillet due to a compressive bending stress.
2. The stress varies linearly with the distance from the load application point. The area in the vicinity of the point force is under-stressed. Therefore, the cross-sectional thickness can be reduced in this region.
3. The maximum stress will reduced by increasing the fillet radius.

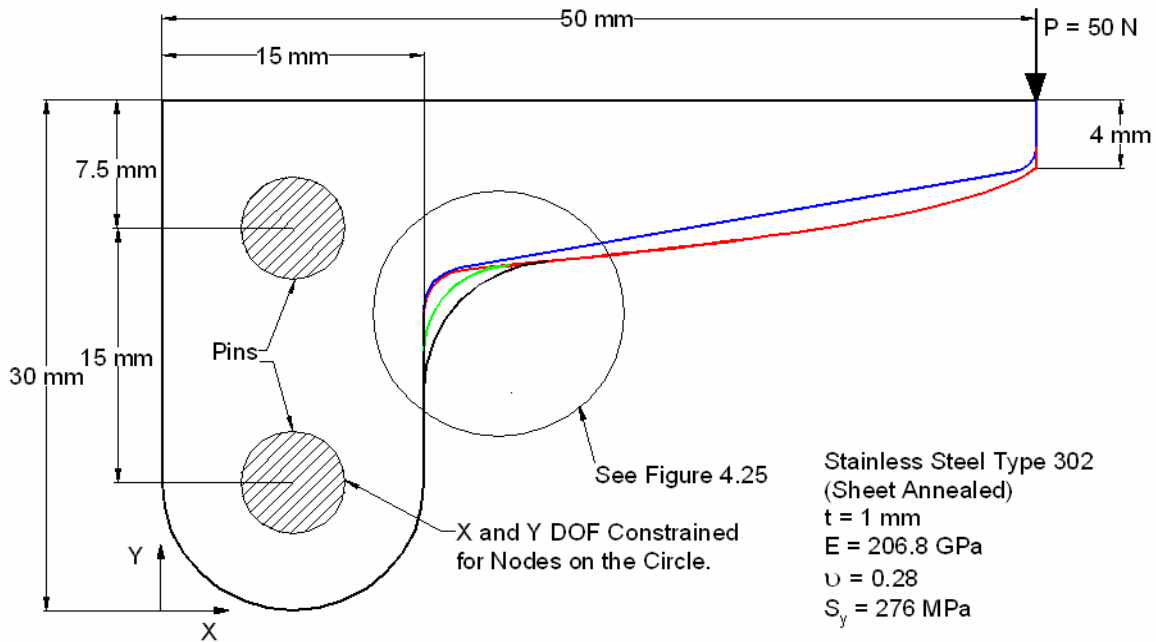


Figure 4.24 Support geometry

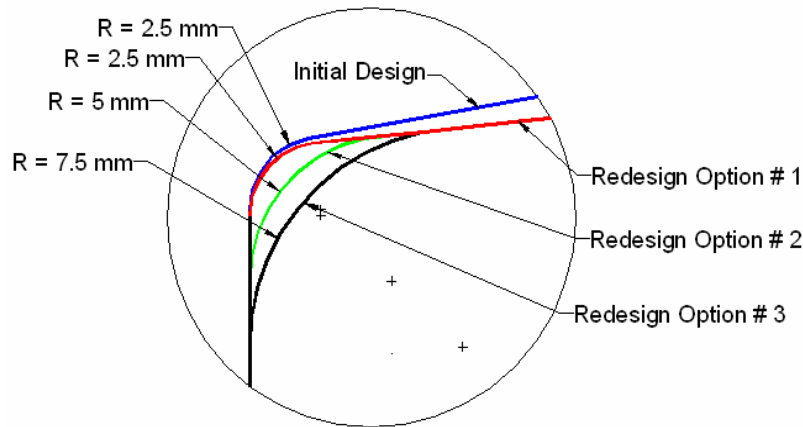
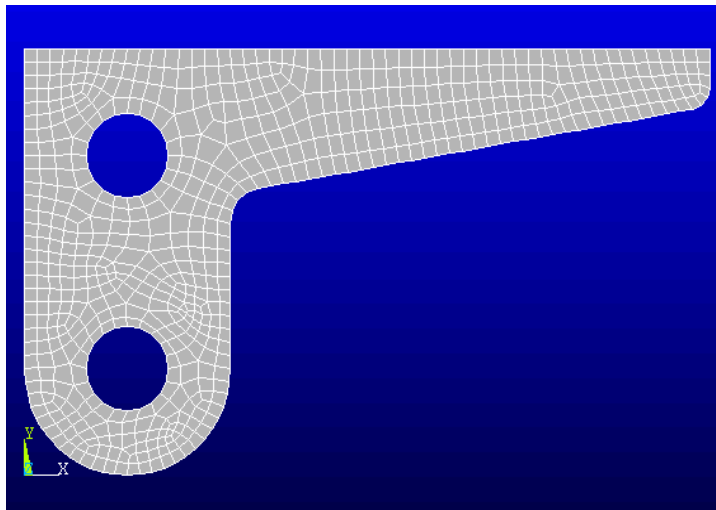


Figure 4.25 Initial design and redesign options for case study # 3

4.4.1 FEM Model and ANSYS Analysis

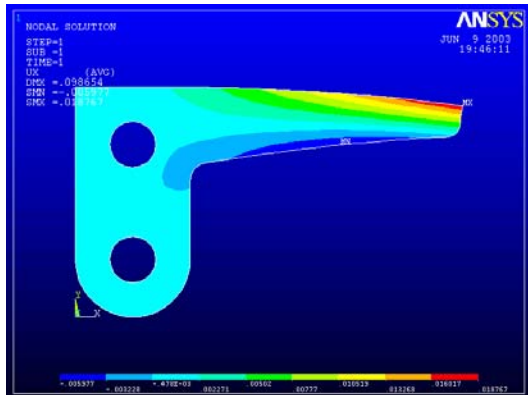
Figure 4.24 shows the initial problem and it represents a first design concept proposed by the engineer. Since the support is like a cantilever beam, the maximum bending stress will be lower at the free end and increases near the support. The initial design considered a tapered support such that the depth varies from minimum to maximum away from the free end. The ANSYS analysis solution is generated using the ANSYS solver for the initial design. The mesh consists of element type PLANE42 and the problem is assumed plane stress with thickness. Figure 4.26 shows the FEM mesh and states the mesh characteristics. The results of ANSYS analysis are shown in Figure 4.27. Tables 4.25 and 4.26 shows the displacement and the stress results, respectively.



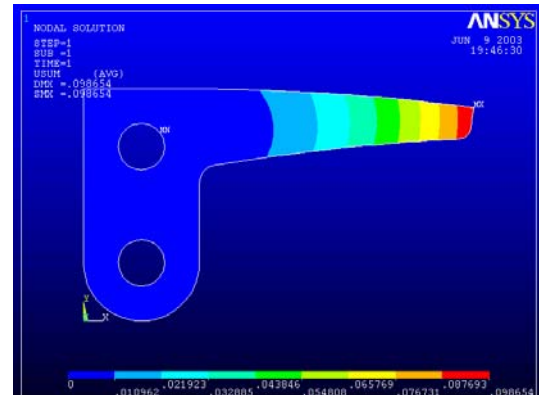
Mesh Characteristics

349 Four-node Quad Elements
415 Nodes
2 DOF/Node
830 Total DOF
Plane Stress

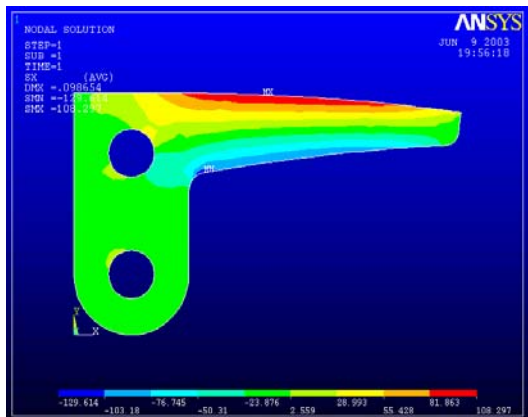
Figure 4.26 FEM Mesh for Initial Design of Case Study # 3.



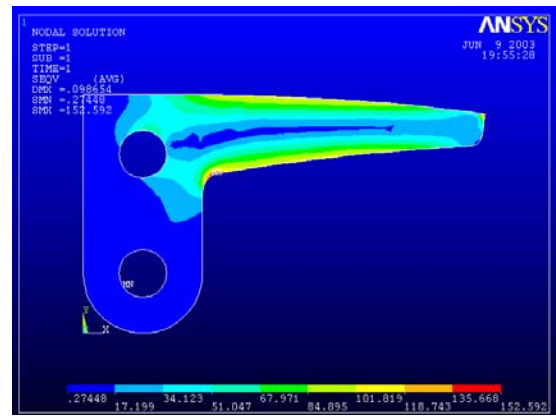
(a) U_x – Displacement (mm)



(b) U_{SUM} – Displacement vector sum (mm)



(c) σ_x – Normal Stress (N/mm²)



(d) σ_{VM} – von Mises Stress at Fillet (N/mm²)

Figure 4.27 Contour plot of results.

Table 4.25 Maximum Deflections (mm)

	U_x	U_y
Node #	43	43
Value	0.18767×10^{-1}	-0.9685×10^{-1}

Table 4.26 Minimum and Maximum stress components (N/mm²)

		σ_x	σ_y	σ_{xy}	σ_{vM}
Minimum	Node #	2	43	5	176
	Value	-129.61	-121.55	-62.146	0.27448
Maximum	Node #	56	192	179	5
	Value	108.30	19.739	33.690	152.59

One can observe that the absolute maximum stress is at the fillet and is compressive. The von Mises stress at the fillet is 152.6 N/mm². The material has yield strength of 276 N/mm² resulting in a safety factor of 1.81. The aim in this redesign process is to have an optimum shape with a safety factor of about 2.

4.4.2 Redesign Option # 1: Optimum thickness for uniform stress distribution

The tapered shape is designed to have a uniform stress distribution as discussed earlier. From Figure 4.27 (d) it can be seen that the von Mises stress distribution is approximately uniform at the outer fiber. A straight taper is not the optimum shape for a uniform stress distribution. For the cantilever beam with point load we know that the bending stress varies linearly. The maximum at the support end and minimum, i.e., zero at the end where the load is getting applied. Therefore, at any distance x from the load, the maximum bending stress is,

$$\sigma_x^{\max} = \frac{M \cdot y}{I} = \frac{(P \cdot x) \cdot \frac{h}{2}}{\frac{1}{12} \cdot b \cdot h^3}$$

where,

σ_x^{\max} = Maximum bending stress allowable.

P = Applied load.

h = Height of cross-sectional area

b = Width of cross section (it is the thickness for the plane stress problem which is 1.)

Using this information the variation of height h with respect to x is given as,

$$h = \sqrt{\frac{6 \cdot P}{\sigma}} \cdot \sqrt{x}$$

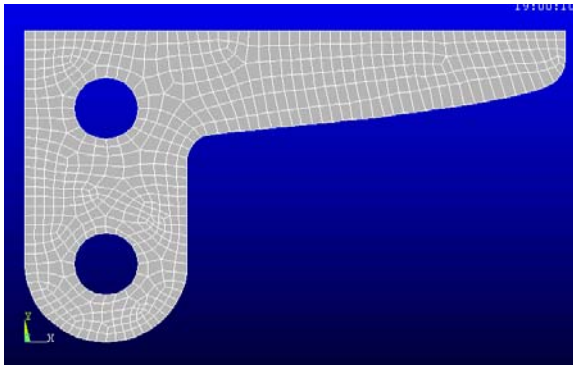
This equation shows that for uniform bending stress distribution, the height h must be function of \sqrt{x} . Thus, for Redesign Option # 1 the geometry is modified to be the function of \sqrt{x} as shown in Figure 4.28(a). Tables 4.27 and 4.28 state the displacement and stress results for the reanalysis, respectively. The contour plots of the results are shown in Figure 4.28.

Table 4.27 Maximum Deflections (mm)

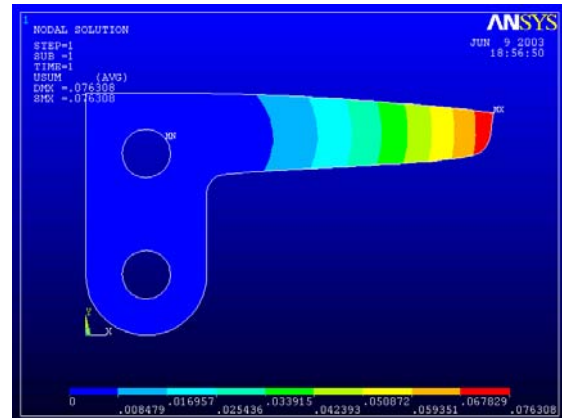
	U_X	U_Y
Node #	43	43
Value	0.15196×10^{-1}	-0.74779×10^{-1}

Table 4.28 Minimum and Maximum stress components at fillet (N/mm²)

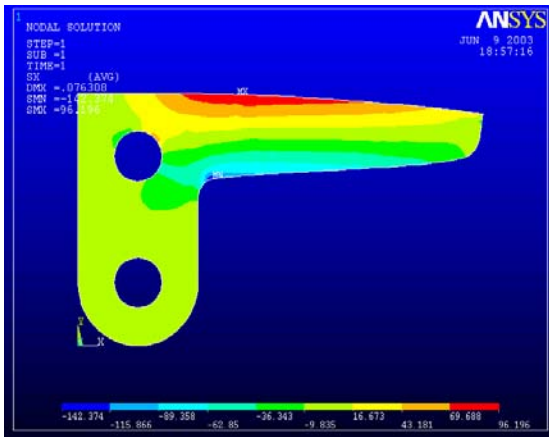
		σ_x	σ_y	σ_{xy}	σ_{VM}
Minimum	Node #	2	43	5	176
	Value	-142.37	-124.86	-62.044	0.25278
Maximum	Node #	51	192	179	5
	Value	96.196	19.546	33.477	159.40



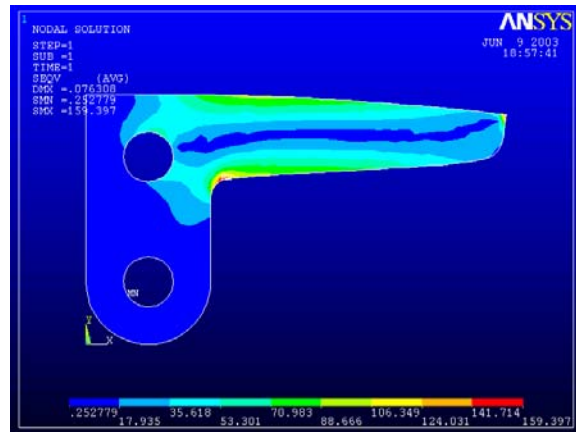
(a) FE Mesh for the Model



(b) U_{SUM} – Displacement Vector Sum (mm)



(c) σ_x – Normal Stress (N/mm²)



(d) σ_{VM} – von Mises Stress (N/mm²)

Figure 4.28 Contour plots for Redesign Option # 1.

The von Mises Stress contour plot shows that the stress is approximately uniform throughout the length of the support. To compare the reanalysis results, the same mesh is solved using the ANSYS solver (ANSYS Direct Analysis) and a fine mesh (# of elements

= 1508, # of nodes = 1654) to obtain the displacement and the stress results at the fillet. Table 4.29 shows a comparison of all these results. The reanalysis is based on three reduced basis vectors.

Table 4.29 Comparison of maximum results for Redesign Option # 1.

Maximum Quantities		Fine Mesh *	ANSYS Direct Analysis	Reanalysis +
Compressive σ_x N/mm ²	Value	-152.47	-138.77	-142.37
	Node #	-	2	2
σ_{VM} N/mm ²	Value	165.71	152.39	159.40
	Node #	-	5	5
U_Y $\times 10^{-1}$ mm	Value	-0.74888	-0.74787	-0.74779
	Node #	-	43	43

* Theoretical value of displacement is based on a very fine mesh of four-node quadrilateral elements (# of elements = 1508, # of nodes = 1654)

+ Reanalysis based on initial design using three basis vectors.

The result demonstrates that for three reduced basis vectors yields a % error in maximum displacement U_Y of 0.01% when compared to the ANSYS Direct Analysis. Being higher in absolute value, U_Y is considered as the basis of comparison. The % error in the maximum compressive stress σ_x is 2.6 % compared with ANSYS direct analysis results and is 6.6% when compared with the fine mesh. The von Mises stress yields the % error of 4.6 % compared with the ANSYS direct analysis and 3.8 % when compared with the fine mesh. Overall, the von Mises stresses the safety factor of 1.73. However, this value is too low since a factor of safety of 2 is required. Therefore, the fillet must be changed.

4.4.3 Redesign Option # 2: Fillet Radius of 5 mm

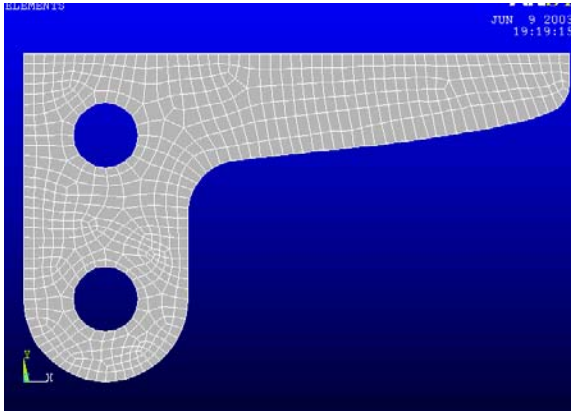
Keeping the optimum shape of the taper, the fillet radius is increased from 2.5 to 5 mm in Redesign Option # 2 as shown in Figure 4.25. The reason why the fillet size is increased is to reduce the stress level at the fillet in turn increasing the safety factor. After performing the reanalysis the results are presented in Tables 4.30 and 4.31 for displacement and stresses, respectively. Figure 4.29 shows the contour plots of results.

Table 4.30 Maximum Deflections (mm)

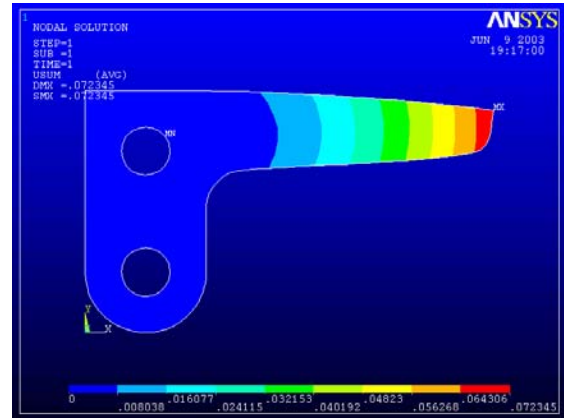
	U_X	U_Y
Node #	43	43
Value	0.14729×10^{-1}	-0.70830×10^{-1}

Table 4.31 Minimum and Maximum stress components (N/mm²)

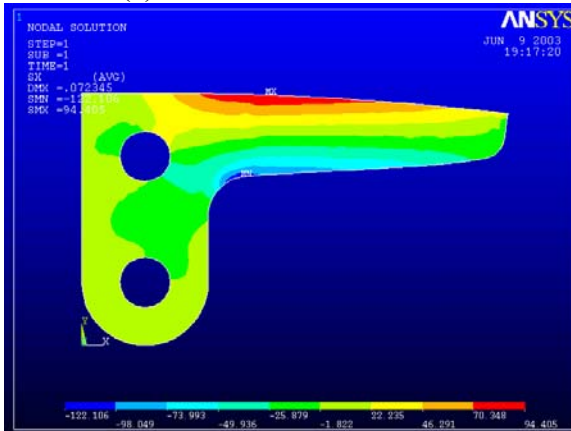
		σ_x	σ_y	σ_{xy}	σ_{VM}
Minimum	Node #	38	43	5	83
	Value	-122.11	-122.09	-45.530	0.24185
Maximum	Node #	53	192	179	43
	Value	94.405	16.467	30.070	140.95



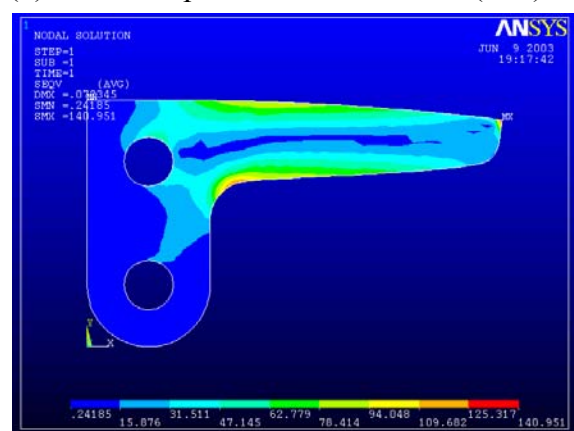
(a) FE Mesh for the Model



(b) U_{SUM}– displacement vector sum (mm)



(c) σ_x – Normal Stress (N/mm²)



(d) σ_{VM} – vonMises Stress (N/mm²)

Figure 4.29 Contour Plots for Redesign Option # 2

The maximum von Mises stress at the fillet has been reduced due to increase in fillet size. Comparing the reanalysis results, the same mesh is solved using the ANSYS solver a very fine mesh (# of elements =1430, # of nodes = 1572). Table 4.32 shows a comparison of all these results. The reanalysis is based on three number of reduced basis vectors.

Table 4.32 Comparison of maximum results at fillet for Redesign Option # 2.

Maximum Quantities		Fine Mesh *	ANSYS Direct Analysis	Reanalysis +
Compressive σ_x N/mm ²	Value	-125.92	-121.71	-122.11
	Node #	-	38	38
σ_{VM} N/mm ²	Value	132.29	123.55	126.96
	Node #	-	39	39
U_Y $\times 10^{-1}$ mm	Value	-0.70602	-0.70850	-0.70830
	Node #	-	43	43

* Theoretical value of displacement is based on a very fine mesh of four-node quadrilateral elements (# of elements = 1430, # of nodes = 1572)

+ Reanalysis based on initial design using three basis vectors.

From the results it is seen that three reduced basis vectors yields the % error in maximum displacement of 0.03% when compared to the ANSYS Direct Analysis results. The % error in maximum compressive stress σ_x is 0.3 % when compared with ANSYS direct analysis and is 3.0% when compared to the fine mesh. The % error for von Mises stresses is 2.76 % compared with the ANSYS direct analysis and 4.02 % when compared with the fine mesh. Overall, the von Mises stresses yields a safety factor of 2.2 which is very good. Designer can stop here having the safety factor above 2.

4.4.4 Redesign Option # 3: Fillet Radius of 7.5 mm

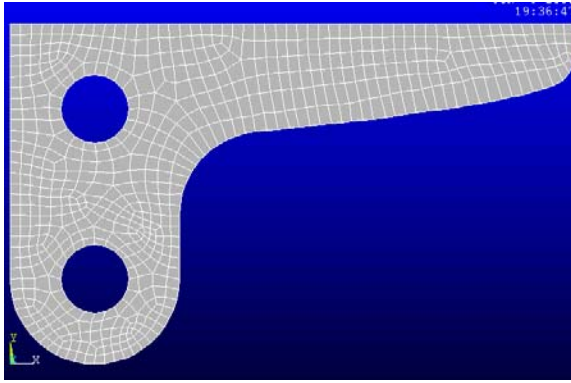
Keeping the optimum shape of the taper, the fillet radius was increased from 2.5 to 5 mm in Redesign Option # 2 resulting in a safety factor of 2.2. In redesign Option # 3 the fillet radius is further increased to 7.5 to demonstrate the use of reanalysis method. The reanalysis results are presented in Tables 4.33 and 4.34 for displacement and stresses, respectively. Figure 4.30 shows the contour plots for the results.

Table 4.33 Maximum Deflections (mm)

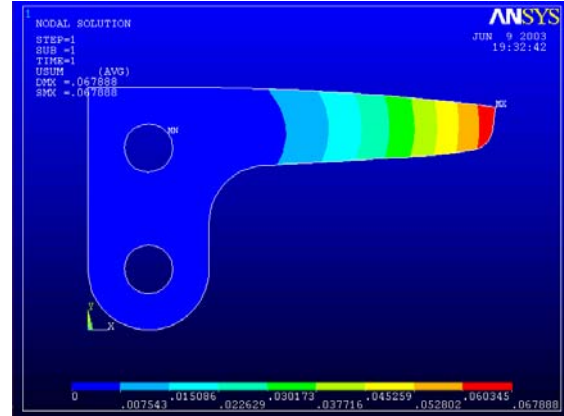
	U_X	U_Y
Node #	43	43
Value	0.14165×10^{-1}	-0.66394×10^{-1}

Table 4.34 Minimum and Maximum stress components (N/mm²)

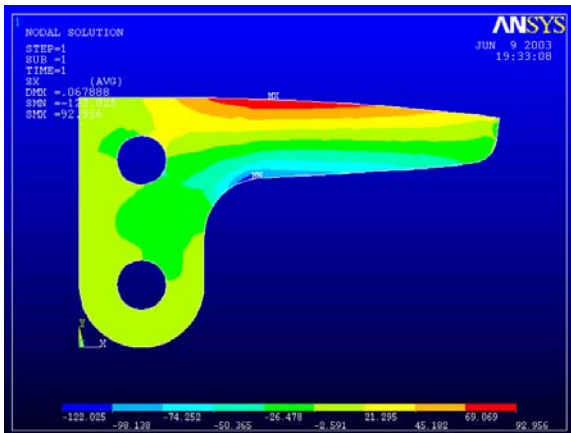
		σ_x	σ_y	σ_{xy}	σ_{VM}
Minimum	Node #	36	43	38	83
	Value	-122.03	-122.36	-39.579	0.21127
Maximum	Node #	54	82	179	43
	Value	92.956	15.071	26.577	141.26



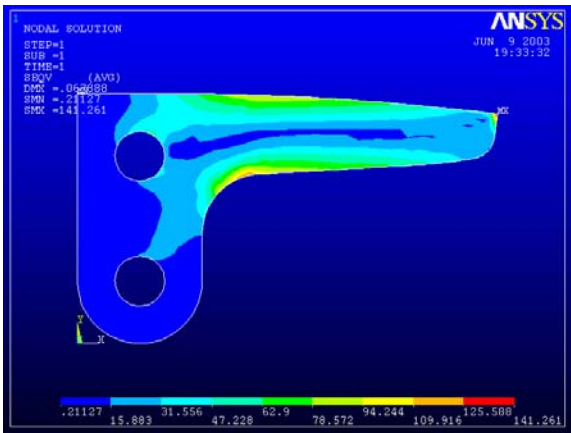
(a) FE Mesh



(b) U_{SUM} – Displacement Vector Sum (mm)



(c) σ_x – Normal Stress (N/mm^2)



(d) σ_{VM} – von Mises Stress (N/mm^2)

Figure 4.30 Contour plots for Redesign Option # 3

The reanalysis results, are compared to the ANSYS direct analysis solution and also for a very fine mesh (# of elements = 1447, # of nodes = 1587). Table 4.35 shows a comparison of these results. The reanalysis is based on three reduced basis vectors.

Table 4.35 Comparison of maximum results for Redesign Option # 3.

Maximum Quantities		Fine Mesh *	ANSYS Direct Analysis	Reanalysis +
Compressive σ_x N/mm ²	Value	-113.74	-118.58	-122.03
	Node #	-	36	36
σ_{VM} N/mm ²	Value	117.98	118.40	121.79
	Node #	-	36	36
U_Y $\times 10^{-1}$ mm	Value	-0.60665	-0.66519	-0.66394
	Node #	-	43	43

* Theoretical value of displacement is based on a very fine mesh of four-node quadrilateral elements (# of elements = 1447, # of nodes = 1587)

+ Reanalysis based on initial design using three basis vectors.

From the results it is seen that based on three reduced basis vectors the % error in maximum displacement is 0.2 when compared to the ANSYS Direct Analysis results. The % error in maximum compressive stress σ_x is 2.9 % when compared with ANSYS direct analysis and it is 7.29% when compared with the fine mesh. The % error in is higher when compared with respect to the fine mesh but it is lower with respect to the ANSYS direct analysis which is really our base of comparison since it is the solution for the same mesh. The von Mises stresses the % error is 2.9 % compared with the ANSYS direct analysis results and 3.2 % when compared with fine mesh. Overall, the maximum von Mises stress yields a safety factor of 2.3 which is very high. Thus, it is good to use the redesign option # 2 which yields the safety factor of only 2.02 and it should be selected as the final design.

4.4.5 Conclusion for Case Study # 3

This problem demonstrates using reanalysis in design process to improve a design. As shown, the initial design concept of the support is tried with three different design options and the finite element analysis of each was carried easily. In the initial design considered a tapered beam and the safety factor was 1.8. The shape was then modified to be optimum in Redesign Option # 1. It was found that besides yielding a uniform stress distribution, the fillet geometry reduced safety factor to 1.73. Thus, further modifications of the fillet radius were considered. In redesign Option # 2 the fillet radius was changed to 5 mm yielding a safety factor of 2.2. Furthermore, increasing the fillet radius to 7.5 yielded a larger safety factor of 2.3 providing the designer more design options. Table 4.36 provides a comparison of the results for initial and three redesign options. It can be observed that each design option reduced the von Mises stress at the fillet and also the displacement. This is also a criterion to be considered while reducing the cross section area.

Table 4.36 Comparison of results for the three redesign options.

Maximum Quantities	Design Options						
	Initial Design: Fillet Radius 2.5 mm	# 1: Optimum Shape of Taper		# 2: Fillet Radius 5 mm		# 3: Fillet Radius 7.5 mm	
	ANSYS Direct Analysis	ANSYS Direct Analysis	Reanalysis ⁺	ANSYS Direct Analysis	Reanalysis ⁺	ANSYS Direct Analysis	Reanalysis ⁺
Compressive σ_x N/mm ²	-129.61	-138.77	-142.37	-121.71	-122.11	-118.58	-122.03
σ_{VM} N/mm ²	152.59	152.39	159.40	123.55	126.96	118.40	121.79
Safety Factor	1.8	1.8	1.7	2.2	2.2	2.3	2.3
U_Y ($\times 10^{-1}$ mm)	-0.9685	-0.7479	-0.74779	-0.7085	0.7083	0.6652	0.66394

⁺ Based on three reduced basis vectors.

5. Conclusion

A prototype graphically driven finite element reanalysis technique has been developed for machine elements that can be used by an engineer/company in the initial design stage. A prototype has been integrated into the commercial finite element code ANSYS. The finite element system allows an engineer to modify part geometry and instantaneously view the results due to geometric changes. This means that the optimization process is engineer-driven as opposed to mathematically-driven. The anticipated advantages of using the technique in the initial design stage could result in a shortened time to market, improved product design and reduced product development cost for a company.

Three case studies were presented to demonstrate the usability, accuracy and reliability of the prototype software system. The first case study considered a plate with a hole subjected to a tensile distributed load. Different hole geometries were explored to determine their effect on the stress concentration factor in a plate. An engineer can modify the geometry of a given hole and displacement and stress results can be instantaneously viewed. A reanalysis method is used to solve each modified problem and the same problem was solved using the ANSYS Direct solver to verify reanalysis accuracy. This was also done for the other two case studies. The numbers of reduced basis vectors used in the reanalysis were varied from one to five to explore displacement and stress solution accuracy. It was determined from the three case studies that as the number of reduced basis vectors increases, solution accuracy increased. Therefore, three reduced basis vectors should be used to reduce computational effort while maintaining accuracy.

The second case study considered a plate with a fillet under tension loading. The goal was to obtain a fillet geometry that would minimize the stress concentration factor. In this case study the engineer, instead of trying traditional circular or elliptical fillets, can obtain better results by creating an optimum free-form fillet reducing the stress concentration.

The third case study considered a more practical problem than the first two which are commonly found in undergraduate mechanics of materials textbooks. The problem considered redesigning a cantilever L-shaped support bracket subjected to a concentrated force at its free end. The optimum shape of the cantilever support was first determined by the engineer with the goal of obtaining a uniform stress distribution. After the optimum cantilever shape was obtained then different fillet sizes were explored at the intersection of the L-shaped bracket to obtain an optimum shape for a high safety factor.

6. Future Work

In the case studies in Chapter 4 it was shown how the combined approximation reanalysis method described in Section 2.4 can be used to solve a reanalysis finite element problem. The advantages of implementing the reanalysis method during the early design process are as follows:

1. Helps designer to consider and evaluate alternate approaches and explore design options.
2. Reduces product development cost.
3. Helps in formulating an improved design.
4. Shortens the time to market.
5. Reduces the knowledge gap.

In spite of these advantages, the following five items are proposed as future work:

1. ***Improved ANSYS Output Environment.*** The system developed in this work is based on ANSYS 5.7. The new version of ANSYS is 6.1. Some portions of this work, such as accessing the ANSYS result file (*file.rst*), is not supported in version 6.1. Initially the idea was to use ANSYS 6.1, however, ANSYS technical support notified me that there are few bugs when reading the result file. They have modified the entire structure of result file. The newer and corrected method of reading and writing the result file will be implemented by ANSYS in their newest version that is currently being released. That is why this work used the older version, i.e., ANSYS 5.7. The FORTRAN code to read the result file need to be modified slightly depending on the structure of the result file for the newer release coupled with the advantage of the improved user friendly interface of ANSYS 6.1. Furthermore, since the GUI of ANSYS 6.1 has changed, especially the “Main Menu,” the current method developed in UIDL to modify the main menu must be modified to be compatible with ANSYS 6.1.
2. ***Use of Combined Approximation Method for Changing the Number of DOFs.*** There are three types of changes which can be made to the finite element mesh as follows:
 - (a) When the nodes or elements are deleted, i.e., when the total number of DOFs is reduced.
 - (b) When the nodes and elements are added in the mesh, i.e., when the total number of DOF is increased. This is more analogous to mesh refinement.
 - (c) When the geometric positions of the nodes are changed keeping the total number of DOFs unchanged (considered in this work).

The combined approximation reanalysis method used in this work applies when there is a change in nodal coordinates, i.e., case (c) above. Thus, the method is applicable only when the total number of DOFs in the mesh remains the same and only when the nodal coordinates are changed. Reanalysis methods have also been developed when the total number of DOFs in the mesh is changed [5.1, 5.2],

i.e., case (b) above. Although such a method is available, no effort has been made in any literature to solve the finite element problem for stress applications. Kirsch [5.1] has used this method for structural reanalysis where he considered the optimization of structures. For layout optimization, this method is typically helpful when the members and joints are added or deleted during the solution process. Gullickson [5.2] has used this method in solving a one-dimensional finite element problem. However, he used this method for generating the displacement results and not stresses.

The reanalysis method is very useful especially when there is a need to refine the mesh. Usage of combined approximation method to solve the mesh refinement problem will now be discussed. In order to utilize the CA method, a problem must be stated as follows. Consider the initial stiffness matrix K_0 , let F_0 be the initial force vector and let u_0 be the displacement solution for the system obtained after solving the force-displacement relationship,

$$F_0 = K_0 u_0 \quad (5.1)$$

Changes in the initial stiffness matrix are represented by ΔK , so the new stiffness matrix can be written as,

$$K = K_0 + \Delta K \quad (5.2)$$

and the new analysis equation can be written as,

$$Ku = (K_0 + \Delta K)u = F_0 \quad (5.3)$$

where u is the resulting new displacement solution vector.

Consider refinement of the initial mesh and this means that K may be of a different size than K_0 . Thus, after the solution of the initial problem for u_0 , K_0 must be expanded in order to allow the addition of ΔK . This is accompanied as follows,

$$K_0 \Rightarrow \bar{K}_0 = \begin{bmatrix} K_0 & 0 \\ 0 & I \end{bmatrix} \quad (5.4)$$

where I is the identity matrix. Also note that,

$$K_0^{-1} = \begin{bmatrix} K_0^{-1} & 0 \\ 0 & I \end{bmatrix} \quad (5.5)$$

in order to avoid re-solving the original analysis equation after each mesh refinement and/or change in the K matrix, the CA method will be used (similar to

Section 2.4.1) to approximate the solution to the new problem. As discussed the CA method, as discussed, uses a linear combination of s linearly independent basis vectors to approximate the displacement vector u associated with the new design or mesh. For a reduced basis approximation, the displacement are approximated by,

$$u = y_1 \cdot u_1 + y_2 \cdot u_2 + \dots + y_s \cdot u_s = y \cdot u_B \quad (5.6)$$

where u_B is an array containing s vectors $u_1, u_2 \dots u_s$ as defined below, and y_i are coefficients to be determined.

$$u_1 = u_0 \quad u_2 = -Bu_0 \quad (5.7)$$

$$u_1 = B^2 u_0 \dots u_s = (-B)^{s-1} u_0$$

where u_0 is the initial displacement vector and B is defined as,

$$B = \bar{K}_0^{-1} \Delta K \quad (5.8)$$

Substituting the expression for u in Equation (5.6) into Equation (5.3) and then pre-multiplying by u_B^T results in the equation of following form,

$$(u_B^T K u_B) y = u_B^T F_0 \quad (5.9)$$

using, $K_R = (u_B^T K u_B)$ and $F_R = u_B^T F_0$.

So similar to the expression derived in Section 2.4.2, Equation (5.9) reduces to,

$$K_R y = F_R \quad (5.10)$$

vector y can be determined by solving Equation (5.10). Thus remaining portion of this process is similar to the CA method explained in Section 2.4.2. Therefore, the CA method can be used for the case when not only the nodal coordinates are changed, but also when the total number of DOFs is changed.

3. Three-dimensional Problems. In this work, the reanalysis method was applied to only two-dimensional element types. The element type used here is ANSYS PLANE42. The method can be extended to three-dimensional element types, i.e., SOLID45, which has 8 nodes per element and 3 DOF per node and also plate and shell elements.

4. Contour Plot of Factor of Safety. ANSYS Parametric Design Language (APDL) can be used to obtain a contour plot of the factor of safety for the component

being analyzed. The plot of the contour shape is similar to the stress contour plot. The designer will have to enter the yield stress for the material and ANSYS will generate a safety factor contour plot.

5. Fatigue Analysis. The method can also be extended to perform fatigue analysis of the design problem. The designer will be able to obtain a contour plot regarding the safety of the design in fatigue.

6. Boundary Element Analysis. The combined approximation reanalysis method can also be applied to boundary elements. In boundary elements only the boundary of the geometry is discretized. In stress analysis the maximum stresses almost all the time occurs on the boundary. Furthermore, in case of two-dimensional problems the boundary elements are only lines rather than areas in finite elements [5.3-5.4]. therefore, only nodes on the boundary are moved whereas nodes on the boundary and inside the boundary need to be changed. The reanalysis method can be combined with boundary elements should result in an analysis that is faster and more accurate.

Figure 6.1 shows the similar form of boundary element mesh for the FE mesh shown in Figure 3.4. Same nodes are moved to show the similarity between two problems.

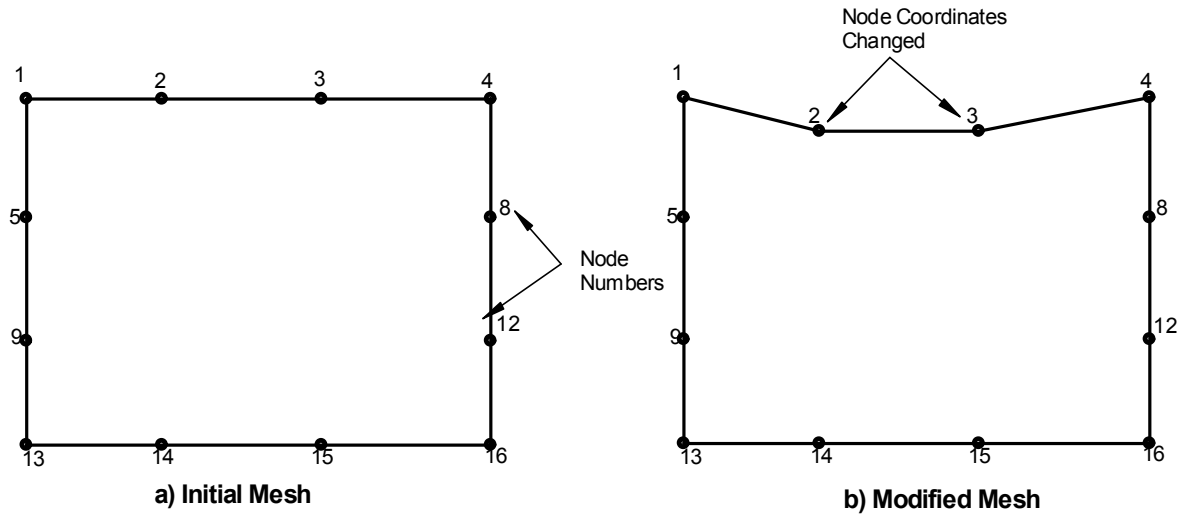


Figure 6.1 BE Mesh

References

- [1.1] Norton, R.L., *MACHINE DESIGN An Integrated Approach*, Second Edition, Prentice-Hall, Upper Saddle River, NJ (2000).
- [1.2] Ertas, A. and Jones, J.C., *The Engineering Design Process*, John Wiley & Sons, Inc., New York, NY (1993).
- [1.3] Dimarogonas, A.D., *Machine Design A CAD Approach*, John Wiley & Sons, Inc., New York, NY (2000).
- [1.4] Suh, N.P., *AXIOMATIC DESIGN Advances and Applications*, Oxford University Press, New York, NY (2001).
- [1.5] Juvinall, R.C. and Marshek, K.M., *Fundamentals of Machine Component Design*, Third Edition, John Wiley & Sons, Inc., New York, NY (1999).
- [1.6] Zahavi, E., *The Finite Element Method in Machine Design*, A Solomon Press Book, Prentice Hall, Englewood Cliffs, NJ (1992).
- [1.7] “Enterprise-wide Solutions: Product Design, Analysis and Management through Engineering Teamwork,” *ANSYS White Paper*, ANSYS Inc. Houston, PA (2002), http://www.ansys.com/customer_stories/white_papers.htm
- [1.8] Berry, D.T. and Leewood, A.R., “FEA for Production Design,” *Machine Design*, pp. 66-67, (September 21, 1989).
- [1.9] Szabo, B.A. and Actis, R.L., “Finite Element Analysis in Professional Practice”, *Computer Methods in Applied Mechanics and Engineering*, v.133 pp. 209-228 (1996).
- [1.10] Roth, G., “The Value of Early Analysis (Part 1),” NAFEMS Publications, East Kilbride, G750 QD, UK (July 2000), <http://www.nafems.org/publications/downloads/Article2.pdf>.
- [1.11] Cotnoir, P., *MFE 540 Design For Manufacturability*, Worcester Polytechnic Institute, Worcester MA, Class Notes for Spring (2002).
- [1.12] Hamrock, B.J., Jacobson, B. and Schmid S.R., *Fundamentals of Machine Elements*, WCB McGraw-Hill, Boston, MA (1999).
- [1.13] Shigley, J. E. and Mischke, C. R., *Mechanical Engineering Design*, McGraw Hill Boston, MA (2001).
- [1.14] Adams, V. and Askenazi, A., *Building Better Products with Finite Element Analysis*, Onward Press, Santa Fe, NM (1999).

- [1.15] Kirsch, U., *Optimum Structural Design-Concepts, Methods and Applications*, McGraw-Hill, New York, NY (1981).
- [1.16] Kirsch U. and Papalambros P.Y., "Exact and Accurate Reanalysis of Structures for geometrical Changes," *Engineering with Computers*, v. 17, pp. 363-372 (2001).
- [2.1] Kirsch, U., *Optimum Structural Design-Concepts, Methods and Applications*, McGraw-Hill, New York, NY, (1981).
- [2.2] Whitesell, J.E., "Rational Approximation in Structural Design Reanalysis," *Journal of Mechanism Transmissions and Automation in Design*, v. 106, pp. 114-118, (March 1984).
- [2.3] Kirsch, U. and Toledano G., "Approximate Reanalysis for Modifications of Structural Geometry," *Computers and Structures*, v. 16, n. 1-4, pp. 269-277, (1983).
- [2.4] Huang, C. and Verchery, G., "An Exact Structural Reanalysis," *Communications in Numerical Methods in Engineering*, v. 103, pp. 103-112, (1997).
- [2.5] Householder, A.S., "A Survey of Some Closed Methods for Inverting Matrices," *SIAM Journal*, v. 5, n. 3, pp. 155-169, (September 1957).
- [2.6] Abu Kassim A.M. and Topping B.H.V., "Static Reanalysis: A Review," *ASCE Journal of Structural Division*, v. 113, n. 5, pp. 1029-1045, (1987).
- [2.7] Sobieszezanski-Sobieski, J. and Haftka, R.T., "Multidisciplinary Aerospace Design Optimization: Survey and Recent Development," *Structural Optimization*, v. 14, pp. 1-23, (1997).
- [2.8] Fox, R.L. and Miura, H., "An Approximate Analysis Technique for Design Calculations," *AIAA Journal*, v. 9, pp. 177-179, (1971).
- [2.9] Noor, A.K., "Recent Advances and Applications of Reduced Methods," *Applied Mechanical Reviews*, v. 47, pp. 125-146, (1994).
- [2.10] Feury, C., "Efficient Approximation Concepts Using Second Order Information," *International Journal of Numerical Methods in Engineering*, v. 28, pp. 2041-2058 (1989).
- [2.11] Kirsch, U. and Liu, S., "Exact Structural Reanalysis by First Order Reduced Basis Approach," *Structural Optimization*, v. 10, pp. 153-158, (1995).
- [2.12] Kirsch, U. and Liu, S., "Structural Reanalysis for General Layout Modifications," *AIAA Journal*, v. 35, n. 2, pp. 382-388, (February 1997).

- [2.13] Kirsch, U. and Moses, F., "An Improved Reanalysis Method for Grillage-type Structures," *Computer and Structures*, v.69, pp. 79-88, (1998).
- [2.14] Kirsch U. and Toledano G., "Approximate Reanalysis for Modifications of Structural Geometry", *Computers and Structures*, v.16, n. 1-4, pp. 269-277, (1983).
- [2.15] Kirsch U., "Reduced Basis Approximations of Structural Displacements for Optimum Design," *AIAA Journal*, v. 29, pp. 1751-1758, (1991).
- [2.16] Kirsch, U., Aisenberger, M., "Approximate Interactive Design of Large Structures," *Computing Systems and Engineering*, v. 2, pp. 67-74, (1991).
- [2.17] Kirsch U. and Papalambros P.Y., "Exact and Accurate Reanalysis of Structures for Geometrical Changes," *Engineering with Computers*, v. 17, pp. 363-372, (2001).
- [2.18] Jennings A. and McKeown J.J., *Matrix Computation*, 2nd Edition, John Wiley & Sons, New York, NY, (1977).
- [2.19] Gullickson, J. and Averill, R.C., "Finite Element Solution Refinement using Combined Approximation Reanalysis," *AIAA*, v. 2, pp. 1181-1188, (2001).
- [2.20] Argyris, J.H., "The Matrix Analysis of Structures with Cutouts and Modifications," *Proceedings 9th International Congress of Applied Mechanics*, University of Brussels, Brussels, Belgium, v. 6, pp. 131-140, (1956).
- [2.21] Argyris, J.H., Bronlund, O.E., Roy J.R. and Scharpf, D.W., "A Direct Modification Procedure for the Displacement Method," *AIAA Journal*, v. 9, n. 9, pp. 1861-1864, (September 1971).
- [2.22] Argyris, J.H. and Kelsey, S., "The Matrix Force Method of Structural Analysis and Some New Applications," *R & M No. 3034, Great British Aeronautical Research Council Technical Report*, London, England, v. 93, pp. 787-828, (February 1956).
- [2.23] Argyris, J. H. and Roy, J. R., "General Treatment of Structural Modifications," *Journal of the Structural Division*, ASCE, v. 98, n. 2, pp. 465-492, (February 1972).
- [2.24] Bennett J.M., "Triangular Factors of Modified Matrices," *Numerische Mathematik*, v. 7, pp. 217-221, (1965).
- [2.25] Best, G., "A Method of Structural Weight Minimization Suitable for High-Speed Digital Computers," *AIAA Journal*, v. 1, n. 2., pp. 478-479, (Feb.1963).

- [2.26] Best, G.C., "The Stress-Area Method of Designing Beams," *Journal of Aeronautical Science*, v.12, n. 3, pp. 298-304, (July 1945).
- [2.27] Bhatia, K.G., "Rapid Iterative Reanalysis for Automated Design," *NASA TN D-7357*, NASA, Washington, D.C., (1973).
- [2.28] Celik, T., "Nonlinear Moment curvature Analysis by Means of Theorems of Structural Variation," *Istanbul Devlet Muhendislik ve Mimarlik Akademisi Dergisi*, v. 6, pp. 81-103, (1981).
- [2.29] Celik, T., "The Theorems of Structural Variation and Their Application in the Elastic-plastic Analysis of Frames," *Istanbul Devlet Muhendislik ve Mimarlik Akademisi Dergisi*, v. 5, pp. 125-138, (1979).
- [2.30] Das, P.C., "Reanalyzing Structures with Small Modifications," *Computer Aided Design*, v. 10, n. 6, pp. 371-374, (November 1978).
- [2.31] Ding. H. and Gallagher, R.H., "Approximate Force Method Reanalysis Techniques in Structural Optimization," *International Journal for Numerical Methods in Engineering*, v. 21, pp. 1253-1267, (1985).
- [2.32] Ertas, R. and Fenves, S.J., "Automatic Analyzer for Iterative Design," *Civil Engineering Studies*, Structural Research Series No. 352, University of Illinois, Urban, IL, (1969).
- [2.33] Fletcher, R. and Powell, M.J.D., "On the Modification of LDLT Factorization," *Mathematics of Computation*, v. 28, n. 128, pp. 1067-1087, (October 1974).
- [2.34] Fox. R.L. and Miura, H., "An Approximate Analysis Technique for Design Calculations," *AIAA Journal*, v. 9, n. 1, pp. 177-179, (January 1971).
- [2.35] Gill, P.E., Golub, G.H. Murray, W. and Saunders, M. A., "Methods for Modifying Matrix Factorizations," *Mathematics of Computation*, v. 28, n.126, pp. 505-535, (April 1974).
- [2.36] Gill, P.E., Murray, W. and Saunders, M. A., "Methods for Computing and Modifying the LDV Factors of a Matrix," *Mathematics of Computation*, v. 29, n. 132, pp. 1051-1077, (October 1975,).
- [2.37] Goodey, W.J., "Solution of Modified Linear Simultaneous Equations," *Air-craft Engineering*, v. 31, pp. 358-359 and 364, (December 1959).
- [2.38] Hoerner, S.V., "Homologous Deformations of Tilttable Telescopes," *Journal of the Structural Division*, ASCE, v. 93, n. 5, pp. 461-485, (October 1967).

- [2.39] Householder, A.S., *Principles of Numerical Analysis*, McGraw-Hill Book Company, New York, NY, (1953).
- [2.40] Householder, A.S., "A Survey of Some Closed Methods for Inverting Matrices," *SIAM Journal*, v. 5, n. 3, pp. 155-169 (September, 1957).
- [2.41] Householder, A.S., *The Theory of Matrices in Numerical Analysis*, Blaisdell Publishing Company, New York, NY, (1964).
- [2.42] Kavanagh, K.T., "An Approximate Algorithm for the Reanalysis of Structures by the Finite Element Method," *Computers and Structures*, v. 2, pp. 713-722, (1972).
- [2.43] Kirsch, U., "Approximate Structural Reanalysis Based on Series Expansion," *Computer Methods in Applied Mechanics and Engineering*, v. 26, pp. 205-223, (1981).
- [2.44] Kirsch, U., "Approximate Structural Reanalysis for Optimization Along a Lines," *International Journal for Numerical Methods in Engineering*, v. 18, pp. 635-651, (1982).
- [2.45] Kirsch, U. and Hoffman, B., "Approximate Behavior Models for Optimum Structural Designs," *Proceedings International Symposium on Optimum Structural Design*, Tuscan, AZ, pp. 7.17-7.26, (1981).
- [2.46] Kirsch, U. and Rubinstein, M.F., "Modification of Structural Analysis by the Solution of a Reduced Set of Equations," *UCLA Paper ENG-0570*, University of California, Los Angeles, CA, (1970).
- [2.47] Kirsch, U. and Rubinstein, M.F., "Reanalysis for Limited Structural Design Modifications," *Journal of the Engineering Mechanics Division*, ASCE, v. 98, n. 1, pp. 61-70, (February 1972).
- [2.48] Kirsch, U. and Rubinstein, M.F., "Structural Reanalysis by Iteration," *Computers and Structures*, v. 2, pp. 497-510, (1972).
- [2.49] Kirsch, U. and Toledano, G., "Approximate Reanalysis for Modifications of Structural Geometry," *Computers and Structures*, v. 16, pp. 269-277, (1983).
- [2.50] Kleiber, M. and Lutoborski, A., "Modified Triangular Factors in the Incremental Finite Element Analysis with Non-symmetric Stiffness Change," *Computers and Structures*, v. 9, pp. 599-602, (1978).
- [2.51] Kosko, E., "Effect of Local Modifications in Redundant Structures," *Journal of the Aerospace Science*, v. 21, n. 3, pp. 206-207, (March 1954).

- [2.52] Kosko, E., "Matrix Inversion by Partitioning," *Aeronautical Quarterly*, v. 8, pp. 157-184, (May 1957).
- [2.53] Law, K.H., "Sparse Matrix Factor Modification in Structural Reanalysis," *International Journal for Numerical Methods in Engineering*, v. 21, pp. 37-63, (1985).
- [2.54] Law, K.H. and Fennes, S.J., "Sparse Matrices, Graph Theory, and Reanalysis," *Proceedings of the International Conference in Civil Engineering*, ASCE, New York, NY, pp. 234-249, (May 12-14 1981).
- [2.55] McNeal, R.H., "Application of the Compensation Theorem to the Modification of Redundant Structures," *Journal of the Aeronautic Scientist*, v. 20, n. 10, pp. 726-727, (October 1953).
- [2.56] Majid, K.I., and Elliott, D.W.C., "Forces and Deflections in Changing Structures," *The Structural Engineer*, v. 51, n. 3, pp. 93-101, (March 1973).
- [2.57] Majid, K.I. and Elliott, D.W.C., "Topological Design of Pin Jointed Structures by Non-linear Programming," *Proceedings of the Institution of Civil Engineers*, v. 55, n. 2, pp. 129-149, (March 1973).
- [2.58] Majid, K.I. and Saka, M.P., "Optimum Shape Design of Rigidly Jointed Frames," *Proceedings of the Symposium on the Application of Computer Methods in Engineering*, v. 1, University of Southern California, Los Angeles, CA, pp. 521-531.
- [2.59] Majid, K.I., Saka, M.P. and Celik, T., "The Theorems of Structural Variation Generalized for Rigidity Jointed Frames," *Proceedings of the Institution of Civil Engineering*, v. 65, n. 2, pp. 839-856, (December 1978).
- [2.60] Melosh, R.J., "Structural Analysis, Frailty Evaluation and Redesign," *Tech Report No. TR-70-15*, v. 1, Air Force Flight Dynamics Lab., Wright-Patterson Air Force Base, Dayton, OH (1970).
- [2.61] Melosh, R.J., Johnson, J.R. and Luik, R., "Survivability Analysis of Structure," *Proceedings of the 2nd Conference on Matrix Methods in Structural Mechanics*, AFFDL-TR-68-150, Wright-Patterson Air Force Base, Dayton, OH (December 1969).
- [2.62] Melosh, R.J. and Luik, R., "Approximate Multiple Configuration Analysis and Allocation for Least Weight Structural Design," *AFFDL-TR-67-59*, Wright-Patterson Air Force Base, Dayton, OH (1967).

- [2.63] Melosh, R.J. and Luik, R., "Multiple Configuration Analysis of Structures," *Journal of the Structural Division*, ASCE, v. 94, n. 11, pp. 2581-2596, (November 1968).
- [2.64] Melosh, R.J. and Luik, R., "Closure on Multiple Configuration Analysis of Structures," *Journal of the Structural Division*, ASCE, v. 96, n. 6, pp. 1239-1241, (June 1970).
- [2.65] Mohraz, B. and Wright, R.N., "Solving Topologically Modified Structures," *Computers and Structures*, v. 3, pp. 341-353, (1973).
- [2.66] Noor, A.K., "Multiple Configuration Analysis via Mixed Method," *Journal of the Structural Division*, ASCE, v. 100, n. 9, pp. 1991-1997, (September 1974).
- [2.67] Noor, A.K. and Lowder, H.E., "Approximate Reanalysis Techniques with Sub structuring," *Journal of the Structural Division*, ASCE, v. 101, n. 8, pp. 1687-1698, (August 1975).
- [2.68] Noor, A.K. and Lowder, H.E., "Approximate Techniques of Structural Reanalysis," *Computers and Structures*, v. 4, pp. 801-812, (1974).
- [2.69] Noor, A.K. and Lowder, H.E., "Structural Reanalysis via a Mixed Method," *Computers and Structures*, v. 5, pp. 9-12, (1975).
- [2.70] Phansalkar, S.R., "Matrix Iterative Methods for Structural Reanalysis," *Computers and Structures*, v. 4, pp. 779-800, (1974).
- [2.71] Row, D.G., Powell, G.H. and Mondkar, D.P., "Solution of Progressively Changing Equilibrium Equations for Nonlinear Structures," *Computers and Structure*, v. 7, pp. 659-665, (1977).
- [2.72] Sack, R.L., Carpenter, W.C. and Hatch, G.L., "Modification of Elements in the Displacement Method," *AIAA Journal*, v.5, n. 9, pp. 1708-1710, (September 1967).
- [2.73] Sobieszczanski, J., "Evaluation of Algorithms for Structural Modification," *Proceedings of the Conference on Finite Element Methods in Civil Engineering*, Vanderbilt University, Nashville, TN, pp. 129-153, (1969).
- [2.74] Sobieszczanski, J., "Structural Modification by Perturbation Method," *Journal of the Structural Division ASCE*, v. 94, n. 12, pp. 2799-2816, (December 1968).
- [2.75] Storaasli, O.O. and Sobieszczanski, J., "Design Oriented Structural Analysis," *AIAA Paper*, pp. 73-538, Williamsburg, VA, (1973).

- [2.76] Storaasli, O.O. and Sobieszczanski, J., "On the Accuracy of Taylor Approximation," *AIAA Journal*, v. 12, n. 2, pp. 231-233, (February 1974).
- [2.77] Topping, B.H.V., "The Application of the Theorems of Structural Variation to Finite Element Problems," *International Journal for Numerical Methods in Engineering*, v. 19, pp. 141-144, (1983).
- [2.78] Topping, B.H.V. and Chan, H.F., "An Exact Formulation of the Theorems of Geometric Variation for Statically Indeterminate Trusses," *Report, Department of Civil Engineering*, University of Edinburgh, Edinburgh, UK, (1983).
- [2.79] Wang, B.P. and Pilkey, W.D., "Efficient Reanalysis of Locally Modified Structures," *Proceedings 1st, Chautagua on Finite Element Modeling*, Schaeffer Analysis, pp. 37-61, (1980).
- [2.80] Wang, B.P. and Pilkey, W.D., "Efficient Reanalysis of Locally Modified Structures," *Department of Mechanical and Aerospace Engineering*, Virginia University, Charlottesville, VA, (1980).
- [2.81] Wang, B.P. and Pilkey, W.D., "Parameterization in Finite Element Analysis," *Proceedings International Symposium on Optimum Structural Design*, Tuscan, AZ, pp. 7.1-7.7, (1981).
- [2.82] Wang, B.P., Pilkey, W.D. and Palazzaolo, A.R., Discussion on "Reanalysis Modal Synthesis and Dynamic Design," *State-of-Art Surveys on Finite Element Technology*, A. K. Noor, and W. D. Pickey, Eds., American Society of Mechanical Engineers, New York, NY, pp. 225-295 (1983).
- [2.83] Weiner, B.L., "Variation of Coefficients of Simultaneous Linear Equations," *Transaction of ASCE*, v. 113, pp. 1349-1390, (1948).
- [2.84] Yang, W.H., "A Method for Updating Cholesky Factorization of a Band Matrix," *Computer Methods in Applied Mechanics and Engineering*, v. 12, pp. 281-288, (1977).
- [2.85] Zielke, G., "Inversion of Modified Symmetric Matrices," *Journal of the Association for Computing Machinery*, v. 15, n. 3, pp. 402-408, (July 1968).
- [2.86] Kavlie, D. and Powell, G.H., "Efficient Reanalysis of Modified Structures," *Journal of Structural Division*, ASCE, v. 97, n. 1, pp. 377-392, (January 1971).
- [2.87] Wiberg, N.E., Discussion of "Efficient Reanalysis of Modified Structures," by Kavlie, D., and Powell, G. H., *Journal of Structural Division ASCE*, v. 97, n. 10, pp. 2612-2619, (October 1971)

- [3.1] “Guide to ANSYS User Programmable Features,” *ANSYS Release 5.6*, ANSYS Inc., Canonsburg, PA (February 2000).
- [3.2] Moaveni S., *FINITE ELEMENT ANALYSIS Theory and Application with ANSYS*, Prentice Hall, Upper Saddle River, NJ (1999).
- [3.3] “Introduction to ANSYS 5.7 Part 1,” *Training Manual*, ANSYS Inc., Canonsburg, PA (January 2001).
- [3.4] “APDL Programmer’s Guide,” *ANSYS Release 5.6*, ANSYS Inc., Canonsburg, PA (February 2000).
- [3.5] “Guide to Interfacing with ANSYS,” *ANSYS Release 5.6*, ANSYS Inc., Canonsburg, PA (February 2000).
- [3.6] “Basic Analysis Procedures Guide,” *ANSYS Release 5.6*, ANSYS Inc., Canonsburg, PA (2003) http://www1.ansys.com/customer/content/documentation/60/Hlp_G_BAS1.html
- [3.7] “ANSYS Command Reference,” *ANSYS Release 5.6*, ANSYS Inc., Canonsburg, PA (2003) http://www1.ansys.com/customer/content/documentation/60/Hlp_C_CmdTOC.html
- [4.1] Gullickson, J. and Averill, R.C., “Finite Element Solution Refinement using Combined Approximation Reanalysis,” *American Institute of Aeronautics and Astronautics*, v. 2, pp. 1181-1188, (2001).
- [4.2] Waldman W., Heller M. and Chen G. X., “Optimal Free-form Shapes for Shoulder Fillets in Flat Plates under Tension and Bending,” *International Journal of Fatigue*, v. 23, pp. 509-523, (2001).
- [4.3] Pilkey, W.D., *Peterson’s Stress Concentration Factors*, Second Edition, John Wiley & Sons Inc., New York, NY (1997).
- [4.4] Thompson, D.W., *On Growth and Form Vol. 2*, Second Edition, Cambridge University Press, New York, NY (1963).
- [5.1] Kirsch, U. and Liu, S., “Structural Reanalysis for General Layout Modifications,” *American Institute of Aeronautics and Astronautics Journal*, v. 35, n. 2, pp. 382-388, (February 1997).
- [5.2] Gullickson, J. and Averill, R.C., “Finite Element Solution Refinement using Combined Approximation Reanalysis,” *American Institute of Aeronautics and Astronautics Journal*, v. 2, pp. 1181-1188, (2001).

- [5.3] Brebia, C. A. and Dominguez J., *Boundary Elements An Introductory Course*, McGraw-Hill Book Company, New York, NY (1989)
- [5.4] Banerjee, P. K., *The Boundary Element Method in Engineering*, McGraw-Hill Book Company, New York, NY (1993)
- [A.1] “Guide to Interfacing with ANSYS,” *ANSYS Release 5.6*, ANSYS Inc., Canonsburg, PA (February 2000).
- [B.1] “APDL Programmer’s Guide,” *ANSYS Release 5.6*, ANSYS Inc., Canonsburg, PA (February 2000).
- [B.2] “ANSYS Command Reference,” *ANSYS Release 5.6*, ANSYS Inc., Canonsburg, PA, http://www1.ansys.com/customer/content/documentation/60/Hlp_C_CmdTOC.html
- [C.1] Ciarlet, P.G., *Introduction to Numerical Linear Algebra and Optimization*, English Edition, Cambridge University Press, New York, NY (1988).
- [C.2] Jennings A. and McKeown, J.J., *Matrix Computation*, Second Edition, John Wiley and Sons, New York, NY (1992).
- [C.3] Golub, G.H. and Van Loan, C.F., *Matrix Computations*, Second Edition, The John Hopkins University Press, Baltimore, MD (1989).
- [E.1] Norton, R.L., *MACHINE DESIGN An Integrated Approach*, Second Edition, Prentice-Hall, Upper Saddle River, NJ (2000).
- [E.2] Pilkey, W.D., *Peterson’s Stress Concentration Factors*, Second Edition, John Wiley & Sons Inc., New York, NY (1997).

A. ANSYS Result File (file.rst) Overview

A.1 Overview

A brief description of the result file generated by ANSYS [A.1] is presented in this appendix. ANSYS writes several binary files to store data created by an analysis. These files are named **Jobname.Ext**, where **Jobname** is the name of analysis file that caused the file to be generated and **.Ext** is an extension indicating the type of data in the file. Characteristics of ANSYS binary files are as follows:

1. An ANSYS binary file is a direct access, unformatted file. The record can be read or written by specifying (as a number) what location to read or write.
2. Before ANSYS actually writes data to a file on disk, it uses a buffer to store data in memory until those buffers become full. A block number designates these buffers. Most access routines use this block number.
3. By default, ANSYS files are external files. The file uses a standardized “external” format that enables transfer across different computer systems.
4. In addition to the file names, ANSYS uses file numbers to identify the files. File handles and other information are associated with the file numbers.
5. Some binary files contain data values that point to the start of certain data (for example, the start of the data steps index table record). Both the ANSYS program and external binary files access routines use these pointers to locate data on the various binary files.

A.2 Result File Structure

The result file has an extension **.rst**. if specific name is not given to an ANSYS analysis job then the default name is **file** and the result file generated after the analysis is called **file.rst**. **File.rst** is the result file when a structural or coupled field analysis is performed by ANSYS. The result file is used to obtain input from ANSYS about the analysis problem. Information regarding the finite element model that is created in ANSYS is required to carry out reanalysis. The reanalysis requires the following information from the result file,

- Number of Degrees of Freedom per Element (NDOFN)
- Total Number of Nodes (NNODE)
- Total Number of Elements (NELE)
- Nodal Constraints (IFIX)
- Element and Node Relation Data (NODE)
- Nodal Coordinate Data (X and Y)
- Nodal Force Data (FORCE)

A complete description of the **file.rst** can be found in reference [A.1]. The manual uses following convention to describe the binary file,

1. Record ID (*recid*) is the identifier for the particular record. Not all records will have record identifiers; they are indicated only for the records whose record pointers are stored in a header.
2. Type (*type*) indicates the type of information the record stores.
The types are,
 i – integer.
 dp – double precision.
 cmp – complex.
3. Number of records (*nrec*) indicates how many records of this description are found here. It is the number by which the concerned '*recid*' is repeated.
4. Record length (*lrec*) indicates the number of items stored in the record.

Below is the description of a few initial records in **file.rst**. Only records that are used in this work will be discussed.

recid	type	nrec	lrec	Content
-------	------	------	------	---------

---	i	1	100	Standard ANSYS file header.
-----	---	---	-----	-----------------------------

---	i	1	40	.RST FILE HEADER
-----	---	---	----	------------------

fun12,	maxn,	nnod,	resmax,	numdof,
maxe,	nelm,	kan,	nsets,	ptrend,
ptrDSI,	ptrTIM,	ptrLSP,	ptrELM,	ptrNOD,
ptrGEO,	0,	0,	0,	units
nSector	0,	ptrend8,	0,	0,
0,	0,	0,	0,	0,
0,	0,	0,	0,	0,
0,	0,	0,	0,	0

few items in header which are used, are described below,

fun12 - unit number (it is 12 for .rst file)

maxn - maximum node number of the model

nnod - the actual # of nodes used in the solution phase

resmax - the maximum # of data sets allowed on the file (default to 1000; minimum allowed is 10)

numdof - number of DOFs per node

maxe - maximum element number of the finite element model

nelm - number of finite elements

kan - analysis type

ptrGEO - pointer to the beginning of the geometry information

units - unit system used

= 0 - user defined units

= 1 - SI

= 2 - CSG

= 3 - British, using feet

= 4 - British, using inches

```

---      i      1      numdof  Degress of freedom per node
                                DOF reference numbers are:
                                UX = 1, UY = 2, UZ = 3, ROTX = 4, ROTY = 5, ROTZ = 6

NOD      i      1      nnod   Nodal equivalence table. This table equates
                                the number used for storage to the actual
                                node number
                                (baclast(i), i = 1,nnod)

```

As described above the variable ptrGEO is the pointer to the beginning of the geometry information. This is nothing but the record identifier (recid) for the geometry information. This pointer can be used to jump directly to the geometry information and results in saving CPU time in reading unnecessary data from the result file. In this way, the pointers provided in these files are very helpful.

The above discussed record identifiers (*recids*) gives the first three values out of the list discussed in Section A.1 which are required further in reanalysis. As described, ptrGEO is used to access geometry information. The record identification Geo contains the following information,

```

GEO      i      1      20      Geometry data header.

                                0,          maxety,   maxrl,    ndnod,    nelm,
                                maxcsy,   ptrETY,    ptrREL,   ptrNLC,   ptrSYS,
                                ptrEID,    0,          0,        0,        0,
                                ptrMAS,   csysiz,    elemsiz,  etysiz,   rlsiz,

                                few items in header which are used, are
                                described below,

                                ptrNLC - pointer to nodal point locations
                                ptrEID - pointer to element index table

```

The nodal point location contains the coordinate data,

```

NLC      Dp      1      7*ndnod  This group contains the node number and
                                coordinates (in the order X, Y, Z, THXY,
                                THYZ, THZX) of each node.

```

The record ID NLC contains the coordinate data and the record is stored as double precision. The storage sequence is node number, X coordinate, Y coordinate, Z coordinate, rotation XY, rotation YZ, and rotation ZX.

ptrEID obtained from the previous data set, is used to find the element node connectivity. The record ID 'EID' and its next *recids* (repeated until the number of elements) gives the node numbers associated with each element in the sequence I, J, K, L,... with I, J, K, L,... forming an anticlockwise sequence.

```

EID      i      1      nelm   Element description table. This record
                                contains the record pointer for each
                                element description.

```

```

---      i      nelm  10+nodelm  Element description. Each of these records
                                     is pointed to by a record pointer given in
                                     record labeled EID. The length of these
                                     records varies for each element. nodelm
                                     shown here is the number of nodes for this
                                     element.

```

The items stored in each record:

```

mat,      type,      real,      secnum,  esys,
Death,    solidm,    shape,    elnum,    0,
NODES

```

few items in header which are used, are described below,

NODES - node numbers defining the elements.

From the next record ID solution information is stored starting with the solution header which describes initial data before starting the solution data.

```

---      i      1      100      Solution data header

0,        nelm,      nnod,      mask,      itime,
iter,      ncumit,    nrf,      maxesz,    nmast,
ptrNSL,    ptrESL,    ptrRF,    ptrMST,    ptrBC
rxtrap,    mode,      isym,      kcmplx,    numdof,
DOFS,

```

Description:

ptrBC - pointer to the boundary conditions.

The pointer to the boundary condition data is used to access further data regarding the boundary conditions and nodal force data. The record identification 'BC' contains pointers to this data. The boundary condition data is stored as follows:

```

BC      i      1      40      Boundary condition index table

numdis,    ptrDIX,    ptrDIS,    numfor,    ptrFIX,
ptrFOR,    0,         0,         0,         0,
0,         0,         0,         0,         0,
0,         0,         0,         0,         0,
0,         0,         0,         0,         0,
0,         0,         0,         0,         0,
0,         0,         0,         0,         0,

```

numdis - number of nodal constraints
ptrDIX - pointer to the table of nodes having nodal constraints.
numfor - number of nodal input force loadings
ptrFIX - pointer to the table of nodes having nodal forces
ptrFOR - pointer to nodal force values

DIX	i	1	numdis	Nodal constraint DOF. This index is calculated as $N*32+DOF$, where N is the node number and DOF is the DOF reference number. Values are in the same order as the DOF number reference table.
FIX	i	1	numfor	Nodal input force DOFs. This index is calculated as $N*32+DOF$, where N is the node number and DOF is the DOF reference number. Values are in the same order as the DOF number reference table.
FOR	dp	1	4*numfor	Nodal forces. This record contains present and previous values of the nodal input force loading at each DOF.

This way all the required data is obtained from the ANSYS result file. Before solving any finite element analysis problem two more items required are the Young's Modulus (EY) and Poisson's Ratio (PR). ANSYS does not store this information in any of the binary files. So this can't be obtained from the ANSYS output file. A different methodology is adapted to obtain this information. This will be discussed in the Appendix B for description on APDL, the ANSYS Parametric Design Language.

A.3 Accessing ANSYS Binary Files

ANSYS binary files are blocked binary files and are difficult to access using simple FORTRAN file access subroutines. ANSYS provides some specific subroutines to read, write from and modify the ANSYS binary file. This collection of routines is called the BINLIB. It is nothing but a shared library which is located in

/ansys57/customize/misc/<platform>/libbin.so (where <platform> is a directory that uniquely identifies the hardware platform version. It is **sun64** for the SUN Solaris machines used in this work).

The FORTRAN source code for these programs is located in **/ansys57/customize/misc** and the files are named **rdresu.F**, **wrtres.F**, **rdsubs.F** and **wrtsub.F**. To link these programs to ANSYS use, **/ansys57/customize/misc/rdrwrt.link** procedure file and specify the program to be built on command line. Valid command line options are **rdresu**, **wrtres**, **rdsubs**, **wrtsub**, and **userprog**. For example to build the program to read the result file,

```
/ansys57/customize/misc/rdrwrt.link rdresu
```

Appropriate files will then be copied from **/ansys57/customize/misc** to the working directory compiled and linked. For reading the information stated in Section A.1 a FORTRAN code is written using the file access subroutines located in above mentioned directory and the program is named **userprog.F** and the program is compiled by typing

```
/ansys57/customize/misc/rdrwrt.link userprog
```

The resulting **userprog.o** file and the executable get created in the working directory. Procedure files available in /asnsys57/bin are used to run the program. After compiling **userprog.F** the resulting executable is **userprog.e57**. This runs by just running **userprog57**.

B. ANSYS Parametric Design Language

B.1 Introduction

APDL stands for ANSYS Parametric Design Language (Section 3.2.4), and is a scripting language that can be used to automate common tasks or even, build a model in terms of parameters [B.1]. APDL also encompasses a wide range of other features such as repeating a command, macros, if-then-else branching, do-loops, and scalar, vector and matrix operations. In this work APDL is not only used for defining the parameters, it is used to make the reanalysis process user friendly so that the user can make the geometric modifications to the finite element model interactively. This appendix provides brief overview of the using APDL for this purpose.

B.2 Defining Element and Material Properties

The reanalysis algorithm was developed only for the four node quadrilateral plane stress / plane strain element type in this work. This element type is defined in the pre-processing phase of ANSYS, as a series of commands. This along with the other material properties including the Young's modulus and Poisson's ratio, are defined using an APDL macro. The reason behind this is, the reanalysis algorithm developed in this work is applicable only for PLANE42 element type with some specific thickness. This method will ensure that the element type is always PLANE42 before starting the reanalysis problem with user option to input the Young's modulus and Poisson's ratio. The commands,

```
ET, 1, PLANE42
KEYOPT, 1, 1, 0
KEYOPT, 1, 2, 1
KEYOPT, 1, 3, 3
KEYOPT, 1, 5, 0
KEYOPT, 1, 6, 0
```

sets the element type to PLANE42, which is four-node quadrilateral element. The KEYOPT (key options) defines the element type as plane stress with the option for user to input the element thickness. Only KEYOPT(2) and KEYOPT(3) are changed while the remaining are used with the default values. These options are,

```
KEYOPT(2)
    0 -- Include Extra Displacement Shapes
    1 -- Suppress Extra Displacement Shapes
KEYOPT(3)
    0 -- Plane Stress
    1 -- Axisymmetric
    2 -- Plane Strain (Z strain = 0.0)
    3 -- Plane Stress with Thickness Input
```

One more significant change in the key option is to suppress the extra displacement shapes. The material properties are assigned to the model in an interactive way, asking the user to input the values of element thickness, Young's modulus and Poisson's ratio have the optional default values of 1, 30×10^6 and 0.3, respectively. This is done using **ASK* command in APDL, e.g., asking the user to input the value of Young's modulus with the optional default value of 30×10^6 is done using the following command,

```
*ASK, YM, YOUNGS MODULUS, 30E6
```

where *YM* is the parameter which stores value of Young's modulus for further analysis.

B.3 Changing a User Defined Toolbar

ANSYS customization features allow the toolbar to be changed. Frequently used ANSYS functions or macros can be added to the ANSYS toolbar and this is done by defining *abbreviations*. An abbreviation is an alias (up to eight characters long). A complete new customized toolbar can also be stored in a file and the toolbar buttons can be set in the file. Figure B.1 (a) shows the ANSYS default toolbar. Figure B.1 (b) shows the modified toolbar. For the computer on which the reanalysis procedure files developed in this work are copied, the modified toolbar will be visible as soon as the user opens ANSYS. This toolbar contains the necessary buttons to carry out a reanalysis.

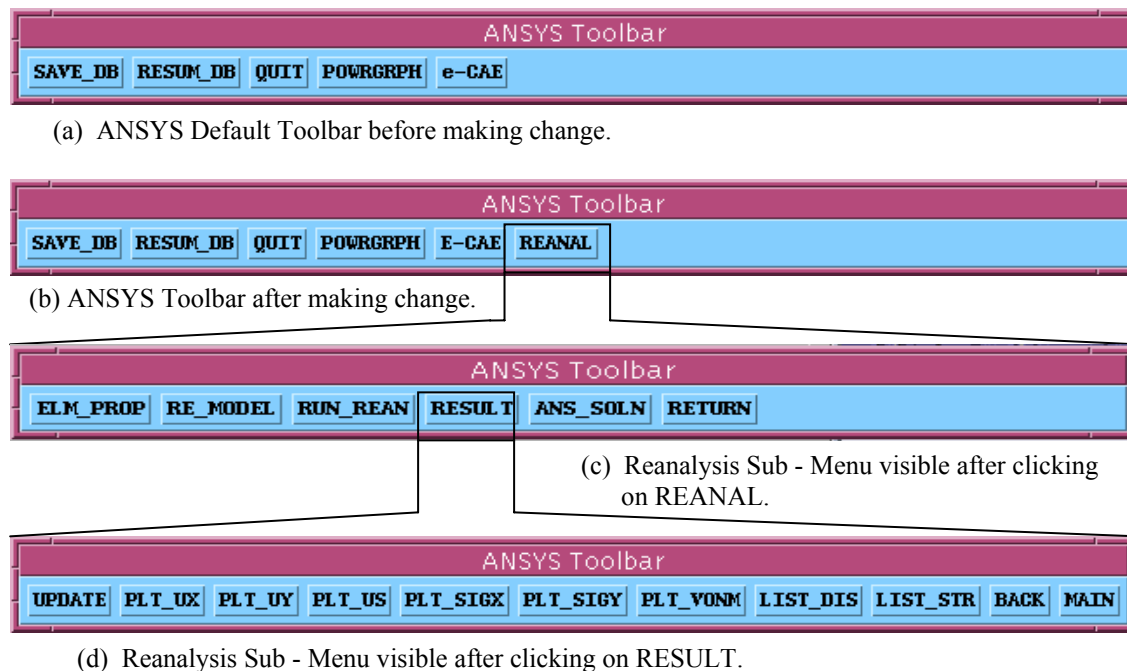


Figure B.1 ANSYS Toolbar before and after making a change.

The “REANAL” button consists of a toolbar for the reanalysis menus. After clicking the REANAL button on the ANSYS toolbar, the reanalysis sub-menu appears as shown in Figure B.1(c). The significance of each button is as follows:

- *ELM_PROP*. Sets the element type and material properties as discussed in Section B.2.
- *RE_MODEL*. Is the button used to modify the geometry. As explained in Section 3.3, after carrying out the analysis if the stresses and displacements are not acceptable, then the mesh geometry is modified. After clicking on the button ANSYS will run an APDL code which allows user to change the coordinate location of nodes graphically. After carrying out the initial analysis ANSYS does not allow the user to change the node coordinates since they are tied down to the areas (solid model) created. So before doing any mesh modifications, the user needs to detach the nodes from the area. The following command is used:

```
MODMSH, DETACH
```

which will detach the nodes and elements from the area. As described in the command reference [B.2] this command releases all associativity between the current solid model and finite element model. ANSYS deletes any attribute assigned to the solid model. However, attributes such as nodes and element assigned to finite element model, are not deleted.

After modifying the nodal coordinates and when the user is satisfied with the modified geometry, upon exiting, nodal coordinates of the modified geometry are written in a file. The nodal coordinates are read during the reanalysis. The command *NX(I)*, *NY(I)* gives the *X* and *Y* coordinates of node *I*, respectively. APDL also allows a DO loop to run the same command again and again. The loop is used to retrieve nodal coordinates and nodal forces as follows,

```
*DO, I, 1, NNODE
  X (I) = NX (I)
  Y (I) = NY (I)
  *GET, F (I, 1), NODE, I, F, FX
  *GET, F (I, 2), NODE, I, F, FY
*ENDDO
```

where the **GET* command retrieves the specified entity and stores it into a user specified parameter. A two-dimensional array *F* is created to store *X* and *Y* directional forces applied at each node. One-dimensional arrays *X* and *Y* store the *x* and *y* coordinated of the node, respectively.

The **VWRITE* command is used to write the obtained parametric data in an external file. The command is,

```
*VWRITE, Par1, Par2... Par10
```

where this command can write ten parameters at a time in the output file. The next line of this command must indicate the format of the parameter to be written in the file, i.e., it must specify if the number is integer, float or character. It is similar to the

FORMAT command used in FORTRAN. Before using this command, the file with a specific name needs to be created using the **CFOPEN* command. and the file is closed by using **CFCLOS* command at the end of session.

- *RUN_REAN*. Runs the FORTRAN code for reanalysis. The executable created after compiling the FORTRAN code (Section A.3) is directly run from ANSYS using the /SYS command. The command used is,

```
/SYS, 'link.link'
```

where *link.link* is the batch file (which is **.link* file in SUN Solaris machines) which contains a series of the command line arguments to run the *userprog57* program.

- *RESULT*. Opens another toolbar window which contains many options to display the displacement and the stress results. This includes graphical contour plots and lists of nodal solutions. Figure B.1 (d) shows the result toolbar. All the operations in this toolbar discussed hereafter,
1. *UPDATE*. Updates the displacement and the stress results in ANSYS database by the reanalysis results. This is extremely important in obtaining the graphical display of the reanalysis results. **VPUT* command is used to replace the displacement values in ANSYS by the displacement values obtained from the reanalysis code. Before using this command, the displacement results are written in a file from the reanalysis program. The file is then accessed using the **VREAD* command. The usage of this command is as follows,

```
*VREAD, DISP(1), ANSYS_DISPL, DAT, adfemcopy, IJK, 2, NNODE
```

where *DISP* is an two-dimensional array which stores the X and Y directional displacement results for each node from the reanalysis. *DISP(1)* denotes the first value in the array. It is not required to have a *DO* loop to read consecutive values in the file. *ANSYS_DISPL.DAT* is the file that contains the displacement results which is in a folder named *adfemcopy*. *IJK* denotes the sequence in which the data from the file is to be stored in the array. The maximum size of array *DISP* is *2xNNODE* where *NNODE* is the maximum number of nodes.

After storing the displacement results in the array *DISP(2xNNODE)*, they are then stored into two different arrays *UX* and *UY*. This is done because the **VPUT* command can only read one-dimensional array. The **VPUT* command is used as follows

```
*VPUT, UX(1), NODE, 1, U, X
```

where *NODE* denotes the nodal parameters are being changed, 1 is the initial node number, *U* denotes the nodal displacement values being changed, and *X* stands for

the nodal displacements in X direction. In a similar manner, the Y displacement values are changed.

The stress values are also update in this operation. The stress results are written in a file outside the reanalysis program. Since only two-dimensional problems are considered in this work, the stress components are σ_x , σ_y and σ_{xy} . These stresses are calculated at the nodal locations. These values are then read from the APDL code and the stress values in the ANSYS database are replaced, in similar manner as the displacements. However, this time instead of using the **VPUT* command, a different procedure is used. The reason why the **VPUT* command cannot be used is that this command can be used to update the nodal stress values globally, i.e., at each node regardless of which element it is associated with. It is obvious that local nodal stresses at the same node but at different elements will be different. Therefore, *DESOL* command is used. This command modifies solution results at a node of an element. Command usage is as follows,

```
DESOL, ELEM, NODE, Item, Comp, V1, V2, V3, V4, V5, V6
```

where, *ELEM* is the element number for which modifications are to be made. *NODE* is the node number. *Item* is the label identifying results. For stress results it is 'S', and *Comp* is the component of the item. Its value depends on which directional stress that need to be updated. It is X for σ_x , Y for σ_y and XY for σ_{xy} . Also, *V1* is the value of the particular stress.

The disadvantage of using *DESOL* compared with **VPUT* is that for updating the stress results for all elements, a **DO* loop has to be used to repeat the command. There is no need to update the von Mises stress value explicitly. ANSYS calculates the von Mises stresses automatically from the stress values provided.

2. *PLT_UX*. Gives the contour plot for X – directional displacement values. *PLNSOL* command is used to obtain this contour plot. The command usage is as follows.

```
PLNSOL, U, X, 0, 1
```

where U corresponds to the displacement results, X defines the direction and Number 0 defines the undisplaced shape key, which shows only the deformed shape and does not overlays the undeformed structure display. The last item defines the scale factor for 2D display for contact items. Since there is no contact item, a default value of 1 is used.

3. *PLT_UY*. Gives the contour plot for Y – directional displacement values. Again *PLNSOL* command is used.
4. *PLT_US*. Gives the contour plot for vector sum of displacement values.

5. *PLT_SIGX*. Gives the contour plot of the σ_x stress values.
6. *PLT_SIGY*. Gives the contour plot of the σ_y stress values.
7. *PLT_VONM*. Gives the contour plot of the von Mises stress.
8. *LIST_DIS*. Gives the list of displacement results. The *PRNSOL* command is used to develop a list of nodal displacement values. For listing the displacement results, the usage is as follows,

`PRNSOL, DOF`

where, DOF corresponds to listing all displacement results.

9. *LIST_STR*. Gives the list of all stress results. Again *PRNSOL* is used to get the required results.
 10. *BACK*. Changes the toolbar back to as shown in Figure B.1 (c).
 11. *MAIN*. Changes the toolbar to the original one, e.g., as shown in Figure B.1 (b).
- *ANS_SOLN*. This allows the user to solve the analysis problem directly using the ANSYS solver instead of the reanalysis. Whenever a user feels that the final geometry obtained is what meets all the design requirements, then this will allow solving the same problem using ANSYS solver. This can also be helpful to compare the ANSYS and last reanalysis results.
 - *RETURN*. Is a command button which returns the ANSYS toolbar to ANSYS default toolbar, i.e., the toolbar shown in Figure B.1 (b).

C. Cost Advantage of Combined Approximation Reanalysis

C.1 Introduction

This appendix describes the cost effectiveness of using the combined approximation (CA) reanalysis solution technique over a traditional finite element solution using a direct method. The redesign problem will be solved using the following five steps as demonstrated in Section 3.3:

1. *Initial Design*. Design the initial geometry.
2. *Analysis and Post-Processing*. Model the new design problem and carry out the finite element analysis. Determine if the stress and the displacement results are acceptable.
3. *Re-modeling*. If the stresses and/or displacements in the step 2 are not acceptable then make changes in geometry.
4. *Reanalysis*. Use the combined reanalysis method developed in this work to solve the finite element problem for the changed geometry.
5. *Repeated Analysis*. Continue carrying out steps 3 and 4 until satisfactory results for the stress and/or displacements are achieved.

In absence of the reanalysis method, the designer will have to model the changed geometry, then mesh it and solve a conventional finite element problem. What is the advantage of using the reanalysis method over a conventional finite element solution approach? Some advantages include:

- i. No need to *re-model* the whole geometry again.
- ii. No need to go in *re-meshing* the whole geometry.
- iii. For small changes in geometry the method is more *efficient* compared with direct analysis.

The advantages of no remodeling and no re-meshing are easily understood. But what is considered to be a small modification? This answer can be obtained by comparing the cost of the combined approximation method versus a new separate conventional analysis.

The criterion generally used for comparing numerical methods is the number of multiplications. The arithmetic operation count in a numerical method is a very important criterion for deciding its acceptability. The arithmetic operations are addition, subtraction, multiplication and division. Generally the count is used to decide the rounding errors. But, it is equally important for the evaluation of the time required for a given set of calculations or a numerical method. It is often a deciding factor for selecting a numerical method for a particular application. Although ‘time’ for the operation is a relative term, since the CPU speed is increasing nowadays with tremendous amount with inventions of faster and faster processors, it is a good tool to compare the numerical method. In this regard, it will be important to keep in mind the following orders of magnitude (which are valid for the more recent computers); the time required for one multiplication is approximately four times that required for an addition (or subtraction),

while the time required for division is approximately ten times that required for an addition (or subtraction) [C.1]. Therefore, only multiplications and divisions will be considered in this work.

C.2 Comparison

In this section basically, two methods will be compared. These are the methods by which the problem under consideration can be solved. Clearly, one way of solving the redesign problem is to solve again. Cholesky decomposition method is generally used to solve the system of linear equations. This is referred to as Method # 1 in this comparison. Method # 2 is the combined approximation reanalysis method. However, before comparing the methods lets first define the following variables:

- n = Total Number of Degrees of Freedom for the Problem (with condition that the total number of degrees of freedom remains same in both designs)
- m = Number of Rows Changed in the Stiffness Matrix
- s = Number of Reduced Basis Vectors
- K_0 = Initial Stiffness Matrix
- u_0 = Initial Displacement Solution
- K = Modified Stiffness Matrix
- ΔK = Change in the Stiffness Matrix
- $K_0 = U_0^T U_0$
- U_0 = Upper Triangular Matrix

C.2.1 Method # 1: Direct Analysis with Cholesky Decomposition Method

This method is called direct analysis since the modified geometry is created, it is re-meshed and the problem is completely re-solved. An assumption has been made that the total number of degrees of freedom are same. Also if the Cholesky decomposition method is used for solving the analysis problem than the total number of multiplications and divisions is determined from the following relationship [C.2],

$$\left(\frac{n^3}{6} + n^2 \right) \quad (C.1)$$

C.2.2 Method # 2: Combined Approximation Reanalysis Method

This method is the combined approximation reanalysis method described in Section 2.4. Table 2.2 gives a detailed list of the steps used and the total number of the multiplications and divisions in each step. The number of reduced basis vectors is assumed to be 3. A portion of Table 2.2 is reproduced in Table C.1.

Table C.1 Method # 2 Cost Analysis

Step No.	Operation	Approximate Number of Multiplications and Divisions
1	$-\Delta Ku_1$	m^3
2	Solve $U_0^T t = -\Delta Ku_1$	n^2
3	Solve $U_0 u_2 = t$	n^2
4	$-\Delta Ku_2$	m^3
5	Solve $U_0^T t = -\Delta Ku_2$	n^2
6	Solve $U_0 u_3 = t$	n^2
7	$u_B = [u_1 \quad u_2 \quad \dots \quad u_s]$	-
8	$u_B^T K$	$3m^2$
9	$(u_B^T K)u_B = K_R$	$9m$
10	$F_R = u_B^T F$	$3m$
11	Solve $K_R y = F_R$	18
12	$u = u_B y$	$3n$
Total Number of multiplications or divisions		$\left[2m^3 + 4n^2 + 3n + (3m^2 + 12m + 18) \right]$

Thus, the total number of multiplications and divisions in Method # 2 is,

$$\left[2m^3 + 4n^2 + 3n + (3m^2 + 12m + 18) \right]$$

Since m is less than n , the terms in parenthesis are relatively very small compared to value of n in the entire expression and, therefore, can be neglected. The total number of multiplications and divisions for Method # 2 are,

$$2m^3 + 4n^2 + 3n \quad (C.2)$$

The comparison to be carried out is to determine a criterion for Method # 2 to be better than Method # 1. An essential criterion is to have less total number of multiplications and divisions that will result in less CPU time to carry out Method # 2. Using Equations (C.1) and (C.2), the following condition must be satisfied,

$$2m^3 + 4n^2 + 3n \leq \frac{n^3}{6} + n^2$$

$$2m^3 \leq \frac{n^3}{6} - 3n^2 - 3n$$

$$2m^3 \leq \frac{n^3}{6} \left(1 - \frac{18}{n} - \frac{18}{n^2} \right)$$

since the value of n (the total number of degrees of freedom) is very large then these terms can be neglected and one can assume,

$$\left(\frac{18}{n} - \frac{18}{n^2} \right) \ll 1$$

therefore, Method # 2 can be considered efficient if,

$$2m^3 \leq \frac{n^3}{6}$$

$$\frac{m^3}{n^3} \leq \frac{1}{12}$$

$$\frac{m}{n} \leq \sqrt[3]{\frac{1}{12}}$$

yielding,

$$\frac{m}{n} \leq 0.4368 \quad (C.3)$$

Thus, when the total number of degrees of freedom changed in the redesigned problem is less than approximately 43%, only then using the combined approximate method is more efficient than re-solving the problem again. In other words, if the total allowable geometrically changed nodes in the modified mesh is less than 43% of the total number of nodes (assuming the total number nodes in both designs are same).

D. User Interface Design Language

D.1 Introduction

The ANSYS User Interface Design Language (UIDL) is a programming language that lets the user customize many components of the ANSYS Graphical User Interface. The configurable components include:

- Items on the ANSYS Main Menu
- Dialogues, including Picking Dialogue
- Online Help

Customizing the GUI lets the user modify many ANSYS menus and dialogs and also integrate locally developed programs into the ANSYS environment.

D.2 UIDL Structure

Each UIDL program consists of a control file header and a series of “building blocks.” A building block is a series of UIDL commands, used to create components of the GUI. There are two types of building blocks:

- Menu Blocks, for Creating Menus
- Function Blocks, for Creating Dialogs

The UIDL processor reads the control file, inserts ANSYS indexing information (which relates the building blocks to the ANSYS GUI) into the control file, and builds the GUI. The UIDL was used to customize the ANSYS GUI to include the reanalysis menu and the subsequent procedures for doing reanalysis using the following three steps:

1. A control file named REANAL.GRN is created and saved in a subdirectory named MENUITEMS.
2. All the remaining control files used by ANSYS are copied in the same folder from `/ansys_inc/ansys57/docu/English/UIDL`.
3. The file named **menulist57.ans**, which contains the pointer to the ANSYS UIDL control files, is copied to the working directory. The name of the new created control file is added in **menulist57.ans**.

D.2.1 Control Files

A control file consists of a control file header and at least one building block menu. A control file name always ends with extension .GRN. ANSYS uses control files to build all the standard dialogs and menus. Here is a list of the standard ANSYS control files and the components of GUI they build:

UIFUNC1.GRN	GUI Function
UIFUNC2.GRN	GUI Function

D.2.1.1 Control File Header

A control file header is set of specific UIDL commands that define information about the control file for the UIDL processor. A line in a control file cannot exceed 80 characters in length. All header commands begin with colon (:). A control file header contains the following four commands in this order:

```
:F NEMENU.GRN
:D Modified on %E%, defines new menus for ANSYS GUI
:I      0,      0,      0
:!
```

where a brief descriptions of these commands is:

- :F** *Filename* Required; name of the control file, must appear in line 1.
- :D** *String* Required; control file description, must appear in line 2. ANSYS writes the date at location (%E%) automatically.
- :I** 0, 0, 0 Required; space holder for ANSYS indexing, must appear on line 3. The 0s (zeros) must be in columns 9, 18, and 27 and must be separated by commas.
- :!** Optional; separates the control file header from the blocks.

When UIDL processes an edited control file, the 0s are placed with indexing information. Each time a control file is modified, the (**:I**) command line must be reinserted with 0s at their proper places.

Once ANSYS is started after creating new control file, ANSYS adds additional information to the end of the control file. ANSYS inserts **:X INDEX ADDED BY ANSYS** at the end of each control file. The name of each block appears, followed by an index number. After each modification in the control file, everything after final **:E END** command must be deleted.

D.2.1.2 Building Blocks

Building blocks follow the control file header in the control file. Building blocks can be menu blocks or function blocks as follows:

1. *Menu Blocks.*
The menu block controls the organization and content of the ANSYS Main Menu in the GUI. The standard ANSYS menu blocks are all contained in the UIMENU.GRN file.
2. *Function Blocks.*
The function block controls the following:
 - Layout and content of the configurable dialogs and prompts.
 - Picking operation.

- Hidden operations which build and pass command.

The standard ANSYS dialogs are stored in the UIFUNC1.GRN and UIFUNC2.GRN files.

D.3 Overview of Building Blocks

Each building block consists of the following three sections:

- Header Section
- Data Controls Section
- Ending Section

Each type of building block has different data controls. Each control file typically contains multiple building blocks. Figure D.1 shows a sample control file containing a menu block for an ANSYS GUI menu. This menu block builds the ANSYS Main Menu.

	Control File	:F NEWMENU.GRN
	Header	:D Menu Control File :I 0, 0, 0 :!
	Block Header Section	:N MenuRoot :S 0, 0, 0 :T Menu :A Main Menu (1)
	Data Controls Section	:D ANSYS ROOT MENU Fnc_Preferences Sep_ (2) Men_Preproc Men_Solution Men_GenlPost Men_TimePost Sep_ (3) Men_Topo K_LN(alpha) Men_DesOpt K_LN(ALPHA) Men_DesOpt_al Men_ProbDesign Men_Aux12 Men_RunStat Sep_ Fnc_UNDO Sep_ Fnc_FINISH K_LN(UTILMENU) (4) Men_UtilMenu
	Ending	:E END

Figure D.1 Control File with ANSYS Main Menu building block.

The structure of control file header is discussed in Section D.2.1.1. The details of the building block are discussed below.

D.3.1 Block Header Section

All header commands begin with a colon (:). Each header section must begin with a **:N** command which defines the unique, internal name of the building block. The next command, **:S**, is a space holder for the index line. This command must have zeros, separated by commas, in columns 9, 16, and 23. The **:T** indicates the type of building block: Menu, or Cmd. Optional UIDL commands, such as **:A** (menu heading) and **:D** (block description), can also be in the header. The header section is processed as soon as the building block is entered by the UIDL processor.

D.3.2 Data Controls Section

This section must include at least one data control. The data controls used depend on the type of building block defined by the **:T** line. In the menu blocks, the data control section contains calls to existing menu blocks (**Men_String**) and to function blocks (**Fnc_String**). In function blocks, the data control section defines the contents of a dialog.

D.3.3 Ending Line

A block must always end with the **:E END** command. At least one separator (**:!** command) should appear between blocks.

D.4 The **menulist57.ans** File

In order for ANSYS to incorporate the changes made in the GUI, the name of the new control file needs to be added to the **menulist57.ans** file. This file contains pointers to all ANSYS control files, which in turn contains the GUI building blocks. ANSYS looks for the **menulist57.ans** using the following search path order:

1. The current working directory
2. The users home login directory
3. **/ansys_inc/ansys57/docu/**directory on the server.

For current work this file is copied into the working directory. All control files including the newly generated file are copied in a separate folder (**MenuItems**) to the working directory. The data in modified **menulist57.ans** file is,

```
/users/projects/sachint/MenuItems/MYMENU.GRN  
/users/projects/sachint/MenuItems/MYFUNC1.GRN  
/users/projects/sachint/MenuItems/MYFUNC2.GRN  
/users/projects/sachint/MenuItems/REANAL.GRN
```


The modified ANSYS GUI information is defined by REANAL.GRN. This file takes precedence over the GUI information defined in the standard ANSYS control files because it appears last in the **menulist57.ans** file.

E. Hand Calculation for Example Problems

This appendix provides the hand solution of the problems solved in Chapter 4 using the reanalysis approach. It is good practice before starting any finite element analysis, to carry out a hand analysis of the problem.

E.1 Problem # 1: Plate with a Hole.

Hand analysis for the initial problem and the redesign problems is performed to determine the maximum stress in the plate.

Plate with a Square Hole. Figure E.1 shows the plate with a square hole and its geometric details applicable to the problem

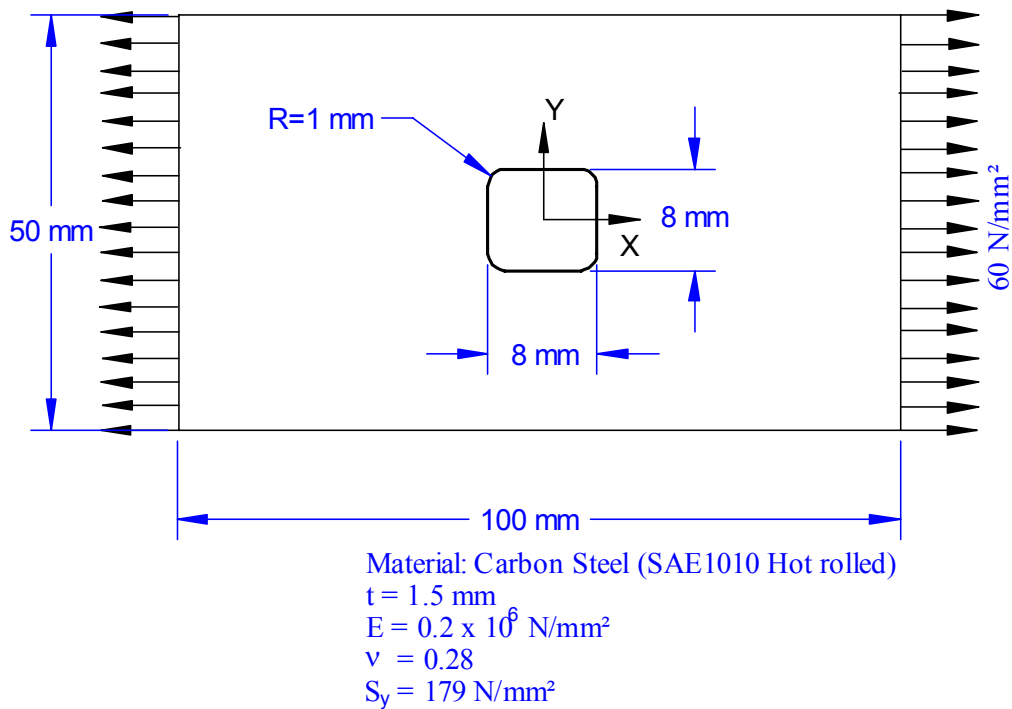


Figure E.1 Plate with a square hole.

Due to the square hole and a fillet there is stress concentration at the fillet. A stress concentration factor is needed to find out the theoretical stress at the fillet. From Norton [E.1] the stress concentration factor for the concerned problem is determined to be 2.22, i.e., $K_t = 2.22$. The maximum nominal stress without the fillet will be at the central axis of the part. And it is the force acting over the smallest area (as shown in Figure E.2) resisting the force.

$$A_{\min} = 1.5 \times (50 - 8) = 63 \text{ mm}^2$$

$$P = 4500 \text{ N}$$

Maximum nominal stress is,

$$\sigma_o = \frac{P}{A_{\min}} = \frac{500}{63} = 71.428571 \cdot \text{N/mm}^2$$

$$K_t = 2.22$$

Maximum theoretical stress at the fillet is,

$$\sigma_{\max} = K_t \cdot \sigma_o = \underline{\underline{158.57}} \text{ N/mm}^2$$

Thus, the maximum stress is 158.57 N/mm².

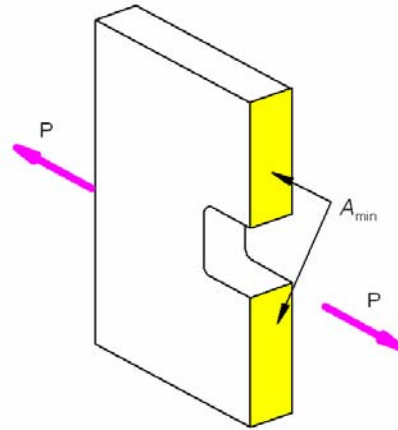


Figure E.2 Cut Section

Using the reanalysis tools discussed in Chapter 3, this geometry was modified to three different geometries (1) Plate with the circular hole, (2) Plate with a horizontal elliptical hole and (3) Plate with a vertical elliptical hole. Keeping all the other material and the geometric properties constant (including the thickness, Young's Modulus and Poisson's ratio) a hand analysis for the stress concentration can also be performed using the stress concentration factors.

Plate with a Circular Hole. Figure E.3 shows a plate with the circular hole. For this geometry the nominal stress will remain same as the previous one since the is the same.

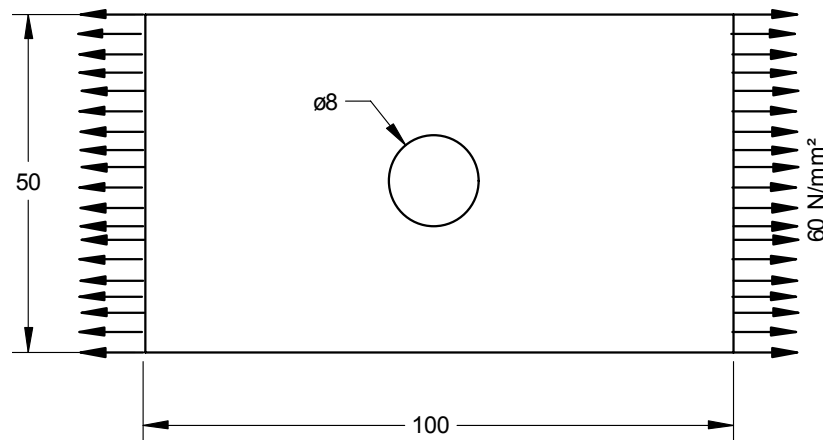


Figure E.3 Plate with circular hole

From Norton [E.1] the stress concentration factor for this problem is $K_t = 2.57017$. from Peterson's Stress Concentration factors handbook [E.2] $K_t = 2.5975$, The maximum stress in the plate is calculated as,

$$\sigma_{\max} = K_t \cdot \sigma_o = \underline{\underline{183.58}} \text{ N/mm}^2$$

Thus, the maximum stress is 183.58 N/mm².

Plate with a Horizontal Elliptical Hole. Figure E.4 shows the problem of plate with an elliptical hole. All the dimensions of the problem are shown in the figure. The nominal stress in this problem will be different than the previous two since the area A_{\min} is greater reducing the nominal stress.

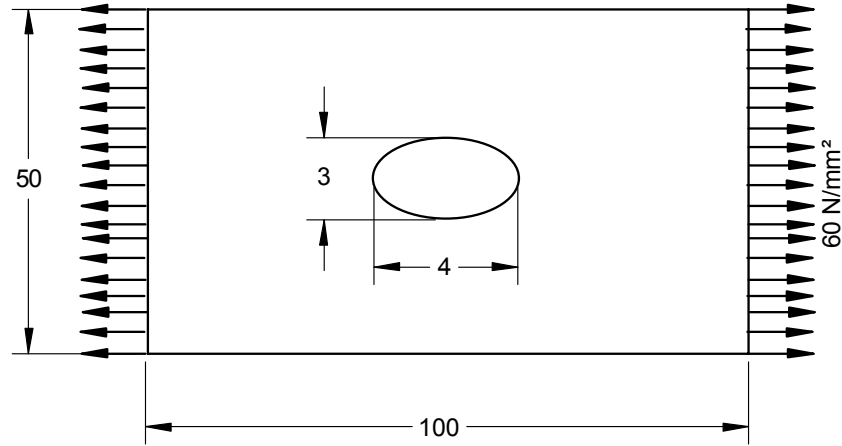


Figure E.4 Plate with a horizontal elliptical hole.

The minimum area resisting is,

$$A_{\min} = 1.5 \times (50 - 6) = 66 \text{ mm}^2.$$

Nominal stress is,

$$\sigma_o = \frac{P}{A_{\min}} = \frac{4500}{66} = 68.182 \cdot \text{N/mm}^2$$

The stress concentration factor = $K_t = 1.94$ [E.2]

Maximum theoretical stress at the fillet is,

$$\sigma_{\max} = K_t \cdot \sigma_o = \underline{\underline{132.27}} \text{ N/mm}^2$$

Plate with a Vertical Elliptical Hole. Figure E.5 shows the problem of plate with a vertical elliptical hole. All the dimensions of the problem are shown in the figure. The nominal stress in this problem will be different than the previous three since the area A_{\min} is smaller reducing the nominal stress.

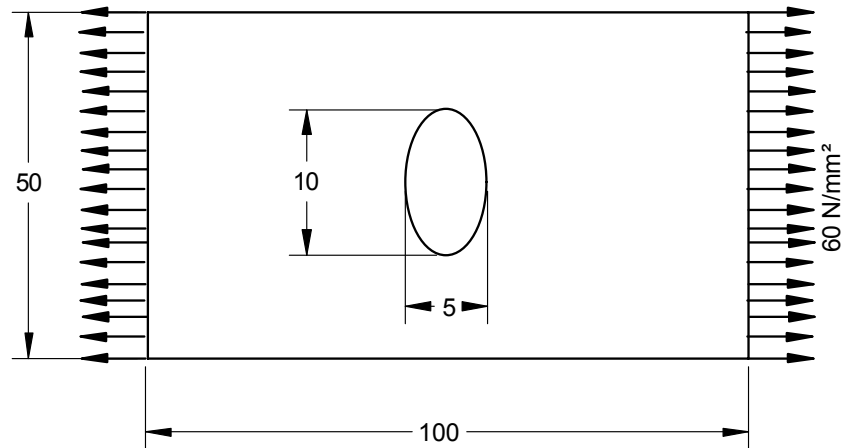


Figure E.5 Plate with a vertical elliptical hole.

For hand analysis, the minimum cross sectional area resisting the force is,

$$\text{Area} = A_{\min} = (50 - 10) \times 1.5 = 60 \text{ mm}^2$$

Total force acting = $P = 4500 \text{ N}$

Nominal Stress,

$$\sigma_o = \frac{P}{A_{\min}} = \frac{4500}{60} = 75 \cdot \text{N/mm}^2$$

Stress concentration factor for this type of elliptical hole was found to be $K_t = 4.132$ [E.2].

Using this, the actual maximum stress will be,

$$\sigma_{\max} = K_t \cdot \sigma_o = \underline{\underline{309.9}} \text{ N/mm}^2$$

Thus the maximum stress in the case when the elliptical hole is vertical is more than the case when elliptical hole is horizontal and the value is 309.9 N/mm^2 .

Displacement Results. The theoretical solution for displacement result for each different case cannot be determined. So the problem is solved neglecting the effect of the hole inside the geometry. Assume that the plate is without any hole, the total displacement in X – direction is given by,

$$U_x = \frac{P \cdot L}{A \cdot E}$$

where,

L = Total Length in X – direction = 100 mm

A = Total Cross-sectional Area = $50 \times 1.5 = 75 \text{ mm}^2$

E = Young's Modulus = $0.2 \times 10^6 \text{ N/mm}^2$

Producing,

$$U_x = \frac{4500 \times 100}{75 \times 0.2 \times 10^6} = 0.03 \cdot mm$$

Thus, when the quarter symmetry model is considered for the plate, then the displacement result will be $U_x = 0.15 \times 10^{-1} mm$.

E.2 Problem # 2: Circular arc fillet.

In Problem # 2, a free-form fillet for optimum value of stress concentration factor is solved. The theoretical value of the stress for the free-form fillet is not known. But in reanalysis # 2, same problem is solved with circular arc fillet. Figure E.6 shows the circular arc fillet.

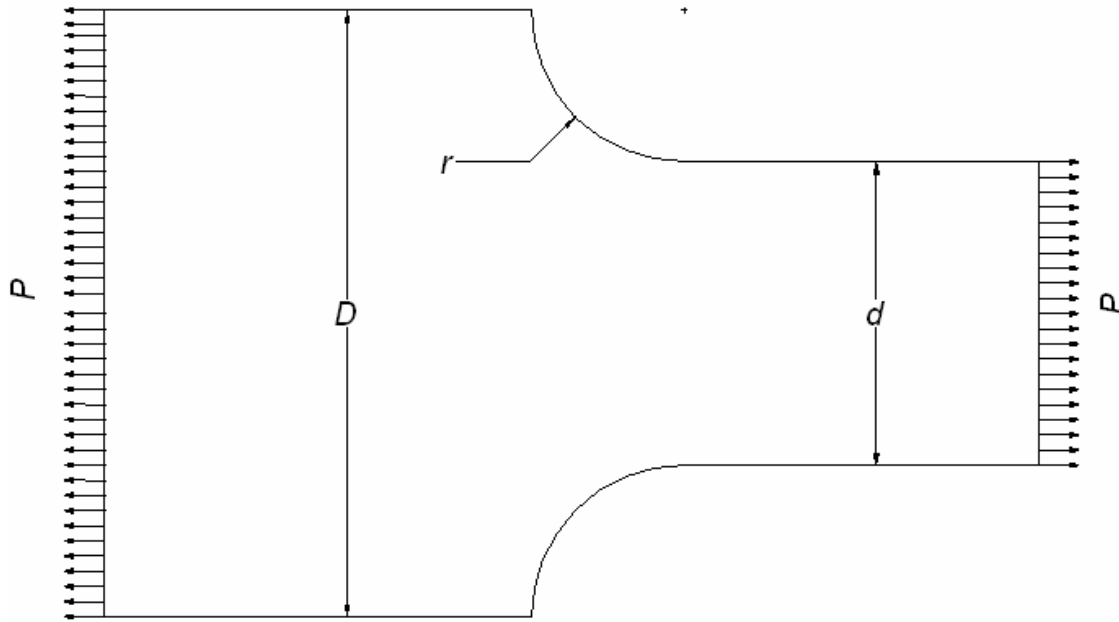


Figure E.6 Circular arc Fillet

The stress concentration factor for this geometry and this type of loading condition can be found out from Norton [E.1]. The notations for this geometry are,

$$D = 20mm,$$

$$d = 10mm,$$

$$r = 5mm,$$

$$\text{Thickness, } h = 1mm$$

From Norton [E.1] the stress concentration factor is given as,

$$K_t = A \cdot \left(\frac{r}{d} \right)^b$$

For $D/d = 2.0$ we get

$$A = 1.09960$$

$$b = -0.32077$$

Using this the stress concentration factor for circular arc fillet,

$$K_t = 1.3734$$

So if the nominal stress applied at the end is 1 N/mm^2 then the maximum stress at the fillet will be **1.3734 N/mm^2** .

Graphically Driven Interactive Stress Reanalysis for Machine Elements in the Early Design Stage

M.S. Thesis Defense Presentation

by

Sachin S. Terdalkar

Advisor: Prof. Joseph J. Rencis



WPI

Mechanical Engineering

Presentation Outline

- ✚ Goal and Objectives
- ✚ Introduction
- ✚ Structural Reanalysis
- ✚ Combined Approximation Reanalysis
- ✚ ANSYS GUI
- ✚ Development Platform
- ✚ Case Studies
- ✚ Cost Analysis
- ✚ Conclusion
- ✚ Future Work

WPI

ME

Goal and Objectives

Goal:

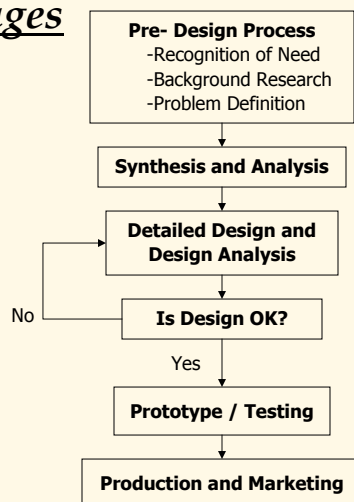
- ✚ Develop a methodology to carry out FEA in the early design stage achieving the advantage of introducing early-analysis in the product development cycle.

Objectives:

- ✚ Instantaneous Stress and Displacement Results
- ✚ Enhanced Computational Performance
- ✚ User Friendly

Introduction

Design Process Stages



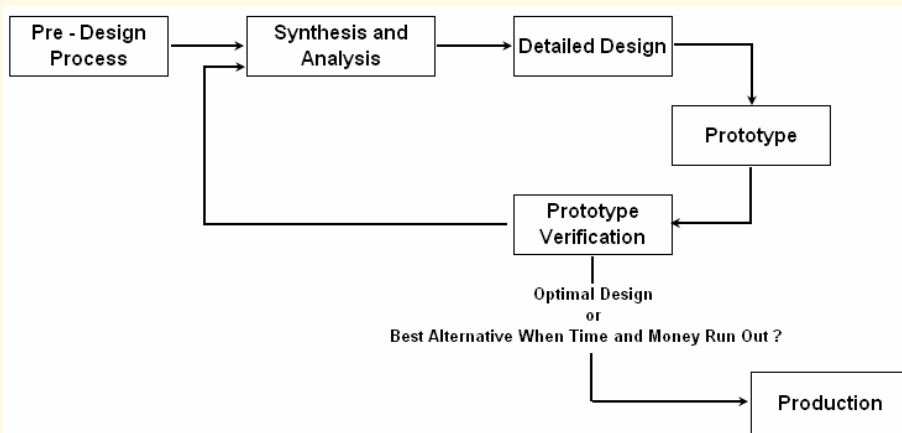
Introduction

Current Status of FEA in Design Process

- ✚ Seldom Used in Daily Engineering Practice
- ✚ Design Engineer Works Independent of Analyst
- ✚ Many Still Apply FEA in Final Design Stage

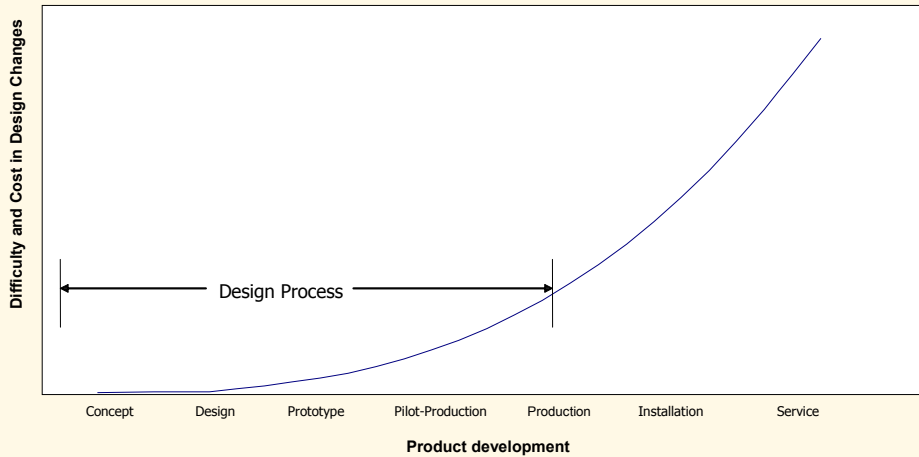
Introduction

Traditional Product Development Cycle



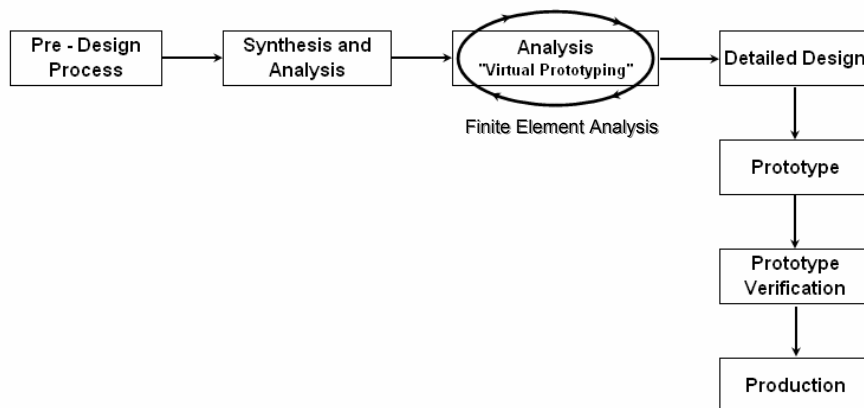
Introduction

Difficulties and Cost in Design Changes



Introduction

Product Development Cycle using Early Analysis



Introduction

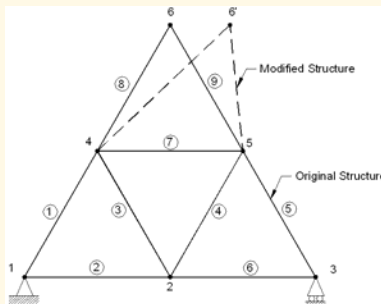
Advantages of Early Analysis

- ✚ Helps designer to consider and evaluate alternate approaches and to explore options
- ✚ Reduced Product Development Cost
- ✚ Improved Product Design
- ✚ Shortened Time to Market
- ✚ Reduction in Knowledge Gap

Structural Reanalysis

Definition

Find the response under the static load of a structure after modifications using the original response of the structure.



Structural Reanalysis

Classifications

- ✚ Direct (Exact)
- ✚ Iterative
- ✚ Approximate
 - ✨ Global Approximations
 - ✨ Local Approximations
 - ✨ Combined (Hybrid) Approximations
(Will be used)

Combined Approximation Reanalysis

Initial Design Problem

$$F = K_0 u_0$$

$$K_0 = U_0^T U_0$$

K_0 Initial Stiffness Matrix

F External Force Array

u_0 Initial Displacement

Modified Design Problem

$$F = Ku$$

$$K = K_0 + \Delta K$$

U_0 Upper Triangular Matrix

K Modified Stiffness Matrix

ΔK Changes in Stiffness Matrix

Define $u_1 = u_0$

Solve, $K_0 u_2 = -\Delta K u_1$

Forward substitution $U_0^T t = -\Delta K u_1$

Backward substitution $U_0 u_2 = t$

Combined Approximation Reanalysis

The matrix of the basis vectors u_B is defined by,

$$u_B = [u_1 \quad u_2 \quad \cdots \quad u_s]$$

Reduced square matrix

$$K_R = u_B^T K u_B \text{ and } F_R = u_B^T F$$

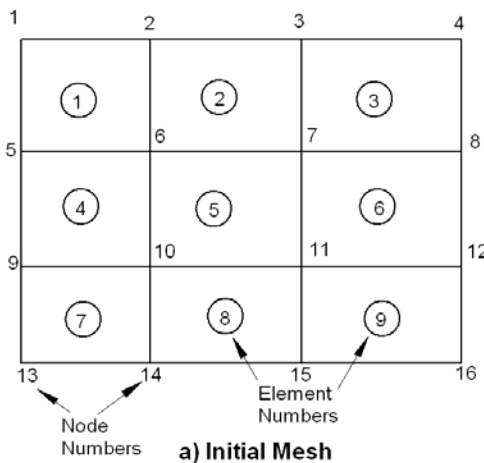
Solving,

$$K_R y = F_R$$

$$u = y_1 u_1 + y_2 u_2 + \cdots + y_s u_s = y u_B$$

Combined Approximation Reanalysis

Finding Change in Stiffness Matrix



Initial Stiffness Matrix

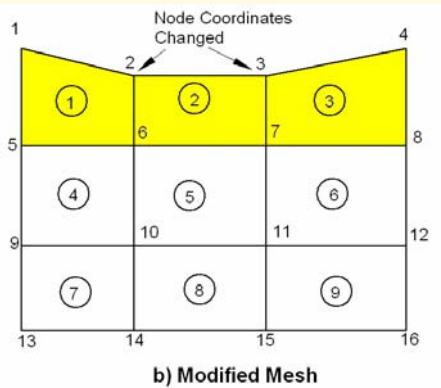
$$K_0 = K_{e_0}^1 + K_{e_0}^2 + K_{e_0}^3 + \cdots + K_{e_0}^9$$

$$K_{e_0}^1, K_{e_0}^2, K_{e_0}^3 \cdots K_{e_0}^9$$

are element stiffness matrices for element numbers 1,2,3,...,9

Combined Approximation Reanalysis

Finding Change in Stiffness Matrix



Modified Stiffness Matrix

$$K = K_e^1 + K_e^2 + K_e^3 + K_{e_0}^4 + K_{e_0}^5 + \dots + K_{e_0}^9$$

Combined Approximation Reanalysis

Finding Change in Stiffness Matrix

Change in the Stiffness Matrix

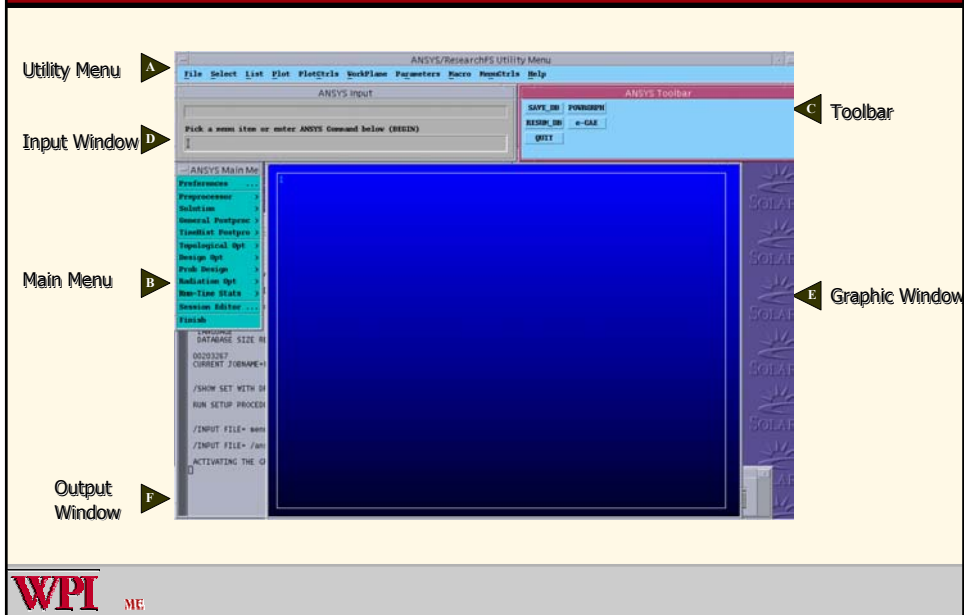
$$\Delta K = K - K_0$$

i.e.

$$\Delta K = (K_e^1 - K_{e_0}^1) + (K_e^2 - K_{e_0}^2) + (K_e^3 - K_{e_0}^3)$$

$$\Delta K = \left[\begin{array}{l} \text{Sum of the differences in element} \\ \text{stiffness matrices of those elements} \\ \text{whose at least one node has} \\ \text{undergone a change in coordinates.} \end{array} \right]$$

ANSYS® GUI



Development Platform

Steps for Solving Reanalysis Problem

1. Initial Problem
2. Analysis and Post-processing
3. Re-modeling
4. Reanalysis
5. Repeated Analysis

Development Platform

1. Initial Design

- ✚ First Design Concept during Design Process
- ✚ Check Stresses and Displacements

2. Analysis and Post-processing

- ✚ ANSYS FEA for Design Concept
- ✚ Post-processing of Analysis Results

3. Re-modeling

- ✚ Modify Current Geometry

Development Platform

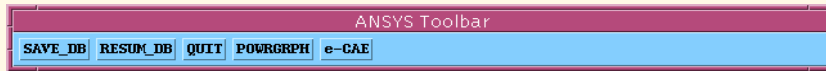
4. Reanalysis

- ✚ Use Reanalysis Algorithm
- ✚ Update Stress and Displacement Results

5. Repeated Analysis

- ✚ Unacceptable Results, repeat Re-modeling and Reanalysis

Development Platform



(a) ANSYS Default Toolbar before making change.



(b) ANSYS Toolbar after making change.



(c) Reanalysis Sub - Menu visible after clicking on REANAL.

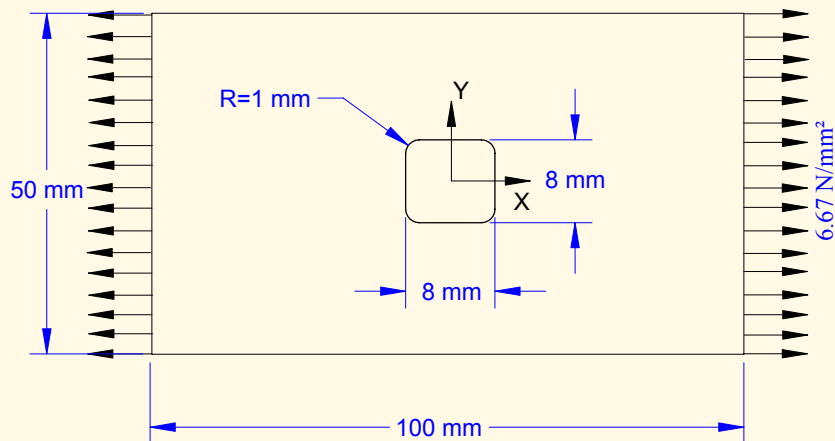


(d) Reanalysis Sub - Menu visible after clicking on RESULT.

Case Studies

Case Study # 1: Plate with a Hole

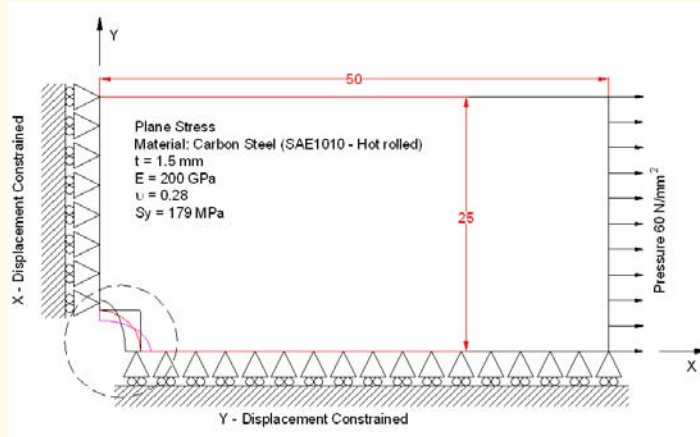
Initial Problem:



Case Studies

Case Study # 1

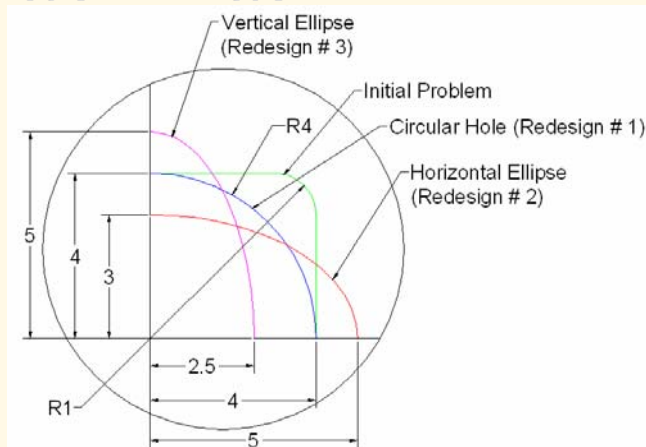
Initial Problem: FE model



Case Studies

Case Study # 1

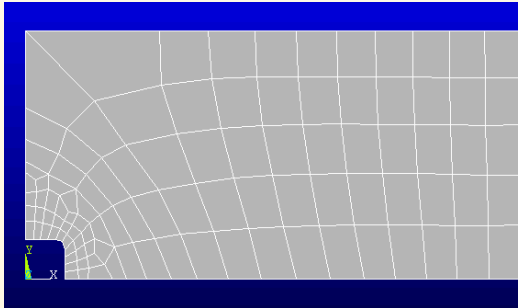
Initial Problem: FE Model



Case Studies

Case Study # 1

Initial Problem: FE Model



Mesh Characteristics:

104 Four-node Quad Elements
130 Nodes
2 DOF/node
260 Total DOF

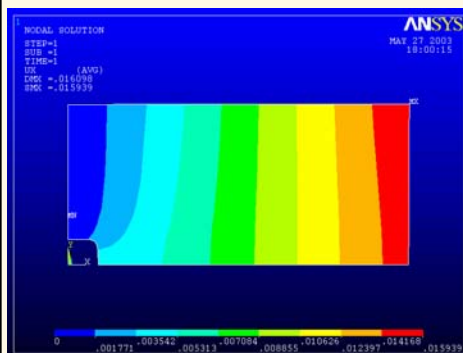
Element and Material Properties:

Material: Carbon Steel
(SAE 1010 – hot rolled)
PLANE42 – Four Node Quad
Plane Stress with Thickness
Poisson's Ratio – 0.28
Young's Modulus – 0.2×10^6 N/mm²
Thickness – 1.5 mm
Yield Stress (S_y) – 179 N/mm²

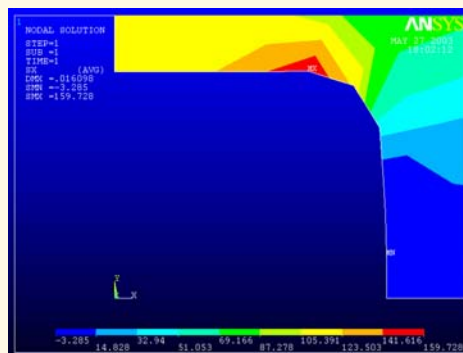
Case Studies

Case Study # 1

Initial Problem: Analysis and Post-processing



U_x – Displacement

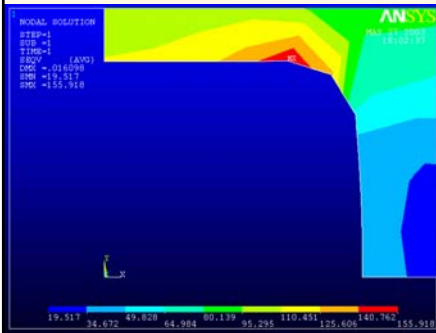


σ_x – Normal Stress at fillet

Case Studies

Case Study # 1

Initial Problem: Analysis and post-processing



σ_{VM} – von Mises Stress at fillet

Maximum Deflection (mm)

	u_x	u_y
Node #	17	22
Value	0.15939×10^{-1}	-0.2634×10^{-2}

Maximum and Minimum stress components (N/mm²)

		σ_x	σ_y	σ_{xy}	σ_{VM}
Minimum	Node #	40	1	102	4
	Value	-3.2847	-50.418	-39.466	19.517
Maximum	Node #	37	37	52	37
	Value	159.73	29.524	2.3933	155.92

$S_y = 179 \text{ N/mm}^2$
Safety Factor = 1.12

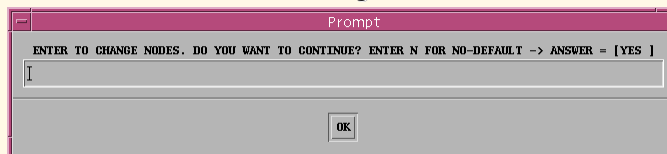
Case Studies

Case Study # 1

Re – modeling



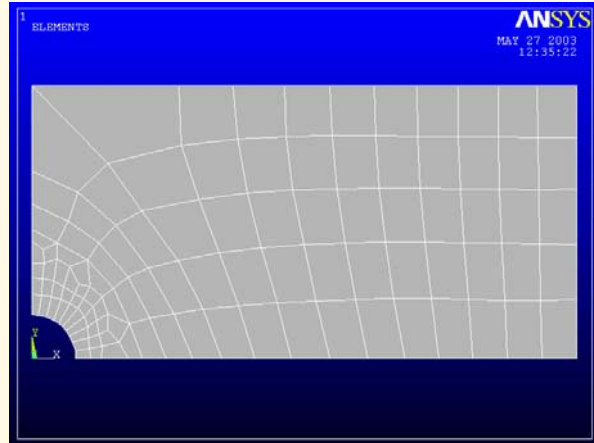
Re – modeling window



Case Studies

Case Study # 1

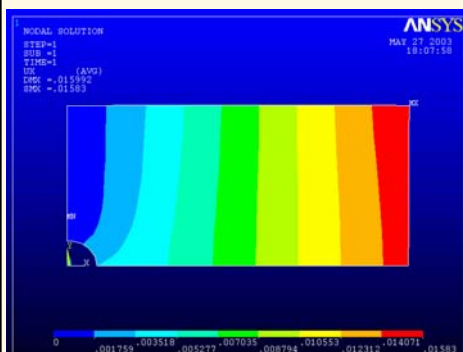
Redesign Option # 1: Plate with Circular Hole



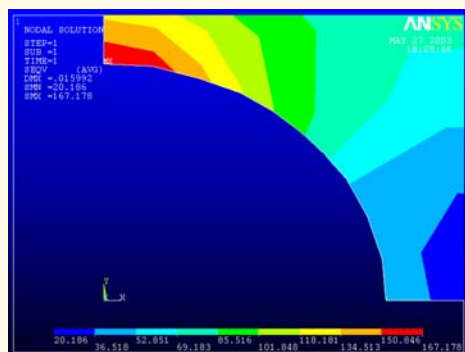
Case Studies

Case Study # 1

Reanalysis Results



U_x – Displacement

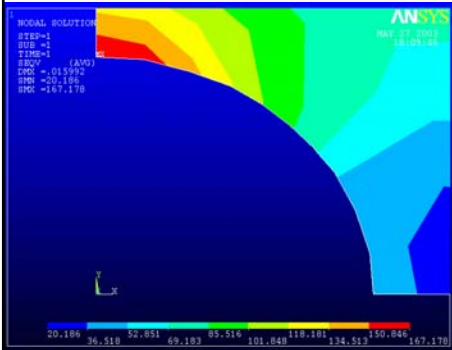


σ_x – Normal Stress at Fillet

Case Studies

Case Study # 1

Reanalysis Results



Maximum Deflection (mm)

	U_x	U_y
Node #	17	22
Value	0.1583×10^{-1}	-0.25617×10^{-2}

Maximum and Minimum stress components (N/mm²)

		σ_x	σ_y	σ_{xy}	σ_{vm}
Minimum	Node #	1	1	1	3
	Value	-3.9486	-54.329	-24.293	20.186
Maximum	Node #	32	32	108	32
	Value	179.03	27.045	4.0545	167.18

$S_y = 179 \text{ N/mm}^2$
Safety Factor = 1.00

Case Studies

Case Study # 1

Reanalysis Results

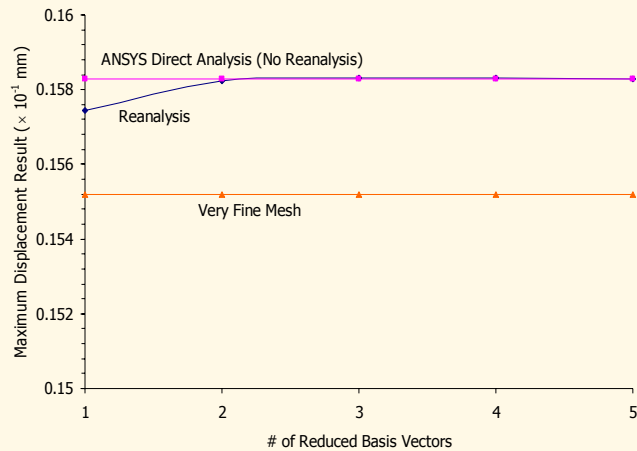
		Theoretical	ANSYS Direct Analysis	Reanalysis				
				RBV – 1	RBV – 2	RBV – 3	RBV – 4	RBV – 5
Maximum σ_x N/mm ²	Value	183.584	176.33	200.25	169.19	179.03	180.25	180
	Node #	-	32	37	32	32	32	32
Maximum σ_{vm} N/mm ²	Value	183.584	164.40	196.58	159.11	167.18	167.92	167.61
	Node #	-	32	37	32	32	32	32
Maximum Displacement $\times 10^{-1}$ mm	Value	0.15518	0.15829	0.15744	0.15824	0.15830	0.15830	0.15839
	Node #	-	17	17	17	17	17	17

RBV – Number of Reduced Basis Vectors used for Reanalysis

Case Studies

Case Study # 1

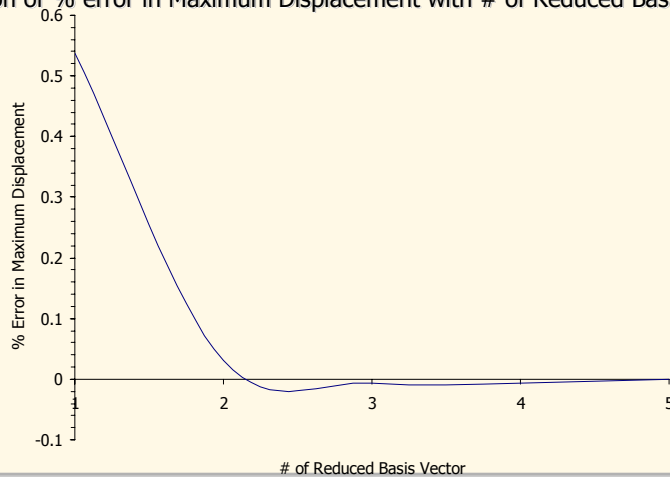
Variation of Maximum Displacement with # of Reduced Basis Vectors



Case Studies

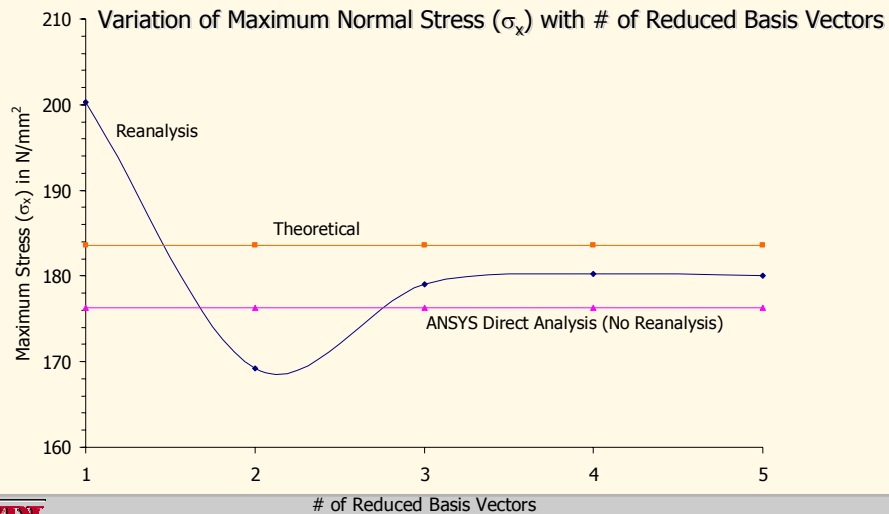
Case Study # 1

Variation of % error in Maximum Displacement with # of Reduced Basis Vectors



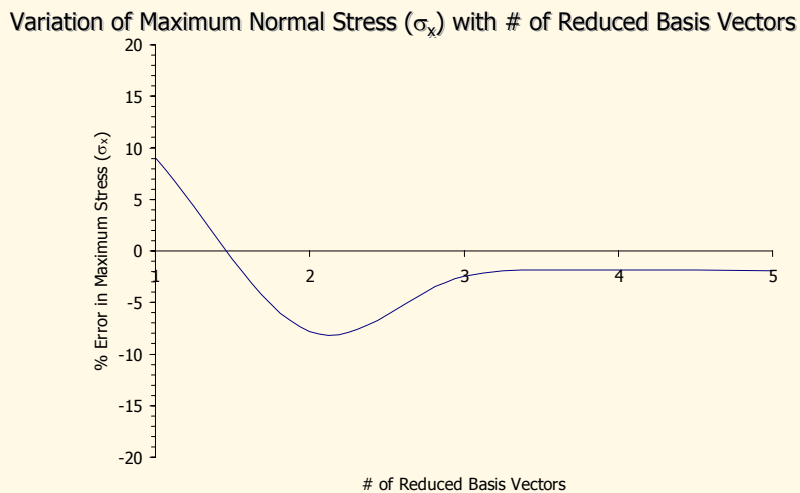
Case Studies

Case Study # 1



Case Studies

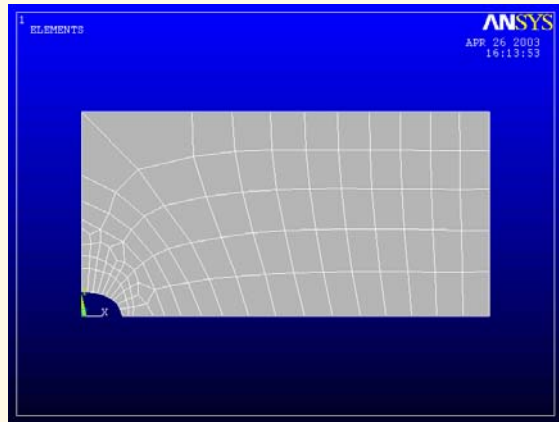
Case Study # 1



Case Studies

Case Study # 1

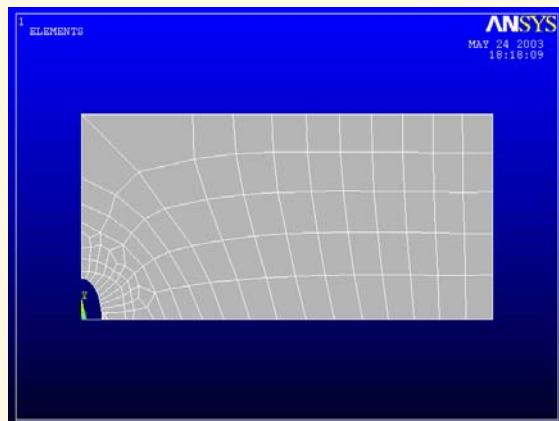
Redesign Option # 2: Plate with Horizontal Elliptical Hole



Case Studies

Case Study # 1

Redesign Option # 3: Plate with Vertical Elliptical Hole



Case Studies

Case Study # 1

Displacement Results

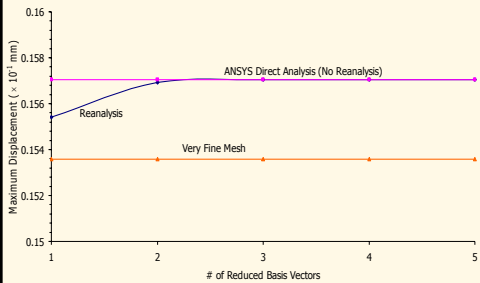


Plate with horizontal elliptical hole

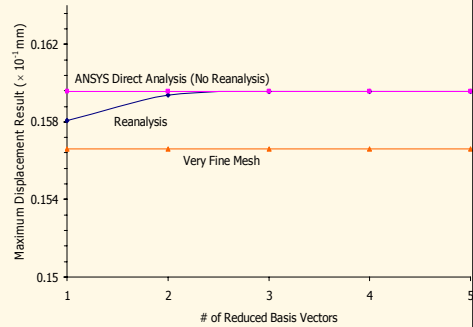


Plate with vertical elliptical hole

Case Studies

Case Study # 1

Stress Results

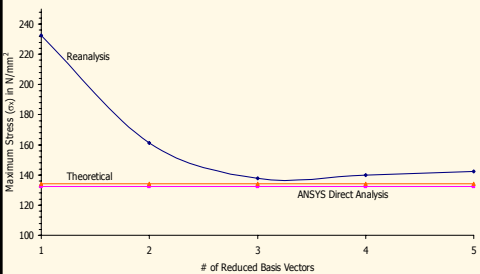


Plate with horizontal elliptical hole

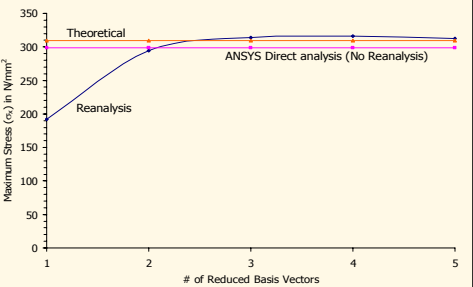


Plate with vertical elliptical hole

Case Studies

Case Study # 1

Reanalysis Result Comparison

Maximum Quantities	Redesign Options								
	# 1: Circular Hole			# 2: Horizontal Ellipse			# 3: Vertical Ellipse		
	ANSYS Direct Analysis	Reanalysis	% Error	ANSYS Direct Analysis	Reanalysis	% Error	ANSYS Direct Analysis	Reanalysis	% Error
σ_x N/mm ²	176.33	179.03	1.53	134.28	137.94	2.72	298.75	314.27	5.19
Safety Factor	1.02	1	-	1.33	1.3	-	0.6	0.57	-
σ_{VM} N/mm ²	164.40	167.18	1.69	126.44	129.53	2.44	274.29	288.70	5.25
Displacement U_x ($\times 10^{-1}$ mm)	0.15829	0.15830	0.0063	0.15704	0.15705	0.0063	0.15958	0.15956	0.013

Case Studies

Case Study # 1

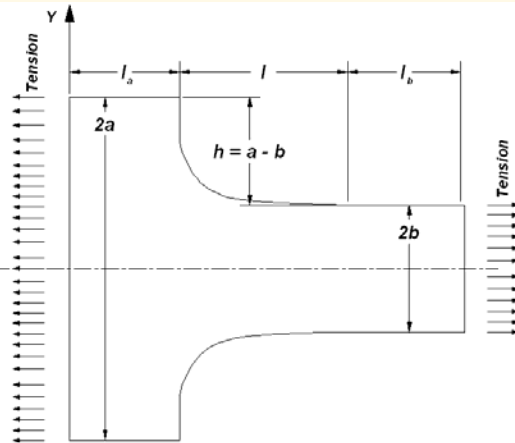
Conclusion:

1. Three different geometries explored
2. Horizontal elliptical hole shows lower stress results
3. The displacement results are very accurate for three reduced basis vectors
4. Stress results are near to the ANSYS Direct Analysis results
5. Accuracy increases as the number of reduced basis vectors is increased

Case Studies

Case Study # 2 : Optimal Free-Form Fillet under Tension

Initial Problem:



Mesh Characteristics:

125 Four-node Quad Elements
156 Nodes
2 DOF/node
312 Total DOF

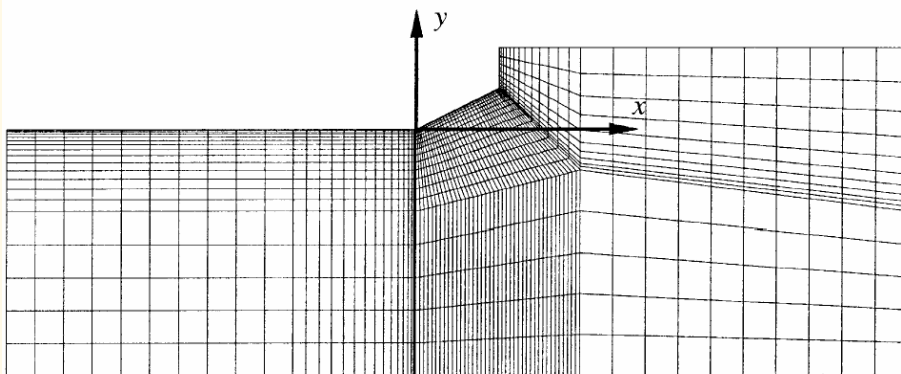
Element and Material Properties:

PLANE42 – Four node quad
Plane Stress with thickness
Poisson's ratio – 0.3
Young's Modulus – 72400 N/mm²
Thickness – 1 mm
 $a/b = 2$
 $l/h = 1$

Case Studies

Case Study # 2

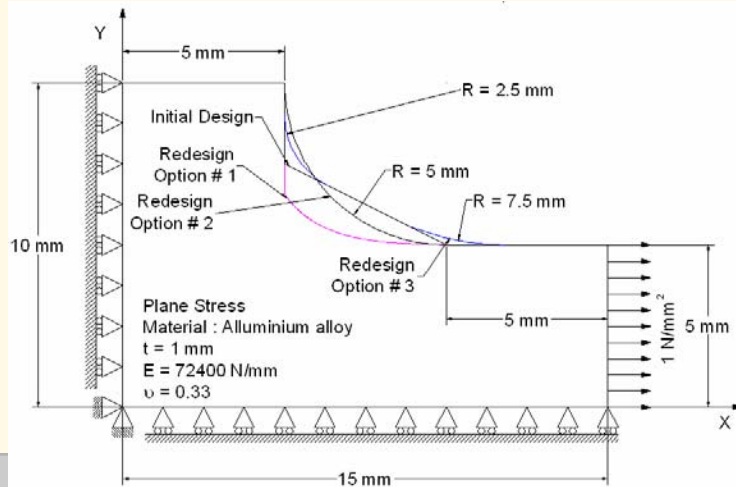
Initial Problem: FEM Mesh used by Waldman [4.2]



Case Studies

Case Study # 2

Initial Problem: FE Model



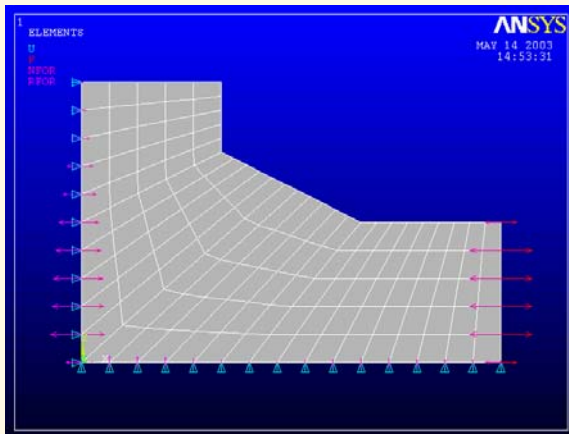
WPI

ME

Case Studies

Case Study # 2

Initial Problem: FE Model



Mesh Characteristics:

125 Four-node Quad Elements
156 Nodes
2 DOF/node
312 Total DOF

Element and Material Properties:

PLANE42 – Four node quad
Plane Stress with thickness
Poisson's ratio – 0.3
Young's Modulus – 72400 N/mm²
Thickness – 1 mm
 $a/b = 2$
 $l/h = 1$

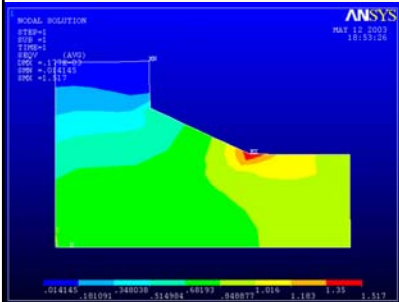
WPI

ME

Case Studies

Case Study # 2

Initial Problem: Analysis and Post-processing



σ_{VM} – von Mises Stress

Maximum Deflection (mm)

	u_x	u_y
Node #	12	1
Value	0.17647×10^{-3}	-0.36526×10^{-4}

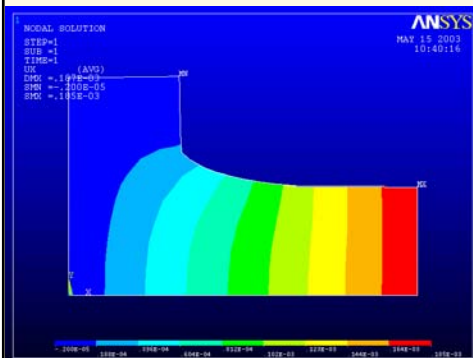
Maximum and Minimum stress components (N/mm²)

		σ_x	σ_y	σ_{xy}	σ_{VM}
Minimum	Node #	52	11	51	52
	Value	-0.154×10^{-1}	-0.1735	-0.3643	0.1414×10^{-1}
Maximum	Node #	32	32	1	32
	Value	1.5184	0.2936	0.104×10^{-1}	1.5167

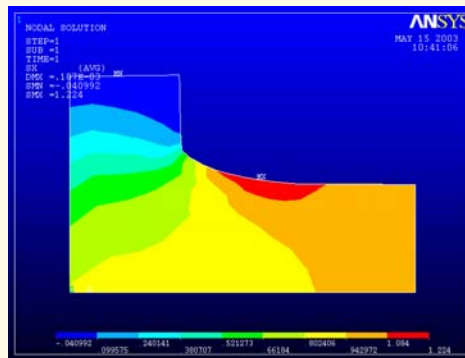
Case Studies

Case Study # 2

Redesign Option # 1: Optimum Shape of fillet



U_x – Displacement

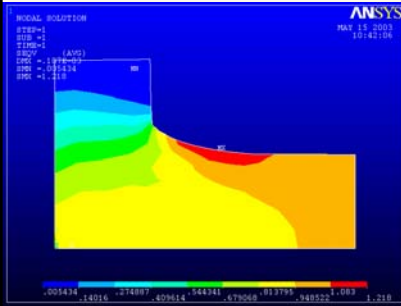


σ_x – Normal Stress

Case Studies

Case Study # 2

Redesign Option # 1: Results



Maximum Deflection (mm)

	U_x	U_y
Node #	27	1
Value	0.18524×10^{-3}	-0.35971×10^{-4}

Maximum and Minimum stress components (N/mm²)

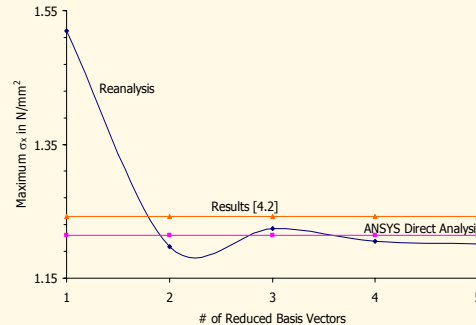
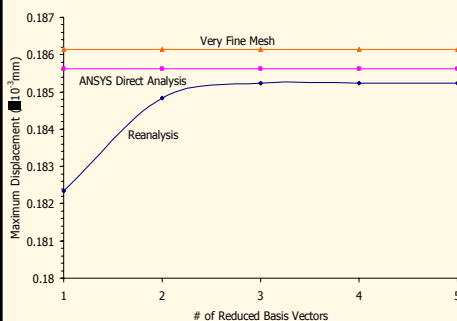
		σ_x	σ_y	σ_{xy}	σ_{VM}
Minimum	Node #	58	10	46	64
	Value	-0.41×10^{-1}	-0.186	-0.372	0.544×10^{-2}
Maximum	Node #	49	46	1	49
	Value	1.2241	0.312	0.144×10^{-1}	1.218

σ_{VM} – von Mises Stress

Case Studies

Case Study # 2

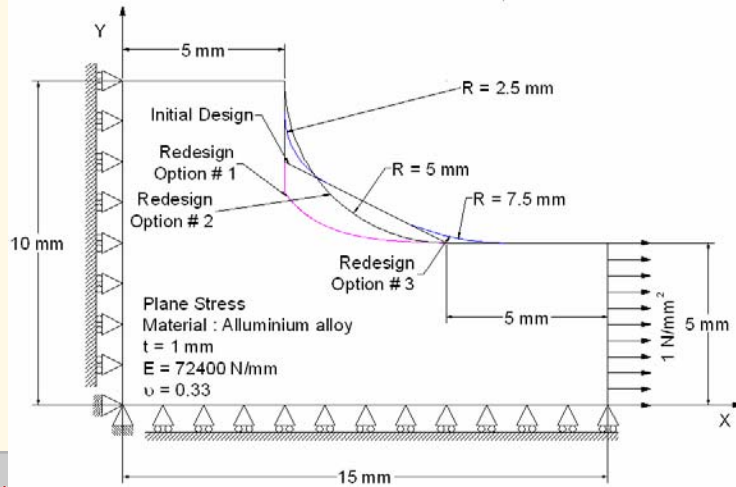
Redesign Option # 1: Displacement and Stress



Case Studies

Case Study # 2

Redesign Option # 2 and 3:



WPI

ME

Case Studies

Case Study # 2

Reanalysis Results:

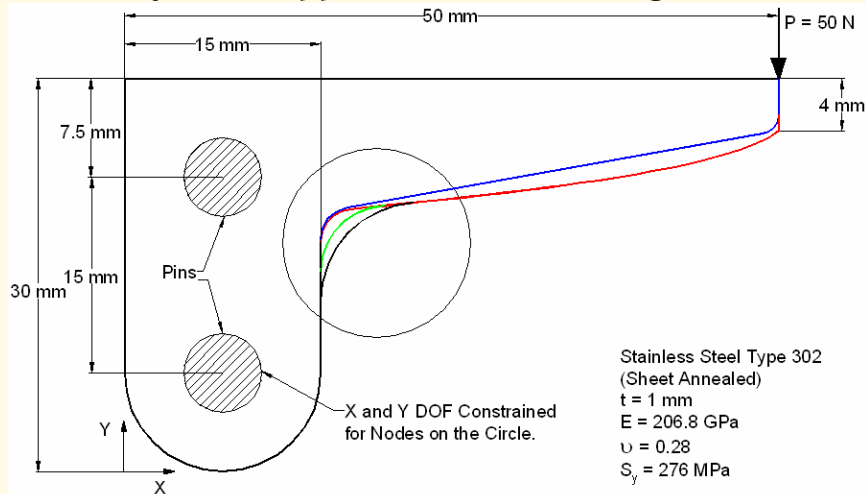
Maximum Quantities	Redesign Options								
	# 1: Free-form Fillet			# 2: Circular Arc Fillet			# 3: Two Circular Arcs		
	ANSYS Direct Analysis	Reanalysis	% Error	ANSYS Direct Analysis	Reanalysis	% Error	ANSYS Direct Analysis	Reanalysis	% Error
σ_x N/mm ²	1.2138	1.2241	0.84	1.3852	1.3892	0.29	1.288	1.2913	0.25
σ_{VM} N/mm ²	1.2127	1.2180	0.44	1.3932	1.4096	1.1	1.2727	1.2749	0.17
U_x ($\times 10^{-3}$ mm)	0.18562	0.18524	0.20	0.18058	0.18024	0.19	0.17543	0.17517	0.15

WPI

ME

Case Studies

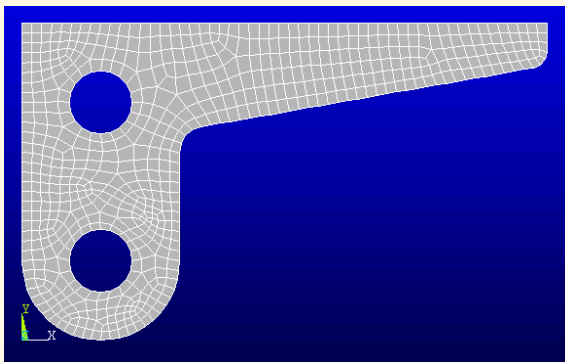
Case Study # 3 : Support Bracket Redesign



Case Studies

Case Study # 3 : Support Bracket Redesign

Initial Problem: FE Model



Mesh Characteristics:

349 Four-node Quad Elements
415 Nodes
2 DOF/node
830 Total DOF

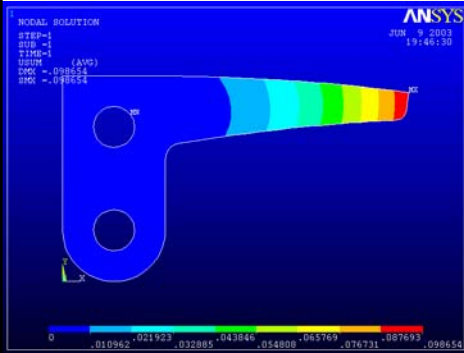
Element and Material Properties:

Material: Stainless Steel Type 302
PLANE42 – Four node quad
Plane Stress with thickness
Poisson's ratio – 0.28
Young's Modulus – 206.8 GPa
Thickness – 1 mm
Yield Stress (S_y) – 276 N/mm²

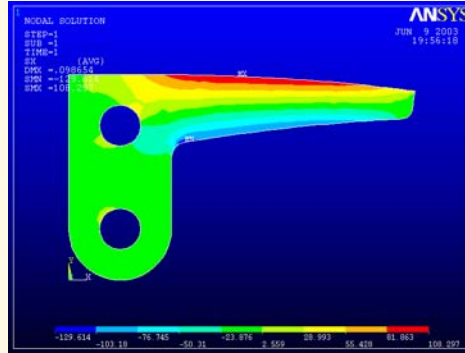
Case Studies

Case Study # 3 : Support Bracket Redesign

Initial Problem: Analysis and post-processing



U_{SUM} – Displacement Vector Sum

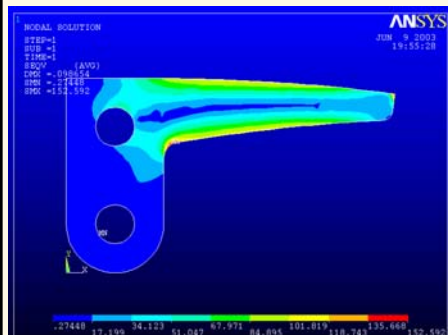


σ_x – Normal Stress

Case Studies

Case Study # 3 : Support Bracket Redesign

Initial Problem: Analysis and post-processing



σ_{VM} – von Mises Stress

Maximum Deflection (mm)

	u_x	u_y
Node #	43	43
Value	0.18767×10^{-1}	-0.9685×10^{-1}

Maximum and Minimum stress components (N/mm²)

		σ_x	σ_y	σ_{xy}	σ_{VM}
Minimum	Node #	2	43	5	176
	Value	-129.61	-121.55	-62.146	0.27448
Maximum	Node #	56	192	179	5
	Value	108.30	19.739	33.690	152.59

$S_y = 276 \text{ N/mm}^2$
Safety Factor = 1.8

Case Studies

Case Study # 3 : Support Bracket Redesign

Redesign Option # 1: Optimum thickness

For the support under point load, the maximum bending stress is,

$$\sigma_x^{\max} = \frac{M \cdot y}{I} = \frac{(P \cdot x) \cdot \frac{h}{2}}{\frac{1}{12} \cdot b \cdot h^3}$$

σ_x^{\max} = Maximum bending stress

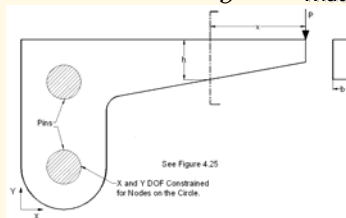
P = Applied Load

h = Height

b = Width = thickness for plane stress problem

Thus,

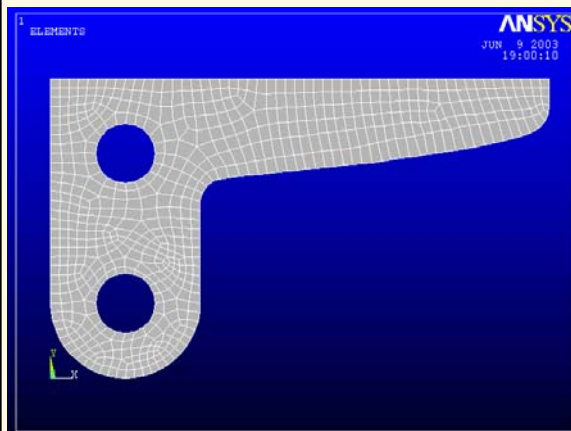
$$h = \sqrt{\frac{6 \cdot P}{\sigma_x^{\max}} \cdot x}$$



Case Studies

Case Study # 3 : Support Bracket Redesign

Redesign Option # 1: Optimum Thickness



Mesh Characteristics:

349 Four-node Quad Elements
415 Nodes
2 DOF/node
830 Total DOF

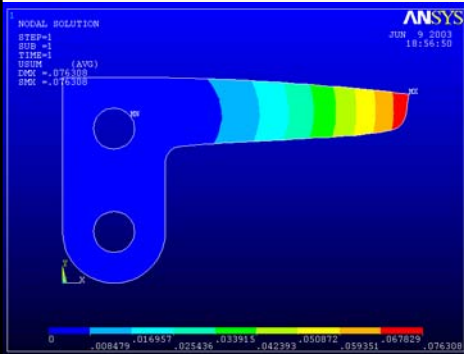
Element and Material Properties:

Material: Stainless Steel Type 302
PLANE42 – Four node quad
Plane Stress with thickness
Poisson's ratio – 0.28
Young's Modulus – 206.8 GPa
Thickness – 1 mm
Yield Stress (S_y) – 276 N/mm²

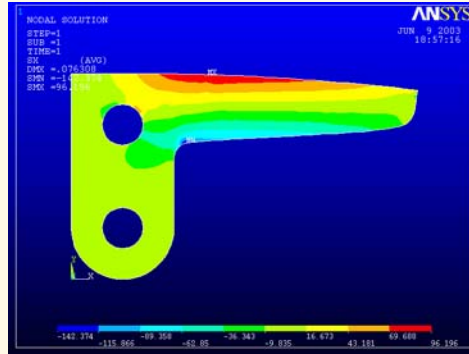
Case Studies

Case Study # 3 : Support Bracket Redesign

Redesign Option # 1: Results



U_{SUM} – Displacement Vector Sum

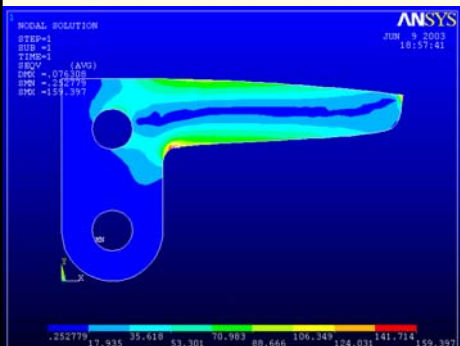


σ_x – Normal Stress

Case Studies

Case Study # 3 : Support Bracket Redesign

Redesign Option # 1: Results



Maximum Deflection (mm)

	U_x	U_y
Node #	43	43
Value	0.15196×10^{-1}	-0.74779×10^{-1}

Maximum and Minimum stress components (N/mm²)

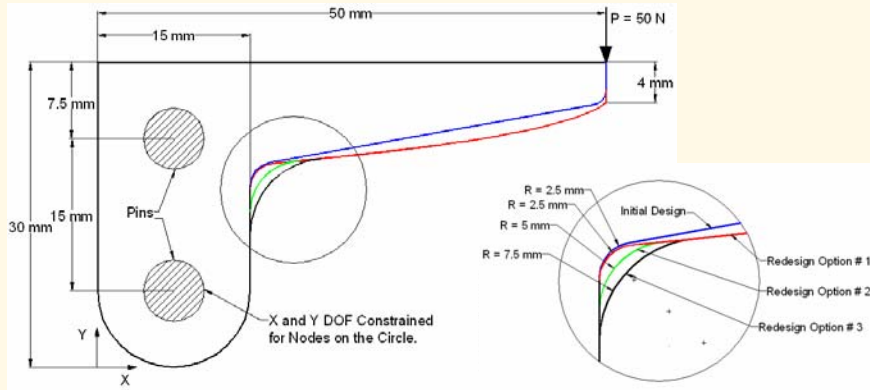
		σ_x	σ_y	σ_{xy}	σ_{vm}
Minimum	Node #	2	43	5	176
	Value	-142.37	-124.86	-62.044	0.2528
Maximum	Node #	51	192	179	5
	Value	96.196	19.546	33.477	159.40

$S_y = 276 \text{ N/mm}^2$
Safety Factor = 1.7

Case Studies

Case Study # 3 : Support Bracket Redesign

Redesign Option # 2 and 3: Increasing the Fillet Radius



Case Studies

Case Study # 3 : Support Bracket Redesign

Reanalysis Results

Maximum Quantities	Design Options									
	Initial Design: Fillet Radius 2.5 mm	# 1: Optimum Shape of Taper			# 2: Fillet Radius 5 mm			# 3: Fillet Radius 7.5 mm		
	ANSYS Direct Analysis	ANSYS Direct Analysis	Reanalysis	% Error	ANSYS Direct Analysis	Reanalysis	% Error	ANSYS Direct Analysis	Reanalysis	% Error
Compressive σ_x N/mm ²	-129.61	-138.77	-142.37	2.59	-121.71	-122.11	0.33	-118.58	-122.03	2.9
σ_{vm} N/mm ²	152.59	152.39	159.40	4.6	123.55	126.96	2.7	118.40	121.79	2.8
Safety Factor	1.8	1.8	1.7		2.2	2.2		2.3	2.3	
U_y ($\times 10^{-1}$ mm)	-0.9685	-0.7479	-0.74779	0.015	-0.7085	0.7083	0.028	0.6652	0.66394	0.19

Cost Analysis

Total number of multiplications and divisions in case of Direct Analysis using Cholesky Decomposition Method

$$\left(\frac{n^3}{6} + n^2 \right)$$

Total number of multiplications and divisions in case of Combined Approximation Reanalysis Method

$$\left[2m^3 + 4n^2 + 3n + (3m^2 + 12m + 18) \right]$$

where,

m = Total number of DOFs changed

n = Total number of DOFs of the system

Since $m \ll n$

Total number of multiplications and divisions in case of Combined Approximation Reanalysis Method

$$2m^3 + 4n^2 + 3n$$

Cost Analysis

For Reanalysis method to be faster than the Direct analysis method

$$2m^3 + 4n^2 + 3n \text{ should be less than } \left(\frac{n^3}{6} + n^2 \right)$$

$$2m^3 + 4n^2 + 3n \leq \frac{n^3}{6} + n^2$$

$$2m^3 \leq \frac{n^3}{6} - 3n^2 - 3n$$

Yielding,

$$\frac{\text{Total \# of DOFs changed}}{\text{Total \# of DOFs of the system}} = \frac{m}{n} \leq 0.4368$$

CA method is most efficient when the coordinates of less than 43% of node out of total number of nodes is changed.

Conclusion

- ✚ Reanalysis method coupled with the design process offers many advantages for improving the design
- ✚ CA method can be effectively used in reanalysis
- ✚ Three reduced basis vectors are sufficient for better accuracy for displacement and stress
- ✚ Reanalysis algorithm using CA method is more efficient up to 43 % of change in node locations

Future Work

- ✚ Improved ANSYS Output Environment
- ✚ Using Combined Approximation Method for Change in # of DOF
- ✚ 3-Dimensional Problems
- ✚ Factor of Safety Plots
- ✚ Fatigue Analysis Plots
- ✚ Boundary Elements